MONTHLY NOTICES

OF THE

ROYAL ASTRONOMICAL SOCIETY

VOL. LXXXVI. MAY 14, 1926. No. 7

Dr. J. H. JEANS, PRESIDENT, in the Chair.

Philip Arthur Curry, B.A., A.Inst.P., Director, Helwan Observatory, Egypt,

was balloted for and duly elected a Fellow of the Society.

The following candidates were proposed for election as Fellows of the Society, the names of the proposers from personal knowledge being appended :—

William Barron Coutts, M.A., B.Sc., F.R.S.E., 74 Vanbrugh Park, Blackheath, London, S.E. 3 (proposed by F. W. Dyson) ;

Idwal Owain Griffith, M.A., 37 Banbury Road, Oxford (proposed by H. Knox-Shaw) ;

Mohammed Ali Higab, M.Sc., The University, Leeds (proposed by S. Brodetsky) ;

Charles Hardman Laver, B.A., B.M., B.Ch., F.R.C.S., The Red House, Redhill, Surrey (proposed by W. H. Steavenson) ;

Mrs. Dorothy Una Ratcliffe, The Hall, Roundbay, Leeds (proposed by S. Brodetsky) ;

Leo Mengersen Waterford, Acting Chief Assistant, Adelaide Observatory, South Australia (proposed by A. L. Kennedy).

Seventy-one presents were announced as having been received since the last meeting, including, amongst others :—

Amateur Telescope-Making [in six parts, by various authors] (presented by Mr. C. Ions).

Tycho Brahe, Opera Omnia, tomus viii. (presented by Dr. Dreyer).

Madison, Washburn Observatory : Publications, vol. 14, pt. 2, Meridian Observations of Comparison Stars, A. S. Flint.

San Fernando Observatory, Carte du Ciel, zone $-3°$ (10 charts).

On Radiative Viscosity and the Rotation of Astronomical Masses.

(Second Paper.) By J. H. Jeans.

1. In the first paper * I showed that the transfer of momentum by radiation plays a predominant part in determining the internal motions of astronomical masses, just as the transfer of energy by radiation plays a predominant part in determining the internal distribution of temperature.†

In the present paper exact equations of motion are obtained and applied to certain special problems of astronomical importance. A summary of the results obtained is given in §§ 15–18; readers who are interested in the astronomical applications of the analysis rather than in the analysis itself may prefer to turn to § 15 at once.

The Transfer of Radiation in Moving Media.

2. Schwarzschild's original investigation assumed the medium through which the radiation travelled to have no relative motion, and recent developments by Eddington, Milne, Rosseland, and others have proceeded on the same supposition. We proceed to study the transmission of radiation in a medium which is supposed, at least for the present, to move in the most general manner possible.

Consider the passage of a ray of light from a point P to an adjacent point Q, at which the medium moves with a velocity δv relative to the medium at P. Let us momentarily take the direction of δv to be that of the axis of x, and suppose the direction-cosines of the ray at P relative to the medium at P to be l, m, n, those of the ray at Q relative to the medium at Q being l', m', n'.

The difference between the two sets of direction-cosines is of course a consequence of the "aberration" of the light received at Q caused by the motion of Q relative to the source of light P. The two sets of direction-cosines are accordingly related by the usual aberrational equations ‡

$$\frac{\kappa(l'+\delta v/\mathrm{C})}{l}=\frac{m'}{m}=\frac{n'}{n}=\kappa\left(1+l'\frac{\delta v}{\mathrm{C}}\right) \quad . \quad . \quad . \quad (1)$$

in which $\kappa^2=1-(\delta v/c)^2$. This system of fractions only represents two independent equations, which we may conveniently take to be

$$l'-l=(ll'-1)\frac{\delta v}{\mathrm{C}} \quad . \quad . \quad . \quad . \quad (2)$$

$$mn'-m'n=0 \quad . \quad . \quad . \quad . \quad (3)$$

Since the direction-cosines of δv are 1, 0, 0, equation (3) merely

* *M.N.*, **86**, 328 (1926).

† R. A. Sampson, *Mem. R.A.S.*, **51** (1894), p. 123; K. Schwarzschild, *Gött. Nach.*, 1906, p. 41.

‡ See, for instance, Jeans, *Electr. and Mag.* (5th ed.), p. 609.

expresses the obvious fact that the directions of δv, of the ray at P, and of the ray at Q are all in one plane.

Let us now refer all directions in space to a fixed frame of reference. Let the direction l, m, n be fixed by co-ordinates θ, ϕ (co-latitude and azimuth), and let the direction l', m', n' have co-ordinates θ', ϕ'. Let the direction of δv have co-ordinates θ'', ϕ'' and write

$$\delta v \sin\theta'' \cos\phi''=du, \qquad \delta v \sin\theta'' \sin\phi''=dv, \qquad \delta v \cos\theta''=dw.$$

Then the condition that δv, (θ, ϕ), and (θ', ϕ') shall be coplanar is

$$\begin{vmatrix} du, & dv, & dw \\ \sin\theta\cos\phi, & \sin\theta\sin\phi, & \cos\theta \\ \sin\theta'\cos\phi', & \sin\theta'\cos\phi', & \cos\theta' \end{vmatrix} = 0,$$

from which we readily obtain

$$\frac{\delta\theta}{\cos\theta(du\cos\phi+dv\sin\phi)-dw\sin\theta}=\frac{\sin\theta\delta\phi}{dv\cos\phi-du\sin\phi} \quad . \qquad (4)$$

where $\delta\theta$ has been written for $\theta'-\theta$ and $\delta\phi$ for $\phi'-\phi$.

Since l has been taken to be the cosine of the angle between the directions of δv and (θ, ϕ), we have

$$l\delta v=du\sin\theta\cos\phi+dv\sin\theta\sin\phi+dw\cos\theta,$$

and there is a similar equation for l'. Inserting these values for l, l' into equation (2), we find that each of the fractions in equation (4) is equal to $-1/C$. Thus the values of $\delta\theta$, $\delta\phi$ are

$$C\delta\theta=-\cos\theta(du\cos\phi+dv\sin\phi)+dw\sin\theta \quad . \quad . \qquad (5)$$

$$C\sin\theta\,\delta\phi=du\sin\phi-dv\cos\phi \quad . \quad . \quad . \quad . \qquad (6)$$

3. An element of solid angle $d\omega$ is given by $d\omega=\sin\theta d\theta d\phi$. Consider the radiation filling at P a small cone of solid angle $d\omega$, and let the corresponding solid angle at Q be $d\omega'=\sin\theta' d\theta' d\phi'$. We have

$$\frac{d\omega'}{d\omega}=\frac{\sin\theta'}{\sin\theta}\frac{\partial(\theta', \phi')}{\partial(\theta, \phi)}$$

$$=1+\frac{2}{C}(du\sin\theta\cos\phi+dv\sin\theta\sin\phi+dw\cos\theta).$$

Let the intensity of the radiation inside this cone at P be $I(\theta, \phi)d\omega$, and let the corresponding intensity in the cone $d\omega'$ at Q be $I(\theta', \phi')d\omega'$. The total energy in this cone is the same at P as at Q, except in so far as this is altered by emission and absorption on the path PQ. Hence we have exactly, as in Schwarzschild's theory,

$$\delta[I(\theta, \phi)d\omega]=E\rho\frac{d\omega}{4\pi}ds-k\rho I d\omega ds,$$

where δ refers to the increase which occurs in the element PQ or ds of

path, E is the emission per unit mass, and R the coefficient of opacity. This may be written in the form

$$\frac{\partial I}{\partial s}ds+\frac{\partial I}{\partial \theta}\delta\theta+\frac{\partial I}{\partial \phi}\delta\phi+\frac{2I}{C}(du\sin\theta\cos\phi+dv\sin\theta\sin\phi+dw\cos\theta)$$
$$=\left(\frac{E\rho}{4\pi}-k\rho I\right)ds \quad . \quad (7)$$

When P, Q are relatively at rest du, dv, dw, $\delta\theta$, and $\delta\phi$ all vanish, and the equation reduces to Schwarzschild's well-known equation. In the general case let the solution of equation (7) be

$$I=I_0+I_1\frac{\partial u}{\partial s}+I_2\frac{\partial v}{\partial s}+I_3\frac{\partial w}{\partial s} \quad . \quad . \quad . \quad (8)$$

On substituting this value for I into equation (8) and equating coefficients of $\partial u/\partial s$, etc., we obtain

$$\frac{\partial I_0}{\partial s}=\frac{E\rho}{4\pi}-k\rho I_0 \quad . \quad . \quad . \quad . \quad (9)$$

$$\frac{\partial I_1}{\partial s}-\frac{\cos\theta\cos\phi}{C}\frac{\partial I_0}{\partial \theta}+\frac{\sin\phi}{C\sin\theta}\frac{\partial I_0}{\partial \phi}+\frac{2\sin\theta\cos\phi}{C}I_0=-k\rho I_1 \quad . \quad (10)$$

$$\frac{\partial I_2}{\partial s}-\frac{\cos\theta\sin\phi}{C}\frac{\partial I_0}{\partial \theta}-\frac{\cos\phi}{C\sin\theta}\frac{\partial I_0}{\partial \phi}+\frac{2\sin\theta\sin\phi}{C}I_0=-k\rho I_2 \quad . \quad (11)$$

$$\frac{\partial I_3}{\partial s}+\frac{\sin\theta}{C}\frac{\partial I_0}{\partial \theta}+\frac{2\cos\theta}{C}=-k\rho I_3 \quad . \quad (12)$$

4. Consider a star, or region of a star, arranged in parallel layers so that the surfaces $E/k=constant$ are perpendicular to the axis of z. The general solution of equation (9) is

$$I_0=\left(1+\frac{1}{k\rho}\frac{\partial}{\partial s}\right)^{-1}\left(\frac{E}{4\pi k}\right)=\left(1-\frac{1}{k\rho}\frac{\partial}{\partial s}+\left(\frac{1}{k\rho}\frac{\partial}{\partial s}\right)^2-\ldots\right)\left(\frac{E}{4\pi k}\right) \quad (13)$$

but it will immediately appear that an adequate solution for the present problem is obtained by taking only the first two terms on the right. The general value of $\partial/\partial s$ is

$$\frac{\partial}{\partial s}=\sin\theta\cos\phi\frac{\partial}{\partial x}+\sin\theta\sin\phi\frac{\partial}{\partial y}+\cos\theta\frac{\partial}{\partial z},$$

but the solution for I_0 reduces to

$$I_0=\left(1-\frac{1}{k\rho}\cos\theta\frac{\partial}{\partial z}\right)\left(\frac{E}{4\pi k}\right)=\left(1+\cos\theta\frac{\partial}{\partial \nu}\right)\left(\frac{E}{4\pi k}\right) \quad . \quad (14)$$

where, as usual, $d\nu=-k\rho dz$.

Since I_0 does not depend on ϕ, equation (10) assumes the form

$$k\rho I_1+\sin\theta\cos\phi\frac{\partial I_1}{\partial x}+\sin\theta\sin\phi\frac{\partial I_1}{\partial y}+\cos\theta\frac{\partial I_1}{\partial z}$$
$$+\frac{1}{C}\left[2\sin\theta\cos\phi I_0-\cos\theta\cos\phi\frac{\partial I_0}{\partial \theta}\right]=0.$$

Clearly $\partial I_1/\partial x$ and $\partial I_1/\partial y$ both vanish, while I_1 is proportional to $\cos\phi$, being given by

$$k\rho I_1+\cos\theta\frac{\partial I_1}{\partial z}=-\frac{\cos\phi}{C}\left[2\sin\theta I_0-\cos\theta\frac{\partial I_0}{\partial\theta}\right] \quad . \quad . \quad (15)$$

There are similar values for I_2 and I_3, given by

$$k\rho I_2+\cos\theta\frac{\partial I_2}{\partial z}=-\frac{\sin\phi}{C}\left[2\sin\theta I_0-\cos\theta\frac{\partial I_0}{\partial\theta}\right] \quad . \quad . \quad (16)$$

$$k\rho I_3+\cos\theta\frac{\partial I_3}{\partial z}=-\frac{1}{C}\left[2\cos\theta I_0+\sin\theta\frac{\partial I_0}{\partial\theta}\right] \quad . \quad . \quad (17)$$

5. The total radiant energy per unit volume, R, is given by

$$R=\frac{1}{C}\int\int I d\omega$$

$$=\frac{1}{C}\int\int\left[I_0+I_1\left(\sin\theta\cos\phi\frac{\partial u}{\partial x}+\sin\theta\sin\phi\frac{\partial u}{\partial y}+\cos\theta\frac{\partial u}{\partial z}\right)+\ldots\right]\sin\theta d\theta d\phi,$$

and on integrating with respect to ϕ we find

$$R=\frac{2\pi}{C}\int\left[I_0+\frac{I_1\sin\theta}{2\cos\phi}\frac{\partial u}{\partial x}+\frac{I_2\sin\theta}{2\sin\phi}\frac{\partial v}{\partial y}+I_3\cos\theta\frac{\partial w}{\partial z}\right]\sin\theta d\theta \quad . \quad (18)$$

We may neglect squares of u/C, v/C, and w/C, and so may insert in this equation values of I_1, I_2, and I_3 calculated on the supposition that u, v, and w all vanish. In such a case the value of E/k is $4\sigma T^4$ where σ is Stefan's constant and T is the absolute temperature, so that

$$I_0=\left(1+\cos\theta\frac{\partial}{\partial\nu}\right)\left(\frac{\sigma T^4}{\pi}\right),$$

and we obtain in succession from equations (15), (16), and (17)

$$I_1=-\frac{\sin\theta\cos\phi}{k\rho C}\left(2+5\cos\theta\frac{\partial}{\partial\nu}\right)\left(\frac{\sigma T^4}{\pi}\right) \quad . \quad . \quad . \quad (19)$$

$$I_2=-\frac{\sin\theta\sin\phi}{k\rho C}\left(2+5\cos\theta\frac{\partial}{\partial\nu}\right)\left(\frac{\sigma T^4}{\pi}\right) \quad . \quad . \quad . \quad (20)$$

$$I_3=-\frac{1}{k\rho C}\left(2\cos\theta+(5\cos^2\theta-1)\frac{\partial}{\partial\nu}\right)\left(\frac{\sigma T^4}{\pi}\right) \quad . \quad . \quad (21)$$

If we insert these values of I_1, I_2, and I_3 in equation (18), we obtain

$$R=\frac{2\pi}{C}\int I_0\sin\theta d\theta-\frac{8\sigma T^4}{3k\rho C^2}\left(\frac{\partial u}{\partial x}+\frac{\partial v}{\partial y}+\frac{\partial w}{\partial z}\right) \quad . \quad . \quad (22)$$

and on further inserting the value for I_0 given by equation (14),

$$R=\frac{E}{kC}-\frac{8\sigma T^4}{3k\rho C^2}\left(\frac{\partial u}{\partial x}+\frac{\partial v}{\partial y}+\frac{\partial w}{\partial z}\right) \quad . \quad . \quad . \quad (23)$$

When the medium is at rest, R and E/k are each equal to aT^4 or $4\sigma T^4/C$. We see that when the medium is in motion R and E/k are no longer equal to one another, and the question of the precise definition of temperature becomes of importance. The precise question we have to settle is whether T is to denote the temperature of the matter at a point or that of the radiation at the same point. A similar question occurs in discussing the kinetic theory of a gas which is not in a steady state. It is of course immaterial which definition of temperature we select, so long as we retain this definition consistently.

Let us agree to define the temperature T to be such that the radiant energy per unit volume is equal to aT^4. Then

$$R=aT^4=4\sigma T^4/C,$$

and equation (23) gives

$$\frac{E}{k}=4\sigma T^4+\frac{8\sigma T^4}{3k\rho C}\left(\frac{\partial u}{\partial x}+\frac{\partial v}{\partial y}+\frac{\partial w}{\partial z}\right) \quad . \quad . \quad . \quad (24)$$

Equation (14) now gives

$$I_0=\left(1+\cos\theta\frac{\partial}{\partial v}\right)\left[1+\frac{2}{3k\rho C}\left(\frac{\partial u}{\partial x}+\frac{\partial v}{\partial y}+\frac{\partial w}{\partial z}\right)\right]\left(\frac{\sigma T^4}{\pi}\right) \quad . \quad (25)$$

On inserting this value for I_0 and the values for I_1, I_2, I_3 found in equations (19) to (21) into equation (8), we obtain a formula which gives the flow of radiation on the supposition that squares of u/C, v/C, and w/C may be neglected.

The Transfer of Momentum.

6. We proceed next to the main object of the paper, a calculation of the momentum transported by the flow of radiation just investigated.

Relative to axes fixed in space, or fixed in the star, let the direction of the ray previously considered be Θ, Φ. Let the velocity of the stellar material at P be du, dv, dw. Further, put $\Theta=\theta+\Delta\theta$ and $\Phi=\phi+\Delta\phi$. Precisely as in § 2 (equations (5) and (6)), we obtain

$$C\Delta\theta=\cos\theta(u\cos\phi+v\sin\phi)+w\sin\theta \quad . \quad . \quad (26)$$

$$C\sin\theta\Delta\phi=-u\sin\phi+v\cos\phi \quad . \quad . \quad . \quad . \quad (27)$$

Let μ_{xx} denote the flow of momentum parallel to Ox across unit area perpendicular to Ox, and let μ_{xy}, μ_{xz} . . . have corresponding meanings. Then

$$\mu_{xx}=\frac{I}{C}\int I(\Theta,\Phi)\sin^2\Theta\cos^2\Phi\,d\omega$$

$$=\frac{I}{C}\int\int I(\theta,\phi)[\sin^2\theta\cos^2\phi+2\sin\theta\cos\theta\cos^2\phi\Delta\theta$$

$$-2\sin\phi\cos\phi\sin^2\theta\Delta\phi]\sin\theta d\theta d\phi \quad . \quad (28)$$

in which we must insert the value for I given in equation (8).

The value of I_0 is given by equation (25). On inserting this in the right-hand member of equation (28), the only terms which survive integration with respect to ϕ are

$$\frac{\pi}{C}\int\left(1+\cos\theta\frac{\partial}{\partial\nu}\right)\left[\left\{1+\frac{2}{3k\rho C}\left(\frac{\partial u}{\partial x}+\frac{\partial v}{\partial y}+\frac{\partial w}{\partial z}\right)\right\}\frac{\sigma T^4}{\pi}\right]\sin^3\theta d\theta$$
$$+\frac{2\pi}{C}\int\left(1+\cos\theta\frac{\partial}{\partial\nu}\right)\frac{\sigma T^4}{\pi}\frac{w}{C}\sin^3\theta\cos\theta d\theta,$$

in which terms in $(u/C)^2$, etc., are again neglected. Effecting the integration with respect to θ, this becomes

$$\tfrac{1}{3}aT^4\left\{1+\frac{2}{3k\rho C}\left(\frac{\partial u}{\partial x}+\frac{\partial v}{\partial y}+\frac{\partial w}{\partial z}\right)\right\}+\frac{2w}{15k\rho C}\frac{\partial}{\partial z}(aT^4).$$

The terms in I_1, I_2, and I_3 can be similarly calculated, and we obtain as the total flow of momentum,

$$\mu_{xx}=\tfrac{1}{3}aT^4+\frac{4}{45k\rho C}\left(\frac{\partial u}{\partial x}+\frac{\partial v}{\partial y}+\frac{\partial w}{\partial z}\right)aT^4-\frac{4}{15k\rho C}\left(\frac{\partial u}{\partial x}\right)aT^4$$
$$+\frac{2w}{15k\rho C}\frac{\partial}{\partial z}(aT^4) \quad . \quad (29)$$

By similar procedure we calculate

$$\mu_{zz}=\tfrac{1}{3}aT^4+\frac{4}{45k\rho C}\left(\frac{\partial u}{\partial x}+\frac{\partial v}{\partial y}+\frac{\partial w}{\partial z}\right)aT^4-\frac{4}{15k\rho C}\left(\frac{\partial w}{\partial z}\right)aT^4-\frac{4w}{15k\rho C}\frac{\partial}{\partial z}(aT^4),$$

$$\mu_{yz}=-\frac{2}{15k\rho C}\left(\frac{\partial w}{\partial y}+\frac{\partial v}{\partial z}\right)aT^4-\frac{v}{5k\rho C}\frac{\partial}{\partial z}(aT^4),$$

$$\mu_{xy}=-\frac{2}{15k\rho C}\left(\frac{\partial v}{\partial x}+\frac{\partial u}{\partial y}\right)aT^4,$$

and the values of μ_{yy}, μ_{zx} can be written down by mere interchange of symbols from μ_{xx}, μ_{xz}.

7. The equations are not symmetrical in x, y, z because we have supposed the stellar material at the point under consideration to be so oriented that the surfaces E/k=constant are perpendicular to the axis of z. It is easy to remove this restriction by a general transformation of axes. This leads to the entirely symmetrical system of equations :

$$\mu_{xx}=\tfrac{1}{3}aT^4+\frac{2aT^4}{15k\rho C}\left[\tfrac{2}{3}\left(\frac{\partial u}{\partial x}+\frac{\partial v}{\partial y}+\frac{\partial w}{\partial z}\right)-2\frac{\partial u}{\partial x}\right]$$
$$+\frac{2}{15k\rho C}\left[\left(u\frac{\partial}{\partial x}+v\frac{\partial}{\partial y}+w\frac{\partial}{\partial z}\right)aT^4-3u\frac{\partial}{\partial x}(aT^4)\right] \quad . \quad (30)$$

$$\mu_{yz}=-\frac{2aT^4}{15k\rho C}\left(\frac{\partial w}{\partial y}+\frac{\partial v}{\partial z}\right)-\frac{1}{5k\rho C}\left(v\frac{\partial}{\partial z}+w\frac{\partial}{\partial y}\right)(aT^4) \quad . \quad . \quad . \quad (31)$$

and similar equations.

When u, v, w all vanish, the equations reduce to

$$\mu_{xx}=\mu_{yy}=\mu_{zz}=\tfrac{1}{3}a\mathrm{T}^4,$$

which of course represents the ordinary pressure of radiation in a medium at rest. The additional terms which result from the motion of the medium fall into two groups.

The first group consists of terms in $\partial u/\partial x$, $\partial u/\partial y$, $\partial w/\partial x$, etc. On comparing these terms with the similar terms in the flow of momentum in a viscous fluid we find that they are precisely the same as if the stellar material had a coefficient of "radiative" viscosity κ_{R} given by

$$\kappa_{\mathrm{R}}=\frac{2}{15k\rho\mathrm{C}}a\mathrm{T}^4 \quad . \quad . \quad . \quad . \quad (32)$$

This is only two-fifths of the value found by the elementary method of the first paper; the numerical difference arises from the cause there explained.

The remaining terms in μ_{xx}, etc., are terms jointly proportional to the velocity u, v, w and to the gradient of $a\mathrm{T}^4$. These represent the flow of momentum caused by the flow of radiant energy through the star.

8. Equations (30) and (31) give the flow of momentum carried by radiation; to this we must add the flow of momentum carried by matter. Expressions for this latter flow can be found in any text-book.* Let p_{G} denote the ordinary gas-pressure and put

$$p=p_{\mathrm{G}}+\tfrac{1}{3}a\mathrm{T}^4 \quad . \quad . \quad . \quad . \quad (33)$$

so that p is the total pressure, gas-pressure plus pressure of radiation.

Further, let κ_{G} denote the coefficient of gaseous or fluid viscosity and put

$$\kappa=\kappa_{\mathrm{G}}+\frac{2}{15k\rho\mathrm{C}}a\mathrm{T}^4 \quad . \quad . \quad . \quad . \quad (34)$$

so that κ represents the total coefficient of viscosity, material plus radiative. Then the total flow of momentum, M_{xx}, . . . is found to be given by

$$\mathrm{M}_{xx}=p+\tfrac{2}{3}\kappa\left(\frac{\partial u}{\partial x}+\frac{\partial v}{\partial y}+\frac{\partial w}{\partial z}\right)-2\kappa\frac{\partial u}{\partial x}$$
$$+\frac{2}{15k\rho\mathrm{C}}\left[\left(u\frac{\partial}{\partial x}+v\frac{\partial}{\partial y}+w\frac{\partial}{\partial z}\right)a\mathrm{T}^4-3u\frac{\partial}{\partial x}(a\mathrm{T}^4)\right] \quad . \quad (35)$$

$$\mathrm{M}_{yz}=-\kappa\left(\frac{\partial w}{\partial y}+\frac{\partial v}{\partial z}\right)-\frac{1}{5k\rho\mathrm{C}}\left(v\frac{\partial}{\partial z}+w\frac{\partial}{\partial y}\right)(a\mathrm{T}^4) \quad . \quad . \quad . \quad . \quad (36)$$

and similar equations.

* Lamb, *Hydrodynamics* (5th ed.), p. 544; or Jeans, *Dynamical Theory of Gases* (4th ed.), p. 243.

The Equations of Motion.

9. Suppose that unit volume of the star contains a mass m of matter moving with a velocity u, v, w. Let this matter generate radiation at a rate g per unit mass per unit time, so that the consequent loss of mass is given by

$$mg=-C^2\frac{Dm}{Dt} \quad . \quad . \quad . \quad . \quad (37)$$

where D/Dt, as usual, denotes differentiation as we follow the moving matter on its path. The rate of change of momentum inside this unit volume is equal to the rate of flow of momentum across its boundaries so that

$$\frac{D}{Dt}(mu)=mX-\frac{\partial}{\partial x}M_{xx}-\frac{\partial}{\partial y}M_{xy}-\frac{\partial}{\partial z}(M_{xz}) \quad . \quad . \quad (38)$$

where, using relation (37),

$$\frac{D}{Dt}(mu)=m\frac{Du}{Dt}+u\frac{Dm}{Dt}=m\left(\frac{Du}{Dt}-\frac{ug}{C^2}\right) \quad . \quad . \quad (39)$$

Replacing m by the more usual symbol ρ, equation (38) becomes

$$\rho\left(\frac{Du}{Dt}-\frac{ug}{C^2}\right)=\rho X-\frac{\partial}{\partial x}M_{xx}-\frac{\partial}{\partial y}M_{xy}-\frac{\partial}{\partial z}M_{xz} \quad . \quad . \quad (40)$$

or, substituting the values for M_{xx}, etc., obtained in the last section,

$$\begin{aligned}\rho\left(\frac{Du}{Dt}-\frac{ug}{C^2}\right)=\rho X&-\frac{\partial p}{\partial x}+\tfrac{1}{3}\kappa\frac{\partial}{\partial x}\left(\frac{\partial u}{\partial x}+\frac{\partial v}{\partial y}+\frac{\partial w}{\partial z}\right)\\
&+\kappa\nabla^2u-\tfrac{2}{3}\left(\frac{\partial u}{\partial x}+\frac{\partial v}{\partial y}+\frac{\partial w}{\partial z}\right)\frac{\partial\kappa}{\partial x}\\
&+2\frac{\partial\kappa}{\partial x}\frac{\partial u}{\partial x}+\frac{\partial\kappa}{\partial y}\left(\frac{\partial u}{\partial y}+\frac{\partial v}{\partial x}\right)+\frac{\partial\kappa}{\partial z}\left(\frac{\partial u}{\partial z}+\frac{\partial w}{\partial x}\right)\\
&-\frac{2}{15}\frac{\partial}{\partial x}\left[\frac{1}{k\rho C}\left(u\frac{\partial}{\partial x}+v\frac{\partial}{\partial y}+w\frac{\partial}{\partial z}\right)aT^4\right]\\
&+\frac{u}{5}\left[\frac{\partial}{\partial x}\left\{\frac{1}{k\rho C}\frac{\partial}{\partial x}(aT^4)\right\}+\frac{\partial}{\partial y}\left\{\frac{1}{k\rho C}\frac{\partial}{\partial y}(aT^4)\right\}+\frac{\partial}{\partial z}\left\{\ldots\right\}\right]\\
&+\frac{1}{5k\rho C}\left[\frac{\partial u}{\partial x}\frac{\partial}{\partial x}(aT^4)+\frac{\partial u}{\partial y}\frac{\partial}{\partial y}(aT^4)+\frac{\partial u}{\partial z}\frac{\partial}{\partial z}(aT^4)\right]\\
&+\tfrac{1}{5}\left[\frac{\partial}{\partial x}\left(\frac{u}{k\rho C}\right)+\frac{\partial}{\partial y}\left(\frac{v}{k\rho C}\right)+\frac{\partial}{\partial z}\left(\frac{w}{k\rho C}\right)\right]\frac{\partial}{\partial x}(aT^4)\\
&+\frac{1}{5k\rho C}\left(u\frac{\partial}{\partial x}+v\frac{\partial}{\partial y}+w\frac{\partial}{\partial z}\right)\frac{\partial}{\partial x}(aT^4) \quad . \quad . \quad . \quad . \quad (41)\end{aligned}$$

These and two similar equations in y and z form the general equations of motion of stellar material.

Internal Motions in a Rotating Star.

10. Let us consider the special problem of the internal motions in a star which is rotating about the axis of z. We transform to cylindrical co-ordinates ϖ, ϕ, z given by

$$x=\varpi\cos\phi, \qquad y=\varpi\sin\phi, \qquad z=z.$$

The velocities are now given by

$$u=\frac{x}{\varpi}\dot{\varpi}-y\dot{\phi}, \qquad v=\frac{y}{\varpi}\dot{\varpi}+x\dot{\phi}, \qquad w=\dot{z} \quad . \quad . \quad (42)$$

and the accelerations by

$$\frac{Du}{Dt}=x\left(\frac{\ddot{\varpi}}{\varpi}-\dot{\phi}^2\right)-\frac{y}{\varpi^2}\frac{\partial}{\partial t}(\varpi^2\dot{\phi}) \text{ etc.}$$

From equations (42) we also obtain

$$\frac{\partial u}{\partial x}+\frac{\partial v}{\partial y}+\frac{\partial w}{\partial z}=\frac{1}{\varpi}\frac{\partial}{\partial\varpi}(\varpi\dot{\varpi})+\frac{\partial\dot{z}}{\partial z},$$

$$u\frac{\partial}{\partial x}+v\frac{\partial}{\partial y}+w\frac{\partial}{\partial z}=\frac{\dot{\varpi}}{\varpi}\left(x\frac{\partial}{\partial x}+y\frac{\partial}{\partial y}\right)+\dot{z}\frac{\partial}{\partial z}+\dot{\phi}\left(x\frac{\partial}{\partial y}-y\frac{\partial}{\partial x}\right).$$

On substituting these values, we find that equation (41) becomes a linear equation in x, y, z, with the coefficient of z equal to zero. In fact the equation assumes the form

$$x\mathrm{P}-y\mathrm{Q}=0 \quad . \quad . \quad . \quad . \quad (43)$$

On substituting into the corresponding y-equation this is found to assume the form

$$y\mathrm{P}+x\mathrm{Q}=0,$$

where P and Q are the same as in equation (43). Thus the two equations are equivalent to P=0, Q=0.

The equation P=0 can at once be obtained from equation (41) by putting $y=0$ therein. It is found to be

$$\begin{aligned}
&\rho\left(\frac{\ddot{\varpi}}{\varpi}-\dot{\phi}^2\right)-\frac{\rho g}{\mathrm{C}^2}\left(\frac{\dot{\varpi}}{\varpi}\right)=\frac{\rho}{\varpi}\frac{\partial\mathrm{V}}{\partial\varpi}-\frac{1}{\varpi}\frac{\partial p}{\partial\varpi}+\frac{1}{3}\frac{\kappa}{\varpi}\frac{\partial}{\partial\varpi}\left[\frac{1}{\varpi}\frac{\partial}{\partial\varpi}(\varpi\dot{\varpi})+\frac{\partial\dot{z}}{\partial z}\right]\\
&\quad+\kappa\nabla^2\left(\frac{\dot{\varpi}}{\varpi}\right)+\frac{2\kappa}{\varpi}\frac{\partial}{\partial\varpi}\left(\frac{\dot{\varpi}}{\varpi}\right)-\frac{2}{3\varpi}\frac{\partial\kappa}{\partial\varpi}\left[\frac{1}{\varpi}\frac{\partial}{\partial\varpi}(\varpi\dot{\varpi})+\frac{\partial\dot{z}}{\partial z}\right]\\
&\quad+\frac{\partial\kappa}{\partial\varpi}\left(\frac{2}{\varpi}\frac{\partial\dot{\varpi}}{\partial\varpi}\right)+\frac{\partial\kappa}{\partial z}\frac{1}{\varpi}\left(\frac{\partial\dot{\varpi}}{\partial z}+\frac{\partial\dot{z}}{\partial\varpi}\right)\\
&\quad-\frac{2}{15\varpi}\frac{\partial}{\partial\varpi}\left[\frac{1}{k\rho\mathrm{C}}\left(\dot{\varpi}\frac{\partial}{\partial\varpi}+\dot{z}\frac{\partial}{\partial z}\right)a\mathrm{T}^4\right]+\frac{\dot{\varpi}}{5\varpi}\left[\Sigma\frac{\partial}{\partial x}\left\{\frac{1}{k\rho\mathrm{C}}\frac{\partial}{\partial x}(a\mathrm{T}^4)\right\}\right]\\
&\quad+\frac{1}{5k\rho\mathrm{C}}\left[\frac{\partial}{\partial\varpi}(a\mathrm{T}^4)\left\{\frac{\partial}{\partial\varpi}\left(\frac{\dot{\varpi}}{\varpi}\right)+\frac{1}{\varpi}\left(\frac{\dot{\varpi}}{\varpi}\right)\right\}+\frac{\partial}{\partial z}(a\mathrm{T}^4)\frac{\partial}{\partial z}\left(\frac{\dot{\varpi}}{\varpi}\right)\right]\\
&\quad+\frac{1}{5\varpi}\frac{\partial}{\partial\varpi}(a\mathrm{T}^4)\left[\frac{1}{k\rho\mathrm{C}}\left(\frac{\partial u}{\partial x}+\frac{\partial v}{\partial y}+\frac{\partial w}{\partial z}\right)+\left(\dot{\varpi}\frac{\partial}{\partial\varpi}+\dot{z}\frac{\partial}{\partial z}\right)\frac{1}{k\rho\mathrm{C}}\right]\\
&\quad+\frac{1}{5k\rho\mathrm{C}}\left[\frac{\dot{\varpi}}{\varpi^2}\frac{\partial}{\partial\varpi}(a\mathrm{T}^4)+\left(\dot{\varpi}\frac{\partial}{\partial\varpi}+\dot{z}\frac{\partial}{\partial z}\right)\left(\frac{1}{\varpi}\frac{\partial}{\partial\varpi}(a\mathrm{T}^4)\right)\right] \quad . \quad . \quad (44)
\end{aligned}$$

Similarly the equation Q=0, obtained by putting $x=0$ in equation (41), is found to be

$$\frac{\rho}{\varpi^2}\frac{\partial}{\partial t}(\varpi^2\dot{\phi})-\rho\frac{g}{C^2}\phi=\kappa\nabla^2\phi+\frac{2\kappa}{\varpi}\frac{\partial\phi}{\partial\varpi}+\left[\frac{\partial\kappa}{\partial\varpi}\frac{\partial\phi}{\partial\varpi}+\frac{\partial\kappa}{\partial z}\frac{\partial\phi}{\partial z}\right]$$
$$+\tfrac{1}{5}\Sigma\frac{\partial}{\partial x}\left\{\frac{1}{k\rho C}\frac{\partial}{\partial x}(aT^4)\right\}$$
$$+\frac{1}{5k\rho C}\left[\frac{\partial\phi}{\partial\varpi}\frac{\partial}{\partial\varpi}(aT^4)+\frac{\partial\phi}{\partial z}\frac{\partial}{\partial z}(aT^4)+\frac{2\dot{\phi}}{\varpi}\frac{\partial}{\partial\varpi}(aT^4)\right] \quad (45)$$

11. Equation (44) contains terms in $\dot{r}$, $\dot{\varpi}$, and $\dot{\phi}$. If the motion of the star approximates throughout to one of pure rotation about the axis of z, then the terms in $\dot{\phi}$ are large in comparison with those in $\dot{r}$ and $\dot{\varpi}$.

Neglecting the small velocities $\dot{r}$ and $\dot{\varpi}$, the equation reduces to

$$\varpi\dot{\phi}^2=\frac{1}{\rho}\frac{\partial p}{\partial\varpi}-\frac{\partial V}{\partial\varpi} \quad . \quad . \quad . \quad . \quad (46)$$

while the similar equation in z reduces to

$$0=\frac{1}{\rho}\frac{\partial p}{\partial z}-\frac{\partial V}{\partial z} \quad . \quad . \quad . \quad . \quad (47)$$

On differentiating the two equations with respect to z, ϖ, and subtracting corresponding sides,

$$\frac{\partial}{\partial z}(\varpi\dot{\phi}^2)=\frac{\partial}{\partial z}\left(\frac{1}{\rho}\right)\frac{\partial p}{\partial\varpi}-\frac{\partial}{\partial\varpi}\left(\frac{1}{\rho}\right)\frac{\partial p}{\partial z}.$$

If p is a function of ρ, the right-hand member vanishes and we obtain Poincaré's theorem * that $\dot{\phi}$ is a function of ϖ only. But p will not in general be a function of ρ, and we proceed to consider the more general case.

12. The elimination of p from equations (46) and (47) gives

$$\varpi\frac{\partial}{\partial z}(\rho\dot{\phi}^2)=\frac{\partial\rho}{\partial\varpi}\frac{\partial V}{\partial z}-\frac{\partial V}{\partial\varpi}\frac{\partial\rho}{\partial z} \quad . \quad . \quad . \quad (48)$$

or, in r, θ co-ordinates

$$r^2\sin\theta\cos\theta\frac{\partial}{\partial r}(\rho\dot{\phi}^2)-r\sin^2\theta\frac{\partial}{\partial\theta}(\rho\dot{\phi}^2)=\frac{\partial\rho}{\partial\theta}\frac{\partial V}{\partial r}-\frac{\partial\rho}{\partial r}\frac{\partial V}{\partial\theta} \quad . \quad (49)$$

A star devoid of rotation arranges itself in spherical layers with a high central condensation of mass (*cf.* § 16 below). When the star is rotating the layers are no longer spherical, but the high central condensation will remain, provided the rotation is not excessive. The gravitational potential at any point of the star can be expanded in the form

$$V=V_0+V_2P_2(\cos\theta)+V_4P_4(\cos\theta)+ \ . \ . \ . \quad . \quad . \quad (50)$$

* *Les Hypothèses Cosmogoniques*, p. 28.

where V_0, V_2, V_4 . . . are functions of r only. Since $\nabla^2 V=-4\pi\rho$, the density can be expanded in the form

$$\rho=\rho_0+\rho_2 P_2(\cos\theta)+\rho_4 P_4(\cos\theta)+ \ldots \quad . \quad . \quad (51)$$

where

$$-4\pi\rho_n=\frac{1}{r^2}\frac{\partial}{\partial r}\left(r^2\frac{\partial V_n}{\partial r}\right)-n(n+1)V_n.$$

In the outer layers of a star V_2 will be small in comparison with V_0 as a consequence of the high central condensation of the star. Also V_4 will be small in comparison with V_2, and so on, and similarly as regards ρ_0, ρ_2, ρ_4, ... Thus in the outer layers of a star, the principal term on the right of equation (49) is

$$\left(\rho_2\frac{\partial V_0}{\partial r}-\frac{\partial\rho_0}{\partial r}V_2\right)\frac{\partial}{\partial\theta}P_2(\cos\theta).$$

The simplest solution of equation (49) is accordingly given by

$$r^2\frac{\partial}{\partial r}(\rho\dot\phi^2)=-3\left(\rho_2\frac{\partial V_0}{\partial r}-\frac{\partial\rho_0}{\partial r}V_2\right) \quad . \quad . \quad . \quad (52)$$

To obtain the most general value for $\rho\dot\phi^2$, equation (48) shows that we must add a function of ϖ, but this function must be zero, or otherwise the star would be rotating with infinite velocity at its surface at which $\rho=0$. Thus equation (52) gives the solution of equation (48) to a first approximation. To a second approximation, it is readily verified that the solution is of the form

$$\rho\dot\phi^2=\alpha+\beta P_2(\cos\theta),$$

where α and β are functions of r only.

13. As we shall soon see, the most important configurations are those in which the outer layers are approximately spherical, so that ρ is, to a first approximation, a function of r only. In this case $\dot\phi^2$ is approximately a function of r only in the outer layers. The remaining motion of the star will now be approximately radial at every point, so that

$$\frac{\dot\varpi}{\varpi}=\frac{\dot r}{r},$$

and equation (45) assumes the form

$$\frac{\rho}{r^2}\frac{\partial}{\partial t}(r^2\dot\phi)-\frac{\rho g}{C^2}\dot\phi=\frac{\kappa}{r^2}\frac{\partial}{\partial r}\left(r^2\frac{\partial\dot\phi}{\partial r}\right)+\frac{2\kappa}{r}\frac{\partial\dot\phi}{\partial r}+\frac{\partial\kappa}{\partial r}\frac{\partial\dot\phi}{\partial r}$$
$$+\frac{1}{5r^2}\frac{\partial}{\partial r}\left[\frac{r^2}{k\rho C}\frac{\partial}{\partial r}(aT^4)\right]+\frac{1}{5k\rho C}\left[\frac{\partial\dot\phi}{\partial r}\frac{\partial}{\partial r}(aT^4)+\frac{2\dot\phi}{r}\frac{\partial}{\partial r}(aT^4)\right].$$

Multiplying by r^4 and simplifying,

$$r^2\rho\left(\frac{\partial}{\partial t}-\frac{g}{C^2}\right)(r^2\dot\phi)=\frac{\partial}{\partial r}\left[\kappa r^4\frac{\partial\dot\phi}{\partial r}+\frac{r^4\dot\phi}{5k\rho C}\frac{\partial}{\partial r}(aT^4)\right] \quad . \quad . \quad (53)$$

This equation admits of a very simple interpretation. Using relation (37), with ρ replacing m, we find that the left-hand member is equal to $\frac{D}{Dt}(\rho r^4\dot{\phi})$ and so is proportional to the rate of increase of angular momentum in a shell of unit thickness. Thus the expression in square brackets on the right must be proportional to the flow of angular momentum across a sphere of radius r; clearly the first term represents the transfer produced by viscosity, including radiative viscosity, while the second term represents the transfer produced by the star's outpouring of radiant energy. The flow of energy per unit area at any point, H, is given by

$$H=-\frac{1}{3k\rho C}\frac{\partial}{\partial r}(aT^4) \quad . \quad . \quad . \quad . \quad (54)$$

so that the equation can be written in the form

$$\frac{D}{Dt}(\rho r^4\dot{\phi})=\frac{\partial}{\partial r}\left[\kappa r^4\frac{\partial\dot{\phi}}{\partial r}-\tfrac{3}{5}Hr^4\dot{\phi}\right] \quad . \quad . \quad . \quad (55)$$

in which the physical interpretation becomes obvious.

The first paper showed that viscosity was not sufficiently potent to establish a steady state in the central regions of the star. In the outer layers conditions are different; ρ is small and its presence on the left-hand of equation (53) shows that $\dot{\phi}$ can change rapidly until a steady state is attained. This steady state is one in which the flow of momentum across every sphere concentric with the centre of the star is the same; on account of their small mass, the star's outer layers do not exercise any appreciable fly-wheel action, merely transferring momentum as they receive it. The equation expressing this steady state is

$$\kappa r^4\frac{\partial\dot{\phi}}{\partial r}-\tfrac{3}{5}Hr^4\dot{\phi}=\text{cons}=-\tfrac{3}{5}H_0r_0^4\omega \quad . \quad . \quad . \quad (56)$$

the constant on the right being determined from conditions at the surface of the star, at which we are supposing that H, r, $\dot{\phi}$ have the values H_0, r_0, ω.

Equation (56) is a linear differential equation of the first order, so that its complete solution can be written down immediately. The solution is, however, too general to be of much physical interest except in special cases.

14. In the outermost layers of all of the star, κ is very small, so that the first term on the left-hand of equation (56) may be neglected, and $Hr^4\dot{\phi}$ becomes constant. Since Hr^2 is constant throughout these outermost layers, $r\dot{\phi}^2$ must also be constant. Thus $\dot{\phi}$ varies as $1/r^2$; the rotation increases as we pass inwards, varying inversely as the square of the distance from the centre. The angular velocity is now so arranged near the surface that radial convection currents do not disturb it; convected matter arrives at any spherical surface with precisely the angular velocity appropriate to that surface.

Further inside the star the value of κ cannot be neglected in this

way. When κ is appreciable, but ρ is still treated as small, so that Hr^2 is constant, equation (56) provides the relation

$$\tfrac{3}{5}H_0 r_0^2(r^2\dot{\phi}-r_0^2\omega)=\kappa r^4\frac{\partial\dot{\phi}}{\partial r},$$

and on inserting on the right the approximate value $\dot{\phi}=r_0^2\omega/r^2$, this gives

$$\dot{\phi}=\omega\left[\frac{r_0^2}{r^2}-\frac{10\kappa}{3H_0 r}\right] \quad . \quad . \quad . \quad . \quad (57)$$

In an ideal star of very great mass, viscosity is wholly radiative, so that κ reduces to κ_R given by equation (32). On inserting this value for κ and the value of H from equation (54), equation (56) becomes readily integrable, the integral being

$$\dot{\phi}=\omega\left[\frac{r_0^2}{r^2}-\frac{2r_0^2}{T^6}\int_r^{r_0}\frac{T^6dr}{r^3}\right] \quad . \quad . \quad . \quad (58)$$

This completes the mathematical analysis.

Summary and Discussion.

15. We have first (§§ 2–9) obtained the general equations of internal motion of a star, account being taken of radiative as well as of gaseous viscosity (a previous investigation having shown that the former will generally preponderate over the latter), as also of the disturbance of momentum caused by the flow of radiation through a star. The equations so obtained are then used to examine the internal motions of a star in which the rotation is all about the same axis.

Viscosity has previously been found inadequate to produce a steady state in the central regions of a star. The present investigation shows conditions to be very different in the outer layers ; here a steady state is not only possible, but is rapidly attained. On account of their very low density, these outer layers exercise very little " fly-wheel " action, and merely transmit onwards the momentum they receive. They rapidly reach a steady state in which the angular velocity of every ring is determined by the condition that it passes forward just as much angular momentum as it receives from behind.

We have found that, to a first approximation, the angular velocity of any ring of stellar matter surrounding the axis of rotation depends only on its distance from the centre of the star. Thus the rotation of the star is by concentric spherical shells, each shell rotating as a rigid body.

In the outermost layers of the star the angular velocity $\dot{\phi}$ has been found to vary as $1/r^2$, where r is the distance from the centre of the star. As we pass to deeper layers the value of $r^2\dot{\phi}$ falls off. The coefficient of viscosity κ becomes very small at the star's surface, and so long as κ^2 can be neglected the value of $\dot{\phi}$ is given by equation (57) ; if radiative viscosity alone is taken into account, $\dot{\phi}$ is given by equation (58) in which κ^2 is not neglected.

16. If a star is supposed to be made throughout of uniform material which generates energy at a uniform rate, I have shown * that λ, the

* *M.N.*, **85** (1925), p. 196.

ratio of gas-pressure to pressure of radiation, is proportional to $T^{\frac{1}{4}}$ in a star of very small mass, and to $T^{\frac{1}{2}}$ in an ideal star of very great mass. Thus a star of very small mass will be arranged like a sphere of gas in adiabatic equilibrium with γ, the ratio of the specific heats, equal to 1·308, while a star of very great mass will be arranged like a sphere in adiabatic equilibrium with $\gamma = 1{\cdot}286$. When the star rotates these arrangements will still prevail approximately, so long as the rotation is not rapid.

In fig. 1 the two inner curves show the variations of density and temperature in a star arranged according to the intermediate value

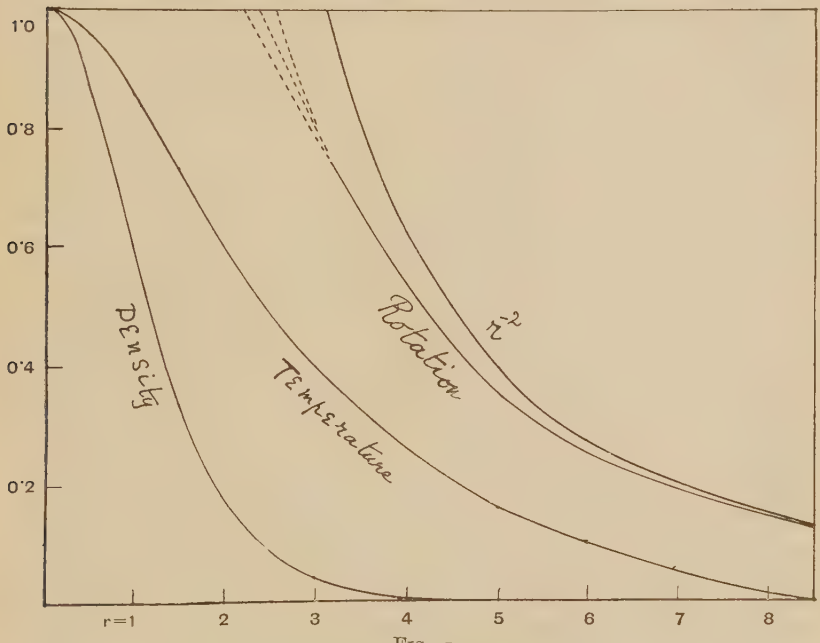

FIG. 1.

$\gamma = 1{\cdot}300$. The high degree of central condensation of mass, as shown by the density curve, is noteworthy. At a distance $\frac{1}{2}r_0$ from the centre of the star, the density has already fallen to 0·0086 times the central density; a sphere of radius $\frac{1}{2}r_0$ encloses 94 per cent. of the total mass of the star within one-eighth of the star's volume. Even a sphere of radius $\frac{1}{3}r_0$ (volume $\frac{1}{27}$ times volume of star) encloses 74 per cent. of the star's mass, the density at its surface being only 0·06 times the central density.

17. The curve marked "rotation" in fig. 1 gives the angular velocity $\dot{\phi}$ as calculated from equation (58), but it is clear that for all practical purposes the curve $1/r^2$ gives an adequate approximation to the angular velocity. The simple $1/r^2$ curve gives the arrangement of angular velocity known as "convective," in which matter conveyed by a radial convection current reaches any distance from the centre with its

angular velocity automatically adjusted, by the principle of conservation of angular momentum, to the value appropriate to that distance from the centre. We can interpret it also as being the arrangement such that radiation can traverse the star without any interchange of momentum occurring on balance between it and the matter of the star If the outer surface of a star were rotating faster than required by the $1/r^2$ law, it would have to impart a tangential velocity to the radiation passing through it, and this would slow down the rotation of these outer layers until they conformed to the $1/r^2$ law.

Viscosity tends to disturb the $1/r^2$ arrangement, trying always to equalise the angular velocity throughout the star. The compromise which is reached is shown by the "rotation" curve in fig. 1, which necessarily represents more uniform rotation than that given by the $1/r^2$ curve. Since $r^2\dot{\phi}$ falls off as we pass into the interior of a star, matter brought to the surface of a star by convection ought to show some lag relative to the velocity of the surface.

In the dense central regions of the star the rotation-law fails entirely; the rotation here depends on the past history of the star. The law may be expected to give a tolerable approximation down to a sphere of radius about $\frac{1}{3}r_0$, so that such a sphere ought to rotate in about one-ninth of the period of the star's surface. A sphere of radius $\frac{1}{3}r_0$ in the sun ought to rotate in less than 3 days, except that we must admit some uncertainty as to whether the sun has had time to settle down thoroughly since its recent ejection of planets. In general the outer layers of stars are mere veils concealing the more energetic rotations within. The slowness of their rotation combined with the high central condensation of the star must result in nearly all stellar surfaces being approximately spherical.

The stream of radiation which leaves a star not only carries off angular momentum with it, but generally lessens the angular momentum per unit mass of the star. Arguments which assume constancy of angular momentum, such as the famous argument of Babinet on the origin of the solar system, can no longer claim any validity.

18. Finally, the law that the rotation $\dot{\phi}$ is the same for all points at the same distance from the star's centre is only a first, and somewhat rough, approximation. To a better approximation the rotation in any sphere of a given radius r is of the form

$$\dot{\phi}=\mathrm{A}+\mathrm{B}\mathrm{P}_2(\cos\theta),$$

where A, B are constant, and P_2 is the second zonal harmonic. In terms of the latitude λ this becomes

$$\dot{\phi}=a+b\sin^2\lambda,$$

which is the observed law of rotation for the solar surface. The physical interpretation of this law which is involved in our theory is that the more rapidly rotating inner layers are of spheroidal shape; these come nearest to the star's surface at its equator, and their drag results in the observed equatorial acceleration.

On the Possibility of the Emission of High-speed Atoms from the Sun and Stars. By E. A. Milne, F.R.S.

1. *Radiation-Pressure and the Doppler Effect.*—In some recent papers * I have investigated the problem of the equilibrium of atoms at high levels in the solar or any stellar atmosphere under radiation-pressure. Such a study is an essential preliminary to the consideration of another problem, in some ways more interesting, namely, that of the expulsion of atoms under radiation-pressure. This problem has been considered recently by M. C. Johnson † and R. K. Sur.‡ The object of the present note is to point out a feature of escape under radiation-pressure which does not seem to have been previously noticed, and to trace its consequences.

Briefly put, the new feature is this. When an atom is being expelled under radiation-pressure, radiation-pressure exceeds gravity, and the atom is being accelerated away from the star. Owing to the Doppler effect, the increasing outward velocity causes the atom to absorb in a wave-length which is steadily shortening, in a frame of reference fixed relative to the star. The region of the spectrum in which the atom absorbs moves towards the violet. If the atom is accompanied with a sufficiently large crowd of other atoms, the absorption line they cause will move off towards the violet. But if the atom is solitary, or accompanied by a relatively small number of atoms, the absorption produced will not be sufficient to form an appreciable absorption line. The atom or atoms will then move out into the violet wing of the absorption line from which they started, and may even climb right out of the absorption line into the adjacent continuous spectrum. To some extent in the wing, and most emphatically in the continuous spectrum, they will be exposed to much fiercer radiation than they were in the absorption line in which they started. They will therefore be subjected to an increasing outward acceleration during their progress through the wing of the absorption line, until, arrived in the continuous spectrum, they possess an acceleration far above that with which they began.

This will continue in general until the inverse square law eventually reduces the acceleration to zero as the atoms move further and further in space from the parent star, and the atoms will get right outside the gravitational field of the star with a definite, very large, limiting velocity. The rough estimate made below indicates that the limiting velocity acquired will be of the order of 1600 km. sec.$^{-1}$ in the case of the sun, and of a similar order of magnitude for the stars in general.

We have said that this steady movement to the violet will in general

* "An Astrophysical Determination of the Average Life of an Excited Calcium Atom," *M.N.*, **84**, 354, 1924; "The Equilibrium of the Calcium Chromosphere," *M.N.*, **85**, 111, 1924; "The Equilibrium . . ., Second Paper," *M.N.*, **86**, 8, 1925.

† "Emission of Hydrogen and Helium from a Star by Radiation-Pressure," *M.N.*, **85**, 813, 1925; "Velocities of Ions under Radiation-Pressure," *M.N.*, **86**, 300, 1926.

‡ "On Selective Radiation Pressure and the Accelerated Motion of Ca^+ Vapour in Eruptive Prominences," *Astrophys. Journ.*, **63**, 111, 1926.

continue until the inverse square effect comes in. Exceptions will occur when the absorption line from which the atoms start is bordered, in the stellar spectrum, by another absorption line close to it on the violet side. In their progress across the continuous spectrum the accelerated atoms may "tumble into" the neighbouring absorption line. This will cause a sudden drop in the acceleration. If the neighbouring line cuts sufficiently deeply into the continuous spectrum, it may even reduce the acceleration to zero, radiation-pressure just balancing gravity once again. But it cannot make it negative. For if it did, the velocity would begin to be reduced, and the atoms would begin to progress redwards across the spectrum, thus returning to a region

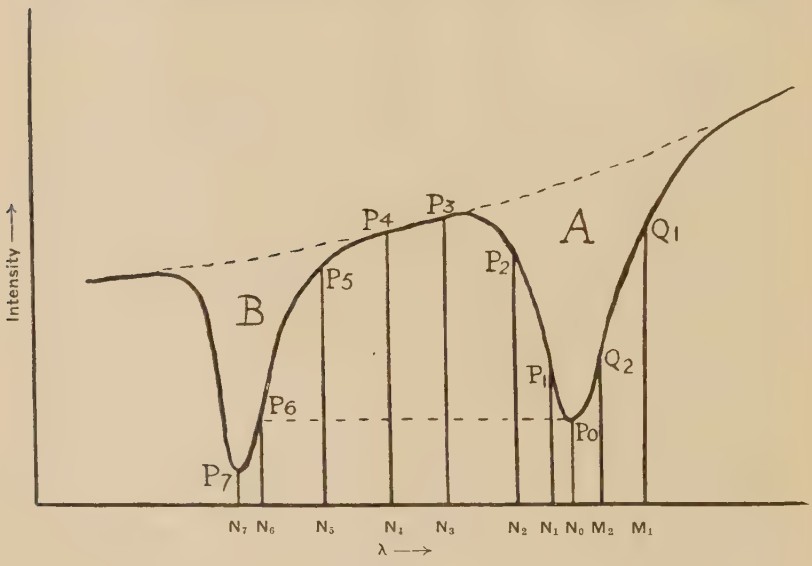

FIG. 1.

in which the acceleration is positive again. It is clear, in fact, that once the outward acceleration is reduced to zero, nothing further can happen. The atoms will stay in the part of the spectrum they happen to be in, and will go on escaping with uniform velocity. If, however, the neighbouring line is not too deep, the atoms may climb out of it on the blue side just as they did out of their original line, and continue moving across the continuous spectrum.

2. *Diagrammatic Representation.*—This sequence of events is best followed by means of a diagram showing the spectral energy curve of the star in the neighbourhood of an absorption line. Such a curve, showing two lines, is shown in fig. 1. Their wave-lengths correspond to the abscissæ marked N_0 and N_7. We will call the lines A and B respectively. Line A is supposed to be a chromospheric or high-level line. The residual intensity in A, namely, the ordinate P_0N_0 in the diagram, is supposed to be just sufficient to support an atom at rest

against gravity. (In the case where two stationary states alone are concerned, the residual intensity F_ν has been shown in the papers cited to be given by the formula

$$F_\nu = \frac{8\nu^2\tau mg}{c} \cdot \frac{q_1}{q_2}$$

where the symbols have their familiar meanings.)

Suppose now we fix attention on a particular atom, at rest. It will not remain at rest. Random fluctuations in the rates of absorption and emission of quanta, random fluctuations in the directions of emission of quanta, and random encounters with other atoms will from time to time give it small inward or outward velocities. There will, in fact, be a permanent velocity-distribution amongst the high-level atoms, analogous to the Maxwellian velocity-distribution originated amongst the molecules of a gas by their collisions. It can be shown, following Einstein, that atoms moving with sufficiently small velocities (" thermal " velocities *) undergo a slight reduction or increase in the radiation-pressure acting on them, according as they are receding from or approaching the source of radiation—the dilution effect of " running away from the radiation," and its opposite. This ensures a steady state.† The nature of the resulting velocity distribution is intimately connected with the contour of the absorption line in the immediate neighbourhood of its centre, more precisely with the value of $(\partial I_\lambda/\partial\lambda)_{\lambda=\lambda_0}$, in an obvious notation. The main contour of the absorption line has probably originated in the reversing layer, in a way which has hitherto baffled explanation.

So much for the small fluctuations of velocity which every atom undergoes. But now suppose that by an exceptional succession of absorptions or collisions, or for some other reason, an atom acquires an outward velocity which is large compared with the usual velocity of thermal agitation, though small compared with the velocities that will subsequently be mentioned. A velocity of 5 or 10 km. sec.$^{-1}$ would probably be adequate. The atom will then begin to absorb a wave-length corresponding to some point such as N_1 in the diagram. The corresponding intensity-ordinate is N_1P_1, which is well in the wing of the line. Now the ordinate N_0P_0 is the measure of an intensity just sufficient to support the atom against gravity. Since $N_1P_1 > N_0P_0$, the atom will now be accelerated outwards. Its acceleration will in fact be

$$\frac{N_1P_1 - N_0P_0}{N_0P_0} g,$$

approximately.‡ Hence the outward velocity will increase. The wave-

* A calcium atom in a gas at 5000° has an average thermal velocity of 1·76 km. sec.$^{-1}$, corresponding to about 0·02 A for the K line. The average component in the line of sight is about 1·0 km. sec.$^{-1}$, or about 0·01 A.

† This question of the steady-state velocity-distribution in the upper chromosphere is a somewhat intricate one, and will be made the subject of a future communication.

‡ This expression requires correction by a term of the order of v/c, to allow for the effect of the atom " running away from the radiation." But the correction is of negligible importance in this connection.

length in which the atom absorbs will move off still further to the violet, to some point such as N_2. Here the ordinate representing the intensity, N_2P_2, is still greater, and the atom is accelerated still more. At N_3 it has climbed out of the line and is exposed to the full brunt of the continuous spectrum. The wave-length continues moving to the violet. Whether the acceleration now increases or decreases depends on whether we are to the red side or the blue side of the maximum of the whole spectrum. The diagram shows it decreasing, but in any case the changes in intensity due to this are small compared with the relatively abrupt change occurring as the atom climbs out of its absorption line.

By the time the representative point gets to N_4, the inverse square law may have had scope to assert itself, and the velocity may be tending to a limit. If not, the representative point may reach the next absorption line, B. If this contains, in its redward wing, an ordinate N_6P_6 equal to N_0P_0, the atom will there have a radiation-pressure just equal to gravity, and the representative point will remain at N_6, the atom having the corresponding velocity. If not, the atom will climb out of this line also, and we have to consider the spectrum to the violet side of B.

The sequence of events just described may seem at first sight fantastic, but I can see nothing in it not solidly based on established physical principles. Once the atom has left home on the violet side, an increasing acceleration is inevitable. It must move faster and faster until supplies fail in virtue of the inverse square law cutting down the radiation. It finishes up as a high-speed atom moving with uniform velocity, gravitationally entirely free from the parent star. The prodigal never returns.

The effect is a unilateral one. Suppose an atom at rest in the chromosphere becomes accidentally endowed with an appreciable *downward* velocity. Its representative point will be displaced to the red, to some point such as M_1, in the redward wing of the absorption line. The ordinate here, M_1Q_1, exceeds N_0P_0, and consequently the atom will be exposed to a radiation-pressure exceeding gravity. The consequential upward acceleration will begin to destroy the downward velocity, and the representative point will move towards the blue. At M_2 the process will still be going on. The upward acceleration is decreasing, but remains positive so long as the atom has an appreciable downward velocity. Eventually the representative point returns to N_0. The wandering atom is, so to speak, gently deposited at the foot of its own absorption line, once again at rest.

Summarising, atoms which get a start in an outward direction are subjected to an increasing outward acceleration, finally leaving the star with a large limiting velocity; atoms which get a start in an inward direction are gradually arrested.

3. *Numerical Estimate.*—We proceed to estimate the limiting velocity which an outward-moving atom will acquire. An exact calculation becomes possible only when the precise contour of the absorption line, and the contours of the neighbouring absorption lines on the high-frequency side, are known in detail. To simplify the calculation and concentrate on essentials we shall suppose the original absorption line

to have the V-shaped contour shown in fig. 2. We suppose further the adjacent continuous spectrum to be of constant intensity, and we ignore the possible presence of neighbouring lines. It will readily be seen that, however roughly, the calculation which follows gives the order of magnitude of the limiting velocity communicated to the atom.

Let λ_0 be the wave-length of the centre of the absorption line, I_0 the residual intensity in the centre of the line, I_1 the intensity of the adjacent continuous spectrum. Let $\delta\lambda$ be the half-width of the V-depression formed by the line in the continuous spectrum, so that $\lambda_0 \pm \delta\lambda$ are the

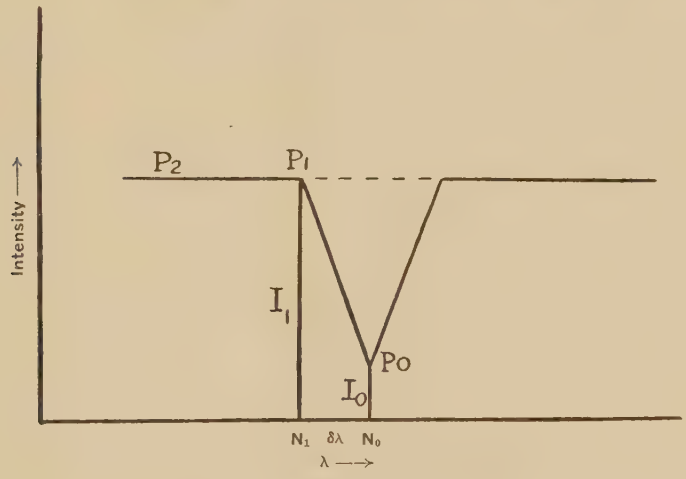

FIG. 2.

boundary wave-lengths of the depression. The intensity I at a point in the violet half of the line at wave-length λ is given by

$$I - I_0 = (I_1 - I_0)\frac{\lambda_0 - \lambda}{\delta\lambda} \quad . \quad . \quad . \quad . \quad (1)$$

The velocity v corresponding to λ is given by

$$v/c = (\lambda_0 - \lambda)/\lambda_0 \quad . \quad . \quad . \quad . \quad (2)$$

The outward acceleration at λ_0 is zero, radiation-pressure and gravity just balancing. At λ, the outward acceleration is

$$g\frac{I - I_0}{I_0},$$

for an atom not far from the surface of the star.* If a is the radius of the

* The calculation ignores the varying Doppler effect for the radiation coming from different parts of the star's disc. The necessary correction is estimated in a paper to be communicated at the June meeting of the Society.

star, the acceleration of an atom at distance r from the centre of the star is given by

$$\frac{d^2r}{dt^2}=g\frac{a^2}{r^2}\frac{I-I_0}{I_0}, \quad . \quad . \quad . \quad . \quad (3)$$

in virtue of the inverse square law.

Eliminating I and λ by means of (1) and (2), and writing $\dot{r}$ for v, we find

$$\ddot{r}=\dot{r}\frac{a^2g}{r^2}\frac{I_1-I_0}{I_0}\frac{\lambda_0}{c\delta\lambda}.$$

Now put

$$V=c\delta\lambda/\lambda_0,$$

so that V is the Doppler velocity corresponding to the half-width of the line. Then

$$\ddot{r}=\frac{I_1-I_0}{I_0}\frac{a^2g}{V}\frac{\dot{r}}{r^2} \quad . \quad . \quad . \quad . \quad (4)$$

We integrate this, assuming the atom has initially an outward velocity v_0. The result is

$$v-v_0=\frac{I_1-I_0}{I_0}\frac{ag}{V}\left(1-\frac{a}{r}\right) \quad . \quad . \quad . \quad (5)$$

Now let r_1 be the distance at which the representative point reaches the point P_1 in fig. 2, *i.e.* the distance at which the atom acquires a velocity equal to the half-width velocity V. Equation (5) then gives

$$V-v_0=\frac{I_1-I_0}{I_0}\frac{ag}{V}\left(1-\frac{a}{r_1}\right) \quad . \quad . \quad . \quad (6)$$

If V_∞ is the velocity of escape from the star under gravity only (parabolic velocity), we have

$$\tfrac{1}{2}V_\infty{}^2=ag,$$

whence (6) may be written in the form

$$2V(V-v_0)=\frac{I_1-I_0}{I_0}V_\infty{}^2\left(1-\frac{a}{r_1}\right) \quad . \quad . \quad . \quad (7)$$

After P_1, the atom will be accelerated according to the law

$$\ddot{r}=\frac{I_1-I_0}{I_0}\frac{ga^2}{r^2},$$

which gives, on integration,

$$v^2-V^2=\frac{I_1-I_0}{I_0}V_\infty{}^2\left(\frac{a}{r_1}-\frac{a}{r}\right) \quad . \quad . \quad . \quad (8)$$

Adding (7) and (8) to eliminate r_1 we have

$$v^2+V(V-2v_0)=\frac{I_1-I_0}{I_0}V_\infty{}^2\left(1-\frac{a}{r}\right).$$

Hence the limiting velocity v_∞ acquired as $r\to\infty$ is given by

$$v_\infty{}^2=V_\infty{}^2\left[\frac{I_1-I_0}{I_0}-\frac{V(V-2v_0)}{V_\infty{}^2}\right] \quad . \quad . \quad . \quad (9)$$

From what has been said, we may neglect v_0 in comparison with V. Thus finally we have

$$v_\infty^2 = V_\infty^2\left[\frac{I_1-I_0}{I_0} - \frac{V^2}{V_\infty^2}\right] \quad . \quad . \quad . \quad (10)$$

Let us apply this to Ca^+ atoms on the sun. For the sun we have $V_\infty = 615$ km. sec.$^{-1}$, the same of course for all atoms. The intensity-ratio usually adopted for the K line of Ca^+ gives $I_0/I_1 = 1/9$. The K line is very wide, and the value to take for the width is uncertain. Schwarzschild's measured contour of the line indicates that we may take $\delta\lambda = 8$Å. This gives $V = 611$ km. sec.$^{-1}$—a value as it happens practically identical with V_∞.* Inserting these values, we find

$$\begin{aligned} v_\infty^2 &= 7V_\infty^2, \\ v_\infty &= 1630 \text{ km. sec.}^{-1}, \\ &= 1{\cdot}63\times10^8 \text{ cm. sec.}^{-1}. \end{aligned}$$

This velocity corresponds to a Doppler shift of about 22A. It may be noticed in passing that from (7) we have $a/r_1 = \frac{3}{4}$, so that the atom just gets clear of the absorption line it started from when it has traversed a distance equal to $\frac{1}{3}$ of a solar radius, or 233,000 kms.

A result of the same order of magnitude will be given for most Fraunhofer lines. In fact most lines being considerably narrower than K, V will be smaller, and v_∞ accordingly greater. This is simply the physical fact that the narrower the line, the quicker the atom climbs out of it, and the sooner it is exposed to the full brunt of the radiation. An upper limit (for a given intensity ratio I_0/I_1) is obtained by taking $V = 0$. This gives $v_\infty = 1740$ km. sec.$^{-1}$.

For Capella, we find a radius of $9{\cdot}16\times10^{11}$ cms., assuming Eddington's values, namely, a mass 4·2 ⊙ and a mean density 0·0026. From this we find $V_\infty = 350$ km. sec. Hence the values of v_∞ will be something over half the value found for the sun.

4. *Order of Magnitude for the Stars in general.*—Closely similar values will be given by all stars. It is a peculiar circumstance, to which I have previously drawn attention,† that for stars built on Eddington's model, the value of the gravitational potential at the surface of the star has a minimum within the observed range of stellar masses. This implies that the velocity of escape, V_∞, which is proportional to the square root of the gravitational potential, has a minimum also, and hence that it does not vary greatly within the existing range of stellar masses. It seems worth giving the proof of this, using Eddington's revised theory. In a notation which Eddington's work has made standard, we have ‡

$$\begin{aligned} r^2T_e^4 &\propto L \propto M(1-\beta)/k, \\ k &\propto \rho_c/\mu T_c^{\frac{1}{2}}, \\ T_c &\propto \mu\beta M/r, \\ \rho_c &\propto M/r^3, \end{aligned}$$

* It is somewhat remarkable that the half-width of the strongest line in the sun corresponds to a velocity equal to the velocity of escape from solar gravity.

† *Trans. Camb. Phil. Soc.*, **22**, 507, 1923.

‡ Eddington, *M.N.*, **83**, 107, 1922. Here r denotes the star's radius.

and, in addition, $$V_\infty^2 \propto M/r.$$

Combining these and making free use of Eddington's quartic equation

$$1-\beta \propto M^2\mu^4\beta^4,$$

we find

$$V_\infty \propto T_e^{\frac{1}{2}}\mu^{-\frac{1}{2}}(1-\beta)^{-\frac{3}{8}}M^{\frac{3}{10}} \quad . \quad . \quad . \quad (10)$$

This shows that $V_\infty \propto M^{\frac{3}{10}}$ for very large masses, and that $V_\infty \propto M^{-\frac{3}{5}}$ for very small masses. Hence V_∞ has a minimum in between. From (10) we find

$$\frac{1}{V_\infty}\frac{dV_\infty}{d\beta}=\frac{3}{10}\frac{2\beta-1}{\beta(1-\beta)}. \quad . \quad . \quad . \quad (11)$$

showing that the minimum occurs for $\beta=\frac{1}{2}$, *i.e.* $M=11{\cdot}5\ \odot$. (According to (10) the principal cause of variation in V_∞ is T_e.)

We thus see that for the majority of stars V_∞ will be of the order of a few hundred kms. sec.$^{-1}$, and v_∞ will be from 2 to 3 times this for absorption lines with an intensity ratio I_0/I_1 of the order of $\frac{1}{10}$. The calculation of v_∞ depends, in fact, on surprisingly few constants. On the theory we have sketched it seems inevitable that the space in the neighbourhood of a star should be traversed by at least some atoms moving outwards with a velocity of between 1000 and 2000 kms. sec.$^{-1}$.

5. *Application to Novæ.*—Such a velocity reminds one immediately of the order of magnitude of the line-displacements observed in the spectra of Novæ. A shift to the violet of the order of 1500–1800 kms. sec.$^{-1}$ for absorption lines is often observed.* Now the *origin* of the outward motion in a Nova outburst is obvious; no explosion is required; a sudden brightening of the whole photosphere must inevitably result in the expulsion, under radiation-pressure, of atoms suitably provided with absorption lines. To this extent this is different from the origin we have suggested for casual expulsions from normal stars. But once the expulsion of atoms has started, the same sequence of phenomena will occur. The first shower of atoms to go off (forming a spherical shell concentric with the star) will be rapidly accelerated. The wave-length in which they absorb will move across the spectrum. Ultimately they will acquire a certain limiting velocity. After them, and following close on their heels, we may consider a second shower (really of course shading continuously into the first). This second shower will ultimately attain the same limiting velocity as the first, but in the interval it will always be moving slower, and consequently absorbing a little to the red. Behind this again there will be a third, and so on. Each shower by itself may be insufficient to cause appreciable absorption of the continuous spectrum behind, but all the showers will eventually accumulate in the same part of the spectrum. Thus we may expect a displaced absorption line to develop in the position corresponding to the limiting velocity as the atoms of the first shower are recruited by later arrivals (arrivals in *velocity*, of course, not in space).

Such a process would account for the appearance of an absorption line in a displaced position without its having been observed to traverse

* *Cf.* Stratton, *Astronomical Physics* (1925), p. 146.

the intermediate wave-lengths. For until the atoms have all acquired the same (limiting) velocity, and all absorb in the same wave-length, their absorptions will be spread out over a considerable range of wave-lengths, and as such they might be insufficient to give rise to any definite absorption line.

As the shell of atoms moved further and further away, with its limiting velocity, its absorbing power would gradually weaken, owing to the inverse square law, unless the star continued to send reinforcements. Thus the displaced absorption lines would be expected to fade away ultimately.

It is not easy to say whether our calculation of v_∞ for the sun and Capella may be expected to have much relation with the v_∞ for a Nova. One would want to know more about the pre-Nova state. But it seems likely in any case that v_∞ will be some not too large multiple of V_∞—for example, if a star suddenly brightened 5 magnitudes (100-fold) the limiting velocity would be about 10 V_∞. In this calculation V_∞ is to be calculated for the radius of the star in its pre-Nova state. It is true that the extent of brightening is often much greater than 5 magnitudes, but we are ignorant of the value to take for V_∞. However, assuming as above that V_∞ has the same order of magnitude as for normal stars, the difficulty is rather why the v_∞ observed is not much bigger than it is. The explanation probably is that the atoms do not climb completely out of the absorption line, but are driven off so abundantly that to some extent the absorption line moves in step with them. This would lead to a lower value of v_∞.

6. *The Cause of Aurorœ and Magnetic Storms.*—We have seen that from time to time high-level atoms in the solar atmosphere will be projected by radiation-pressure so as to attain a limiting velocity of about $1{\cdot}6\times10^8$ cms. sec.$^{-1}$. With this limiting velocity they will reach the earth's atmosphere.

Amongst such atoms we may expect those of Ca^+, H, He, Fe, Ti^+, Sr^+, Mg—any atom, in fact, which shows evidence of being supported by radiation-pressure in the chromosphere. A condition for this seems to be that the atom should possess a normal state, or failing that a metastable state, capable of absorbing a frequency in the solar range of appreciable intensities. The case of Ca^+ is sufficiently well known. Hydrogen, as suggested by Russell and Compton, is probably executing transitions between the metastable 2_1 orbits and the 3_2 orbits when absorbing and emitting the Hα line at high levels. Helium is probably supported at high levels in virtue of the metastable 1σ level belonging to the "orthohelium" set of terms. In these and other cases, the conditions favourable for high-level support are just the conditions which will render the atom subject to an increasing outward acceleration if it gets a start. It absorbs, the next emission returns it to its normal or metastable state, and then it is once again in a condition to absorb. Another condition is that the atom in the state in question must not be too readily ionisable—it must not readily lose its series electron.

The calculation of the order of magnitude of the limiting velocity does not depend, it will be noticed, on the mass of the atom. But the exact value of the limiting velocity will depend on the proximity of

deep Fraunhofer lines to the line from which the atom started. Until a detailed energy-curve of the solar spectrum is available, showing the contours of absorption lines, it does not seem possible to make any detailed calculations. But we see the possibility of there being different velocity-showers. An atom which gets trapped in a neighbouring Fraunhofer line will acquire a smaller limiting velocity than one not so trapped. Also an atom whose own line is in a part of the spectrum where the intensity is increasing towards the blue (*i.e.* on the red side of the maximum) will be subjected to a greater acceleration, eventually, than one whose line is in a part of the spectrum where the intensity is decreasing to the blue (*i.e.* on the blue side of the maximum). Thus whilst all atoms getting away will acquire limiting velocities of the same order of magnitude, there will be different velocities for the different atomic species.

The emission of charged particles from the sun at high speeds has been suggested by various writers * as the origin of auroræ and magnetic storms. It was first thought that the particles might be β-particles or α-particles emitted in virtue of radio-activity on the sun. It was shown by Lindemann, however, that the amount of radio-activity thus required was incredibly large, and he suggested instead that the stream of particles might be a cloud of ionised atoms, electrostatically neutral in the mass, projected from the sun by radiation-pressure. If the cloud is neutral, this removes the difficulty that a stream of particles entirely of one sign would disperse laterally in virtue of the mutual electrostatic repulsions.

Lindemann pointed to the velocities observed in solar prominences, and adopted a velocity of 8×10^7 cms. sec.$^{-1}$ on this evidence. He also attempted to show that this would in fact be the order of magnitude of the velocity acquired under radiation-pressure, but the method of calculation he adopted would now scarcely be considered as in accordance with what is known of atomic theory. Further, he ignored the effect of the inverse square dilution of radiation, and he did not consider the consequences of the Doppler effect, to which attention has been directed in the present paper. He estimated the limiting velocity by supposing that a certain definite number of quanta would be absorbed and emitted before the atom became ionised. But the pressure of radiation on an atom depends on the *rate* at which the atom can deal with quanta—a quantity connected with the fundamental atomic constant τ. In the present paper this rate has been evaluated by supposing that for a high-level atom at rest exposed to the residual intensity in a Fraunhofer line, the rate of absorption of momentum is just sufficient to balance the downward pull of gravity. However, the velocity adopted by Lindemann, 8×10^7 cms. sec.$^{-1}$, is sufficiently close to that calculated here, namely $1{\cdot}6\times10^8$ cms. sec.$^{-1}$, to render the consequences at the earth end of the atoms' trajectory of the same general nature as in Lindemann's theory.

7. *Penetrating Power.*—We will first consider the ability of these high-speed atoms to penetrate the earth's atmosphere. In Lindemann's

* In particular, see Chapman, *Trans. Camb. Phil. Soc.*, **22**, No. 16, 1919; and Lindemann, *Phil. Mag.*, **38**, 670, 1919.

theory the ionised atoms were hydrogen nuclei, and he had some difficulty in showing that such particles, moving only at 8×10^7 cms. sec.$^{-1}$, would be able to penetrate the earth's atmosphere down to the lower level of auroræ; that is to say, to within 80-100 kms. of the earth's surface. This difficulty is now considerably lessened, if not entirely removed.

From the general theory of the chromosphere and our knowledge of the high-level atoms in the sun, the atoms we should expect to be driven off most plentifully by the process here considered would be Ca^+ atoms. Any high-level atom might be driven off, but it happens to be possible to make a fairly exact estimate of the penetrating power of a Ca^+ atom moving with a velocity of $1\cdot6\times10^8$ cms. sec.$^{-1}$, and we shall accordingly consider this case in detail.

The atomic weight of calcium is 40. An α-particle from radium has an initial velocity of $1\cdot6\times10^9$ cms. sec^{-1}, and its atomic weight is 4. Thus the Ca^+ atom moves with $\frac{1}{10}$ of the velocity but has 10 times the mass. It therefore has almost exactly the momentum of an α-particle. This suggests consideration of the collisions of α-particles with heavy nuclei. C. T. R. Wilson, Blackett, and others, by the cloud-condensation method originated by C. T. R. Wilson, have obtained photographs showing the collisions of α-particles with heavy nuclei. In such a collision, which gives a " forked track " in the photograph, the momentum of the incoming α-particle is in part communicated to the heavy nucleus. By measurement of the angles between the three tracks concerned, the velocity communicated to the heavy nucleus can be calculated, and measurement of the length of the track of the heavy nucleus gives directly its range. We have therefore by direct observation the range of a heavy nucleus moving initially with a momentum of the order of magnitude of that of the α-particle.*

Collisions of α-particles with calcium nuclei have not of course been observed. But we may avail ourselves of the accidental circumstance that the atomic weight of calcium is practically the same as that of argon, collisions in which have been observed. Mr. Blackett has kindly informed me that his observations (including some unpublished ones) indicate that the range of an argon atom is proportional to its velocity, and that the equivalent air-range at N.T.P. of an argon atom moving with a velocity of $1\cdot6\times10^8$ cms. sec.$^{-1}$ would be about 0·16 cm. Mr. Blackett has suggested to me that a Ca^+ atom might have a slightly shorter range, for reasons which need not be gone into here, but it is clear that as regards order of magnitude, and indeed to a fairly close approximation, we may take it that a Ca^+ atom endowed with a speed of $1\cdot6\times10^8$ cms. sec.$^{-1}$ would have an equivalent air-range of about 0·15 cm.

Lindemann estimated the air-range of one of his hydrogen ions (moving with a velocity of 8×10^7 cms. sec.$^{-1}$) at about 0·00037 cm. Now, according to Chapman and Milne's calculations,† the equivalent

* See, *e.g.*, Blackett, *Proc. Roy. Soc.*, **107** A, 359, 1925.

† *Q. J. Roy. Met. Soc.*, **46**, 384, 1920. If hydrogen is present in the upper atmosphere to an extent indicated by the small traces found near the ground, this air-range should be increased to 1·2 cm.

air-range down to 100 kms. for a particle entering the earth atmosphere is about 0·4 cm. It is at once evident that as far as our rough calculations go, the penetrating power of the Ca^+ atoms projected by radiation-pressure is of the order of magnitude that would enable them to reach the observed lower limit of auroræ. Auroræ are indeed observed down to 80 kms., and in the range from 100 kms. to 80 kms. the equivalent air-range increases from 0·4 cm. to 5·6 cms. To reach this lower level would be only just within the power of the fastest α-particles (those from RaC, range 7 cms.), but the estimate of densities at high levels in the earth's atmosphere is subject to numerous uncertainties. The greater penetrating power of the projected ions found in this paper, as compared with that in Lindemann's, is due partly to their greater velocity, partly to their much greater mass. On the present theory, as already mentioned, the acquisition of high velocities is not confined to light atoms, and a similar order of velocity is indicated for all atoms that are liable to projection under radiation-pressure.*

The fact that atoms projected under radiation-pressure will arrive at the earth with fairly well-defined velocities, as shown above, may be of importance in accounting for the well-defined lower limits of auroral draperies.

8. *Sign of Macroscopic Charge.*—We have now to examine the question of the resultant charge of any group of atoms which may be projected from the sun by radiation-pressure in this way.

When first projected the atom may be either neutral or positively charged. For example, H or He atoms will be neutral, Ca^+, Sr^+, or Ti^+ atoms will be positively charged.

In Lindemann's theory the hydrogen atoms were supposed to be projected as neutral atoms, and afterwards to become ionised. Lindemann showed (by the method afterwards developed in great detail by Saha) that the equilibrium value of the ionisation of such a cloud would be large—that a low-pressure cloud of hydrogen atoms, at a temperature of, say, 6000°, would be practically completely ionised—when in thermodynamic equilibrium. Actually such a cloud would be in a state far removed from thermodynamic equilibrium, and the ionisation formulæ scarcely apply. The cloud would be un-ionised when projected, and it would be a question of how fast it would approach an equilibrium condition. This would depend on the ionising agents available. Collisions would be so rare as to be negligible, and so could not effect ionisation. But a hydrogen atom in the 2_1 (metastable) state has an ionisation potential of $13{\cdot}54/4 = 3{\cdot}4$ volts, and is thus ionised by radiation of wave-length greater than $\lambda 3646$, the limit of the Balmer series. Thus photo-electric ionisations may occur fairly freely and the cloud may become ionised though ejected with the atoms neutral. Helium atoms in the orthohelium state ($1\sigma = 38{,}454$ cms.$^{-1}$) have an ionisation potential of 4·75 volts and are ionised by light of wave-length less than $\lambda 2600$.

* *Note added* 1926 *June* 3.—Since the paper was communicated, Mr. Blackett has kindly put his most recent data at my disposal. From these he estimates that an α-particle moving at $1{\cdot}6 \times 10^8$ cms. sec.$^{-1}$ would have an air-range at N.T.P. of 0·55 mm. Such a penetrating power is too small to account for auroræ, and we are driven to consider more massive atoms than helium.

They would therefore be much less freely ionised. In these and similar cases the precise degree of ionisation cannot be calculated by thermodynamics ; it requires a calculation of the actual number of radiative ionisations that would occur during the passage of the atoms from the sun to the earth. In the absence of such a calculation we must bear in mind the possibility that the atoms may escape too rapidly from the region of intense solar radiation for ionisation to approach completion. In that case a considerable proportion of neutral atoms would arrive in the earth's atmosphere. They could there cause ionisation, just like charged atoms, but they would be undeflected by the earth's magnetic field.

The state of affairs is quite different for an atom such as Ca^+, which is already ionised when ejected. In the first instance it is unaccompanied by any electron. The effect of the ejection, however, is to leave the sun with a negative charge, or with a slightly decreased positive charge if, as is usually supposed, the sun in its steady state has a permanent positive charge arising from the escape of electrons by thermal agitation.* This decrease in the sun's positive charge will facilitate a further escape of electrons, and it is easy to show that every escape of a positive ion such as Ca^+ will be soon followed by the escape of an electron, thus restoring the sun's charge to its previous value. We have, then, equal numbers of positive and negative charges leaving the sun. But it does not at all follow that they will constitute a neutral cloud. For the positive Ca^+ ions are rapidly accelerated by radiation-pressure, whilst the electrons are relatively transparent to radiation, the pressure of which on them is insufficient even to balance gravity.

The scattering coefficient per electron, on the classical theory, has the value $8\pi b^2/3$, where b, the "radius of the electron," is $e^2/mc^2 = 2{\cdot}81\times10^{-13}$ cms. Radiation of flux F per unit area will cause an acceleration f given by

$$f=\frac{8\pi b^2}{3}\cdot\frac{\mathrm{F}}{mc}.$$

Putting $\mathrm{F}=\sigma\mathrm{T}^4$, where σ is Stefan's constant and T is the effective temperature of the sun, we find $f=1{\cdot}52\times10^3$ cms. sec.$^{-2}$. This is only 1/18 of solar gravity, $g=2{\cdot}73\times10^4$ cms. sec.$^{-2}$. Thus the pressure of radiation arising from the whole of the sun's continuous spectrum produces a negligible acceleration.

The electron may or may not be subjected to an attraction from the positive particles which have already left. If the positive particles are escaping equally from all portions of the sun's surface, they will form a spherical shell, which, as is well known, exerts no electrostatic attraction at points inside it. They will then exert no acceleration on the electrons which follow them. If, on the other hand, the positive particles are escaping from one particular locality, they will exert an electrostatic pull on any escaping electrons, and will indeed tend to cause electrons to escape most freely from the portion of the surface nearest to them ; they will "induce" a negative charge in this region, *i.e.* an excess of electrons, and these latter will be the first to escape.

* *Camb. Phil. Trans.*, **22**, 514, 1923.

As for the residual charge on the sun, it will only exert an outward repulsive acceleration on the escaping electrons if its sign is negative, *i.e.* if a number of positive particles have escaped large enough to neutralise the sun's permanent positive charge.

These considerations are only qualitative, and detailed calculations would be required to establish any definite result. But it appears plausible to conclude that the escaping electrons will be subject to a far smaller acceleration than the positive particles, if to any at all; they may indeed only be escaping in virtue of beginning with a velocity in excess of that due to a fall from infinity under gravity—the ordinary condition for escape under thermal agitation. This has important consequences. So far from forming a neutral cloud, the aggregate of charged particles will have a positively charged head and a negatively charged tail, and the head will be moving faster than the tail. Without calculation it does not seem possible to ascertain to what extent the electrons will be mingled with the positive ions. All we can be sure of is that there will be about as many negatives as positives, and that the positives will move the faster. It is worthy of note that in a recent paper Chapman * has concluded that auroræ cannot be explained by a neutral stream, and that the stream must be charged, though less heavily than he at first supposed. The theory of accelerated escape of positive ions under radiation-pressure would seem to provide just what Chapman finds necessary.

9. *Conclusion.*—Further discussion of the origin of auroræ and magnetic storms would be outside the scope of this paper. Here it is intended not so much to urge that ionised atoms, shot out almost at random from the sun and subsequently accelerated by radiation-pressure, are competent to account for certain geophysical phenomena, as to point out that it seems inevitable that such accelerated atoms should be produced, and to trace some of the consequences. The investigation arose out of a desire to study the stability of the solar chromosphere, and the author would welcome criticism from those who are more familiar with the geophysical aspects of the investigation.

One further remark may be made about the originating velocity which in consequence of the Doppler effect leads to the acceleration. No specific origin has been suggested—it has merely been pointed out that an atom which somehow or other begins to move outwards with an appreciable velocity will have that velocity increased. But it is clear that a prominence motion itself might be the start. If a portion of the sun's surface brightens for a short period and then fades again, a number of atoms will be started with outward velocities which will bring them into the wing of the absorption line, provided they are not too numerous to carry the absorption line with them. As far as the theory goes, accelerated atoms may go out from any portion of the chromosphere at any time, but there will be a greater tendency for them to go out from disturbed regions which are the seat of brightness fluctuations.

10. *Summary.*—(1) An atom which, due to some cause or other, begins to move outward from the sun with an appreciable velocity will begin to absorb in the violet wing of the absorption line corresponding

* *Proc. Camb. Phil. Soc.*, **21**, 577, 1923.

to the same atom at rest, owing to the Doppler effect. It will therefore be exposed to more intense radiation. If it was originally a high-level atom in equilibrium under radiation-pressure and gravity, radiation-pressure will now exceed gravity, and the atom will be accelerated outwards. It will therefore move still further out into the wing, where it will be exposed to still more intense radiation, and so on, until it eventually "climbs out of" its absorption line and becomes exposed to the undiminished continuous spectrum.

(2) The atom will ultimately acquire a limiting velocity, in virtue of the weakening of the radiation under the inverse square law. A limiting velocity may also be acquired in virtue of the atom being "trapped" by an adjacent absorption line.

(3) For atoms projected from the sun in this way, from absorption lines of an intensity ratio of the order of $\frac{1}{9}$, the limiting velocity is of the order of $1{\cdot}6\times10^{8}$ cms. sec.$^{-1}$ (1600 kms. sec.$^{-1}$). The velocity will be about the same for light atoms (*e.g.* H, He) and for heavy atoms (*e.g.* Ca^{+}).

(4) A similar order of magnitude will hold for the stars in general; this is a consequence of the fact that the surface value of the gravitational potential, which controls the limiting velocity, has a minimum for stars of mass $11{\cdot}5\ \odot$, and varies only slowly with mass.

(5) The limiting velocity is of the same order of magnitude as the velocity-displacements observed in the spectra of Novæ. Such displacements are probably due to showers of atoms ejected by the increased radiation-pressure when the star brightens and then accelerated, ultimately attaining a limiting velocity. This may lead to the appearance of lines in a displaced position without their having traversed the intermediate wave-lengths.

(6) Particles projected in this way from the sun may be the cause of auroræ and magnetic storms. Comparison is made with Lindemann's theory. On the present theory the particles arrive with greater velocities, and may be much heavier, than on Lindemann's theory.

(7) Use is made of Blackett's observations of the collisions of α-particles with argon atoms to estimate the air-range of Ca^{+} atoms (same atomic weight as argon) moving at $1{\cdot}6\times10^{8}$ cms. sec.$^{-1}$. The equivalent air-range at N.T.P. is about 0·15 cm., which would be just about sufficient for them to penetrate the earth's atmosphere to the 100 kms. level, the observed lower level of auroræ.

(8) Atoms may be projected neutral or ionised. Neutral atoms may become ionised and form neutral clouds, as in Lindemann's theory. Ionised (positively charged) atoms will be followed by an equal number of electrons, but the electrons will not be subject to appreciable radiation-pressure and will probably lag behind. Hence the cloud (if the projected particles are numerous enough to form such) will have a positively charged head and a negatively charged tail.

(9) The phenomenon of accelerated escape will only occur if the atoms are not numerous enough to give rise to an absorption sufficient to "carry their absorption line with them." Random accelerated escape is possible at any time from any portion of the sun's surface, but escape is more probable from disturbed areas.

The Spectrum of φ Persei (Sp. Type Bope) throughout a complete Cycle (1925–1926). By Major William J. S. Lockyer, M.A., Ph.D. (Plate 6.)

In a communication * to the Society in May of last year, the results of a discussion of a series of photographs of the Spectrum of φ Persei (H.D.C. 10516, R.A. $1^h\ 37^m{\cdot}4$, Dec. $+50°\ 11'$, Mag. 4·19, Sp. Type Bope), taken during the years 1924 and 1925, and embracing about two cycles of the star, were presented. The series comprised forty-five photographs taken on as many nights. The greater majority of the negatives covered half the period of the second cycle, it being only then discovered that such rapid changes were in progress that, to follow closely the sequence of events, photographs every third or fourth night were desirable.

The particularly interesting nature of the spectrum of this star, namely, the quick changes in the relative intensities of the bright components of the hydrogen lines, the varying appearances both in intensity and character of the absorption lines of helium, and the duplicate nature of the ionised lines of iron and titanium, led the writer to state in the above communication that when the star came again into a convenient position for observation, a much more complete series of photographs throughout one entire cycle would be attempted.

The present paper is the result of this further research.

Reference may first be made to an interesting and recent communication by J. F. Frédette † of the Dominion Observatory, Ottawa, entitled "The Riddle of φ Persei," since some of his remarks will be mentioned in the present paper.

After the appearance of the writer's previous paper on this star, Mr. Frédette, as he states (*loc. cit.*, p. 187), "decided to look over the old Ottawa plates in order to see whether a second investigation here offered prospects of being profitable."

Referring, in the first instance, to the method adopted by the writer in the determination of the difference of intensity between the bright components of the hydrogen lines, by means of a graduated wedge, on photographs taken with a prismatic camera, he remarks :

"This independent method, free from the influence of ambiguity as to the position, wave-length, as well as the changing character of the central absorption, affords a most important check on the spectrographic results."

In this connection he further remarks :

"One of the causes certainly at work in invalidating the spectrographic method in this case is a periodic photographic encroachment on the central absorption by the brighter emission components. If the intensity distribution in the emission bands be slightly unsymmetrical, the greater and prevalent shift of the absorption would be in the direction of the weaker half of the band. Even in the case of symmetrical dis-

* *M.N.R.A.S.*, **85**, 580, 1925.
† *Journ. Roy. Astr. Soc. Canada*, **19**, 185, 1925.

tribution, if there should be a considerable wave-length equation between absorption and emission, a prevalent photographic shift would also result."

A re-measurement of about fifty of the Ottawa plates, which he has recently completed, shows that "on some odd plates the hydrogen absorption lines were found to be decidedly open to diverse interpretation."

It is interesting therefore to note that this star has again been placed on the regular observing programme of the Dominion Observatory for a trial period, but, pending the completion of the observational data, the published velocities of Cannon, Ludendorff, and Jordan have been rediscussed from this new point of view, and the results which he has obtained are described in the paper to which reference has been made.

The Material Available.

It was originally intended to commence the observations about the time of the occurrence of the maximum positive velocity, as indicated by the intensities of the components of the bright hydrogen lines, but owing to illness I could not begin them until September 9. This, however, was really unimportant, as observations were commenced in time to record the date of the next important phase of the star, namely, the epoch of zero velocity as indicated by the same lines.

The same instrument, namely, the 9-inch prismatic camera, and similar photographic plates were employed as before, only on several occasions duplicate photographs were secured on Barnet Superspeed Ortho Plates (H and D 550).

During the complete cycle, which covered the period 1925 September 9 to 1926 January 13, photographs were taken on 79 nights out of a possible 127, giving a mean percentage of fine nights of 62·2. One hundred and nineteen negatives were secured, 13 of which were discarded, leaving a total of 106 photographs for measurement. On 33 nights more than one negative was obtained. Thus good photographs on each of 71 nights out of the 127 are available.

In order to be certain that a complete period had elapsed the observations were carried on for another eight nights, three of which were fine, and satisfactory negatives were taken.

All the negatives were taken by the writer with the exception of those obtained on three nights. These were secured by Mr. D. L. Edwards during the writer's absence to attend the November and January meetings of the Society.

It was desired, if possible, to secure a good photograph on at least every third or fourth night in order that the record should be as continuous as possible to follow the sequence of changes taking place in the star's spectrum. This necessarily meant that every available fine night had to be utilised, as it could not be forecasted whether the following night would be fine or not. Fortunately the time chosen for this series was very opportune, for on the conclusion of the observations a long spell of cloudy weather set in.

The following brief summary of the weather conditions is given, as it indicates the continuity of the record secured.

TABLE I.

Neg. No.	Date.	M.T. of Exp. U.T.	Julian Day 2420000 +	Phase (Days).	Int. Diffs. H_β. R–V.	Int. Diffs. H_γ. R–V.	Intensity Diffs. of Hyd. Abs. H_ζ–H_ϵ.	Intensity Diffs. of Hyd. Abs. H_ζ–H_δ.	Diff. from Means. H_ζ–H_ϵ.	Diff. from Means. H_ζ–H_δ.	Intensities of Absorption Lines. Ca^+ 3933. I Max. 5.	Ca^+ 3933. Ch.	Hyd. I.	He 4471. I Max. 5.	He 4471. Ch.	He 4026. I Max. 5.	He 4026. Ch.	He 3964. I Max. 5.	He 3964. Ch.	Hyd. Series.
(1).	(2).	(3).	(4).	(5).	(6).	(7).	(8).	(9).	(10).	(11).	(12).	(13).	(14).	(15).	(16).	(17).	(18).	(19).	(20).	(21).
	1925 Sept.	H. M.																		
641	9	22 53	4403·5	26·9	−0·6?	−0·5?	+0·7	−0·6	+0·1	−0·2	2	S	1·6	3	NS	2	VN	5	S	7
643	10	21 53	04·5	27·8	−0·3	−0·2	+0·1	−0·7	−0·5	−0·3	3	S×	1·0	4	S	3	NS	5	S	10
645	12	21 20	06·4	29·8	−0·6	−0·8	−0·5	−1·0	−1·1	−0·6	1	S	0·4	5	S	5	S	4	S	6
647	13	21 42	07·4	30·8	−0·4	−0·2	−0·3	−1·4	−0·9	−1·0	2	S×	0·6	5	VS	5	S	5	S	6
648	14	20 52	08·4	31·8	−0·3	0·0	0·0	−1·5	−0·6	−1·1	2	S×	0·9	5	VS	5	NS	5	S	7
650	20	22 8	14·4	37·8	+1·2	+0·8	+1·0	0·0	+0·4	+0·4	2·5	S×	1·9	5	VS	4·5	NS	4	S	6
651	20	22 30	14·5	37·9																
655	23	20 38	17·4	40·8	+1·0	+0·9	+1·5	+0·5	+0·9	+0·9	1?	S	2·4	5	S	4	N	3	N	6
659	24	21 20	18·4	41·8	+0·7?	+0·7?	+2·2	+1·3	+1·6	+1·7	2	S	3·1	4	S	4	NS	4	S	8
661	25	0 8	19·5	42·9	+1·0?	+0·5?	+1·3	+0·1	+0·7	+0·5	1	S	2·2	4	VS	4	NS	4	S	7
663	26	21 28	20·4	43·8	+0·8	+1·0	+0·7	−0·1	+0·1	+0·3	1	S?	1·6	4	S	4	N	3	S	6
664	27	20 20	21·4	44·8	+1·7	+0·7	+1·1	+0·6	+0·5	+1·0	1	S?	2·0	4	NS	5	N	5	S	7
665	30	19 53	24·3	47·7	+1·7	+1·1	+1·3?	−0·8?	+0·7?	−0·4?	0	..	2·2?	3	NS	3	N	3	S	6
	Oct.																			
667	2	21 25	26·4	49·8																
668	2	22 5	26·4	49·8	+1·2?	+0·4?	+0·5?	−0·2?	−0·1?	+0·2?	2	S	1·4?	2	NS	2	N	2	S	5
669	2	22 45	26·5	49·9																
670	3	19 30	27·3	50·7	+1·1?	+0·6?	+0·5?	−1·0?	−0·1?	−0·6?	0	..	1·4?	0?	VN?	1	N	1?	..	5
671	5	21 1	29·4	52·8	1·1?	+0·8?	+0·1?	−0·6?	−0·5?	−0·2?	0?	..	1·0?	2	NS	1	N	0	..	5
672	6	20 10	30·3	53·7	+1·1	+0·9	+0·9	−0·1	+0·3	+0·3	1·5	S	1·8	2	N	3	VN	4	S	6·5
673	6	21 30	30·4	53·8																

675	8	20	6	32·3	55·7	+1·2	+0·6	+0·4	−0·5	−0·2	−0·1	2	S	1·3	2	VN	3	VN	4	S	7
676	9	20	5	33·3	56·7	+1·6	+0·7	0·0	−0·7	−0·6	−0·3	2·5	S×	0·9	2	VN	2·5	VN	4	S	8
677	9	21	18	33·4	56·8																
678	10	20	23	34·4	57·8	+1·7	+1·0	+0·5	−0·2	−0·1	+0·2	2	S×	1·4	1·5	N	2	VN	5	S	6·5
680	10	23	27	34·5	57·9																
685	11	19	26	35·3	58·7	+1·4?	+0·7?	−0·8?	−1·4?	−1·4?	−1·0?	1	N?	0·1?	1	N	1	VN	5	S	6
686	12	21	52	36·4	59·8	+1·8	+1·1	+0·8	−0·8	+0·2	−0·4	2	S	1·7	2	VN	2	VN	5	S	6
688	14	20	25	38·4	61·8	+2·0	+1·1	+2·1	+1·3	+1·5	+1·7	2	S×	3·0	1	VN	1	VN	5	S	6
695	17	20	11	41·3	64·7	+1·7	+0·9	+2·5	+0·8	+1·9	+1·2	2	S×	3·4	1	VN	1·5	VN	4	S	6
696	17	21	32	41·4	64·8																
700	23	19	14	47·3	70·7																
701	23	20	28	47·4	70·8	+1·1	+0·2	+1·2?	−0·4?	+0·6?	0·0?	1·5	S×	2·1?	1·5	VN	1	VN	4	S	5
702	23	21	39	47·4	70·8																
703	24	20	17	48·3	71·7	+1·5	+0·5	+1·1	0·0	+0·5	+0·4	3	VS×	2·0	2·5	VN	3	VN	5	S	5·5
704	24	22	0	48·4	71·8																
705	25	20	5	49·3	72·7	+1·8?	+0·8?	+1·6	+0·2	+1·0	+0·6	2	S	2·5	1·5	VN	2	VN	4·5	S	7
706	25	20	57	49·4	72·8																
707	27	19	10	51·3	74·7	+1·2	+0·3	+1·7	0·0	+1·1	+0·4	0·5	S×	2·6	1	VN	1·5	VN	4·5	S	5·5
708	27	20	20	51·3	74·7																
709	31	19	40	55·3	78·7	..	..	..	..	..	..	2·0	S×	..	3	NS	2	VN	1	N	5
	Nov.																				
711	3	19	27	58·3	81·7	+1·0	+0·6	+0·9	−0·2	+0·3	+0·2	2·5	S	1·8	2	VN	3	VN	5	S	9
712	3	20	32	58·4	81·8																
713	4	18	32	59·3	82·7	+0·8	+0·7	+1·1	−0·6	+0·5	−0·2	2	S×	2·0	2·5	NS	3	N	5	S	8
714	4	19	52	59·3	82·7																
715	5	18	40	60·3	83·7	+0·9	+0·3	+0·9	0·0	+0·3	+0·4	1·5	VS×	1·8	3	NS	4	VN	5	S	9·5
716	5	19	58	60·3	83·7																
717	7	22	51	62·5	85·9	+0·5	+0·5	+0·6	−1·1	0·0	−0·7	2	S	1·5	3	N	4	NS	5	S	7

TABLE I.—*continued.*

Neg. No.	Date.	M.T. of Exp. U.T.	Julian Day 2420000 +	Phase (Days).	Int. Diffs. H_β R–V.	Int. Diffs. H_γ R–V.	Intensity Diffs. of Hyd. Abs. H_ζ–H_ϵ.	H_ζ–H_δ.	Diff. from Means. H_ζ–H_ϵ.	Diff. from Means. H_ζ–H_δ.	Intensities of Absorption Lines. Ca^+ 3933. I Max. 5.	Ca^+ 3933. Ch.	Hyd. I.	He 4471. I Max. 5.	He 4471. Ch.	He 4026. I Max. 5.	He 4026. Ch.	He 3964. I Max. 5.	He 3964. Ch.	Hyd. Series.
(1).	(2). 1925 Nov.	(3).	(4).	(5).	(6).	(7).	(8).	(9).	(10).	(11).	(12).	(13).	(14).	(15).	(16).	(17).	(18).	(19).	(20).	(21).
719	8	18 17	4463·3	86·7																
720	8	19 7	63·3	86·7	+0·2	+0·4	+1·0	−0·3	+0·4	+0·1	1	S	1·9	1	N	2·5	VN	5	S	6·5
721	9	18 52	64·3	87·7																
722	9	20 2	64·3	87·7	+0·4	+0·2	+0·6	−0·4	0·0	0·0	3	S×	1·5	2	NS	3	NS	4	S	8
724	10	18 37	65·3	88·7																
725	10	19 47	65·3	88·7	+0·4	+0·3	+0·7	−0·7	+0·1	−0·3	3	S×	1·6	2	N	3	VN	4	S	8·5
727	11	21 0	66·4	89·8																
728	11	21 51	66·4	89·8	+0·4?	−0·1	−0·1	−0·7	−0·7	−0·3	2	S×	0·8	1	VN	2	VN	4·5	S	6
729	12	18 37	67·3	90·7																
730	12	20 7	67·3	90·7	0·0	0·0	+0·2	−0·6	−0·4	−0·2	3	S×	1·1	1	NS	1·5	N	5	S	7
731	13	18 12	68·3	91·7																
732	13	19 27	68·3	91·7	0·0	+0·1	+0·4	−0·5	−0·2	−0·1	3	S×	1·3	1	NS	1	N	4	S	8
733	16	21 57	71·4	94·8	+0·4?	−0·3?	+0·4	−1·1	−0·2	−0·7	2	S	1·3	2	N	1	VN	4	S	6
734	17	19 20	72·3	95·7	−0·4?	+0·1?	+1·4	−0·3	+0·8	+0·1	3	S	2·3	1·5	NS	1	VN	3	S	7
735	18	18 7	73·3	96·7	−0·2	0·0	+0·5	−0·6	−0·1	−0·2	2	S	1·4	3	VN	3	VN	3·5	S	7
738	19	18 20	74·3	97·7	−0·4	0·0	+0·3	−0·8	−0·3	−0·4	2	S×	1·2	3	VN	2	VN	4	S	6
744	20	18 11	75·3	98·7	−0·8	−0·1	+1·3	+0·3	+0·7	+0·7	3	S×	2·2	1	VN	2	VN	4	S	9
746	23	19 22	78·3	101·7	−0·8?	−0·2	−0·3	−1·0	−0·9	−0·6	5	S×	0·6	0	..	1	VN	2	N	16
747	25	18 5	80·3	103·7	−0·7	−0·4	0·0	−0·5	−0·6	−0·1	5	S	0·9	0	..	1	VN	3	N	18
748	27	17 48	82·2	105·6																
749	27	18 50	82·3	105·7	−0·9	−1·0	−0·4	−1·1	−1·0	−0·7	5	S	0·5	1	VN	0·5	VN	2	NS	14

750	28	17 50	83·2	106·6	−1·4	−0·8	−0·4	−1·2	−1·0	−0·8	4	S	0·5	1	VN	1	VN	1	N	15·5
751	28	18 51	83·3	106·7																
752	30	18 17	85·3	108·7	−1·3	−0·9	−0·9	−1·6	−1·5	−1·2	4	S	0·0	0	VN?	1	VN	1	N	11
753	30	19 46	85·3	108·7																
	Dec.																			
754	1	17 57	86·3	109·7	−1·3	−0·8	−0·5	−1·1	−1·1	−0·7	4	VS×	0·4	1·5	VN	1·5	VN	1·5	N	14·5
755	1	19 5	86·3	109·7																
756	2	17 58	87·3	110·7	−0·8	−0·9	−0·9	−1·5	−1·5	−1·1	4	S×	0·0	1	VN	1	VN	1·5	N?	15
757	2	19 11	87·3	110·7																
759	3	17 45	88·3	111·7	−1·0	−0·8	−0·5	−1·2	−1·1	−0·8	4	S×	0·4	1	VN	1	VN	1	N	12·5
760	3	18 46	88·3	111·7																
761	5	18 2	90·3	113·3	−0·8	−0·5	−0·4	−0·7	−1·0	−0·3	3	S×	0·5	2	VN	2	VN	1	N	14
764	9	1 11	93·6	117·0	−1·3	−0·3	−0·5	−1·1	−1·1	−0·7	3?	S	0·4	0?	VN?	1	N	2	NS	13
765	9	17 57	94·3	117·7	−1·1	−0·8	−0·3	−1·0	−0·9	−0·6	3	S×	0·6	2	VN	2	VN	3	S	14
767	10	17 37	95·3	118·7	−0·6?	−0·1?	−0·4?	−0·7?	−1·0?	−0·3?	..	..	0·5?							
768	11	19 40	96·3	119·7	−0·9	−0·7	−0·3	−1·2	−0·9	−0·8	3	S×	0·6	2	VN	3	VN	3	S	8
770	12	18 5	97·3	120·7	−1·1	−0·5	−0·1	−0·7	−0·7	−0·3	4	S×	0·8	1	VN	3	VN	3	S	9
772	13	17 57	98·3	121·7	−1·8	−0·7	+1·0	−0·5	+0·4	−0·1	..	..	1·9	3	N	2	VN	3	S	6
773	14	18 2	99·3	122·7	−1·5	−1·2	+2·1	+0·3	+1·5	+0·7	2	S×	3·0	2	VN	1	VN	4	S	7
775	15	23 19	4500·5	123·9	−0·9	−0·6	+1·8?	0·0?	+1·2?	+0·4?	2	S	2·7?	1	VN	1	N	4	S	5
776	16	19 30	1·3	124·7	−1·2	−0·8	+2·2	+0·7	+1·6	+1·1	2	S	3·1	2	VN	2	VN	4	S	6
778	17	18 2	2·3	125·7	−1·4	−0·8	+1·5	+0·1	+0·9	+0·5	1	S	2·4	3	N	2	VN	3	S	5
780	21	17 52	6·3	2·9	−1·6?	−0·7	+1·4?	+0·2?	+0·8?	+0·6?	..	..	2·3?	2?	N	..	..	4?	S	5
781	21	18 50	6·3	2·9																
782	23	19 32	8·3	4·9	−1·0	−0·6	+0·3	−0·4	−0·3	0·0	2	S×	1·2	3	N	2	VN	4	S	12
785	31	17 51	16·3	12·9	−1·3?	−0·5	+0·8	−0·4	+0·2	0·0	2	S	1·7	1	VN	1·5	VN	4	S	6·5
786	31	18 42	16·3	12·9																

TABLE I.—*continued.*

Neg. No.	Date.	M.T. of Exp. U.T.	Julian Day 2420000 +	Phase (Days).	Int. Diffs. H_β R–V.	Int. Diffs. H_γ R–V.	Intensity Diffs. of Hyd. Abs. H_ζ–H_ϵ.	Intensity Diffs. of Hyd. Abs. H_ζ–H_δ.	Diff. from Means. H_ζ–H_ϵ.	Diff. from Means. H_ζ–H_δ.	Intensities of Absorption Lines. Ca^+ 3933. I Max.	Ca^+ 3933. Ch.	Hyd. I.	He 4471. I Max.	He 4471. Ch.	He 4026. I Max.	He 4026. Ch.	He 3964. I Max.	He 3964. Ch.	Hyd. Series.
(1).	(2). 1926 Jan.	(3).	(4).	(5).	(6).	(7).	(8).	(9).	(10).	(11).	5. (12).	(13).	(14).	5. (15).	(16).	5. (17).	(18).	5. (19).	(20).	(21).
787	2	21 55	4518·4	15·0	−1·1?	0·0?	+0·9?	−0·4?	+0·3?	0·0?	..	..	1·8?	..	..	..	..	5	S	6
789	3	18 58	19·3	15·9	−1·0?	−0·4	+0·8	−0·2	+0·2	+0·2	2	S	1·7	1·5	VN	2	VN	4	S	6
791	6	18 18	22·3	18·9	−0·3	−0·2	+1·0	−0·5	+0·4	−0·1	2	S	1·9	2·5	NS	3	NS	4·5	S	5·5
792	6	19 44	22·3	18·9																
793	7	19 30	23·3	19·9	−0·2	−0·3	+1·4	−0·3	+0·8	+0·1	1	S	2·3	3	NS	3	NS	5	S	6
794	7	20 45	23·4	20·0																
795	11	23 16	27·5	24·1	−0·1	0·0	+0·9	−0·2	+0·3	+0·2	2·5	S×	1·8	3	NS	3	NS	4	S	6·5
796	12	0 32	27·5	24·1																
797	12	18 20	28·3	24·9	+0·1	−0·2	+0·7	−0·2	+0·1	+0·2	2·5	S×	1·6	3	NS	4	NS	5	S	8·5
798	12	19 38	28·3	24·9																
799	13	18 20	29·3	25·9	+0·1	−0·2	+0·7	−0·1	+0·1	+0·3	2·5	S×	1·6	3	NS	3	NS	4	S	8
800	13	19 35	29·3	25·9																
					Means		+0·6	−0·4												
801	16	19 55	32·3	28·9	+0·1	−0·4	+0·6	−0·4	..	..	2	S	..	4	VS	4	S	5	S	6
802	19	20 47	35·4	32·0	−0·3	−0·1	+0·1	−0·7	..	..	2?	VS	..	5	VS	4	VS	3·5	S	8
804	21	19 22	37·3	33·9	+0·1	0·0	+0·3	0·0	..	..	1	S	..	5	VS	5	S	3·5	S	8
805	21	20 22	37·4	34·0																

The number of consecutive *cloudy* nights amounted to :

6 on 1 occasion,
5 ,, 2 occasions,
4 ,, 1 occasion,
3 ,, 2 occasions.

On the other hand, the number of consecutive *clear* nights amounted to :

10 on 1 occasion,
7 ,, 1 ,,
5 ,, 2 occasions,
4 ,, 1 occasion,
3 ,, 4 occasions.

All the data available for the research are brought together in Table I. Column 1 gives the Norman Lockyer Observatory number of each negative; column 2 the date of each photograph; column 3 the mean time of each exposure; and column 4 the corresponding Julian date.

Cyclical Change of the Bright Hydrogen Lines.

It was pointed out in the previous paper that each of the hydrogen lines in the spectrum of this star consisted of a broad absorption band on which are superposed two bright lines symmetrically placed with regard to it and separated from each other by a strong, sharp absorption line. It was found that the intensities of these bright components changed, and by measuring the differences of these intensities curves could be drawn for each pair of components showing a period of variation of 126·8 days.

On the assumption that the changes in the intensities of the violet and red components of the bright hydrogen lines were due to the movement of the central absorption lines towards the violet or red it was possible to convert the curves formed by the measured intensity-differences into velocity in the line of sight curves. Thus the maximum of the intensity-difference curve, at which the red component is at its brightest compared with the violet component of the hydrogen line, corresponds with the epoch of maximum negative velocity.

The same procedure of reduction, as was adopted with the previous observations of this star, has been repeated here with the new set of 106 negatives.

The bright components of H_β and H_γ (see Plate 6) were measured on each negative under the wedge three times to form a mean value, and each negative was again similarly measured on two other separate dates. The mean value finally adopted was thus the result of nine separate settings for each line. After the complete series of negatives had been measured, the first twenty-four negatives were again measured in exactly a similar manner in order to find out whether a greater experience in the method of measurement that had been gained would give different values for the earlier measurements. The differences were, however, surpris-

ingly small, but nevertheless the last-mentioned measures were adopted in place of those made earlier.

As the main part of this research is based on the determination of intensity differences by means of the wedge method, it seemed desirable to make some statement as to the accuracy which could be obtained. For this purpose the measures of one negative, namely, No. 651, picked out at random from the series, are reproduced below in Table II.

This negative was one of those belonging to the early part of the series of the observations and was measured twice over as stated in a previous paragraph ; the first measures (A) were made in 1925 in October and November, and the second (B) in 1926 in February and March. The individual wedge readings with their means are given in the schemes marked (A) and (B).

Below the double horizontal lines are the individually derived differences, and in the last line of all the adopted means used in the construction of the curves are added. It will be seen that in both the (A) and (B) series of measures the individual means are equal to or less than one division of the wedge, but it must be pointed out that the greatest divergence indicated, namely, one wedge difference, is very exceptional. The agreement between the final means of the two sets of measures is very satisfactory, the greatest difference being three-tenths of a wedge division.

All the measures were made by the writer, and they involved 4824 settings.

Columns 6 and 7 of Table I. show the mean values obtained for the differences of intensities between the red (R) and violet (V) components of the hydrogen lines : in the case where two or more photographs were taken on the same night the mean has been adopted. The question mark against some of the figures denotes measures which should receive a little less weight.

These figures form the basis of the two curves for H_β and H_γ respectively at the upper part of fig. 1 : at the bottom is the scale for the dates of observation and the corresponding Julian dates. At the extreme top are printed the conditions of the motions in the line of sight according to the various phases, and just below these the scale for the phases themselves. These phase dates are also given in Table I., column 5, against each negative number.

The zero for this phase scale corresponds to the epoch of maximum of the positive velocity (minimum of curves in fig. 1) which would fall outside the figure on the left-hand side. This zero is calculated from an earlier minimum recorded by the writer in his previous paper as having occurred on 1924 December 3, corresponding to the Julian Day 2424123. Adopting the star's period as 126·8 days, and noting that two periods have elapsed since then, the date of the minimum for the present zero phase would be 1925 August 13, or, in Julian Days, 2424376·6.

From the fact that the present series of observations is continuous, but did not commence at zero phase, it was considered desirable to plot the data in the manner here shown and not commence the curve from zero phase, as this would involve placing the data, observed after zero phase, in front of the earlier series of observations.

Table II.

Measure of Negative of φ Persei No. 651.

A.

1st Series. 1925.	H_β. V.	H_β. R.	H_γ. V.	H_γ. R.	H_ζ.	H_ϵ.	H_δ.
Oct. 17	12·5	13·7	12·9	12·9	13·3	12·9	13·1
	12·6	14·4	12·8	13·2	14·1	12·9	13·7
	12·8	14·2	12·7	13·0	13·4	12·5	13·4
Means	12·6	14·1	12·8	13·0	13·6	12·8	13·4
Oct. 28	12·8	13·9	12·9	13·9	12·5	12·1	12·1
	12·8	13·3	13·6	13·5	12·5	12·0	12·4
	13·2	13·3	12·5	13·7	12·5	12·9	12·8
Means	12·9	13·5	13·0	13·7	12·5	12·3	12·4
Nov. 6	13·2	14·8	12·6	13·7	12·8	11·6	12·6
	12·8	14·8	12·7	13·5	13·2	12·0	12·8
	12·9	14·1	12·5	12·9	12·6	11·8	12·3
Means	13·0	14·6	12·6	13·4	12·9	11·8	12·6

	H_β. R–V.	H_γ. R–V.	H_ζ–H_ϵ.	H_ζ–H_δ.
Oct. 17	+1·5	+0·2	+0·8	+0·2
,, 28	+0·6	+0·7	0·2	+0·1
Nov. 6	+1·6	+0·8	+1·1	+0·3
Means	+1·2	+0·6	+0·7	+0·2

B.

2nd Series. 1926.	H_β. V.	H_β. R.	H_γ. V.	H_γ. R.	H_ζ.	H_ϵ.	H_δ.
Feb. 26	14·3	15·3	14·4	15·0	15·1	13·8	15·0
	14·2	15·6	14·2	14·9	15·0	14·1	14·9
	14·5	15·8	14·2	15·0	15·1	14·0	14·9
Means	14·3	15·6	14·3	15·0	15·1	14·0	14·9
Mar. 2	14·2	14·8	13·1	13·9	13·4	12·6	13·6
	14·1	14·9	13·1	13·6	13·9	12·9	13·2
	14·2	14·9	13·1	14·0	13·6	12·5	13·3
Means	14·2	14·9	13·1	13·8	13·6	12·7	13·4
Mar. 8	13·8	14·9	13·0	14·0	14·0	13·2	14·3
	13·8	14·9	13·1	13·8	14·2	13·1	14·0
	13·8	14·8	13·1	13·5	14·1	13·1	14·0
Means	13·8	14·9	13·1	13·8	14·1	13·1	14·1

	H_β. R–V.	H_γ. R–V.	H_ζ–H_ϵ.	H_ζ–H_δ.
Feb. 26	+1·3	+0·7	+1·1	+0·2
Mar. 2	+0·7	+0·7	+0·9	+0·2
,, 8	+1·1	+0·7	+1·0	+0·0
Means	+1·0	+0·7	+1·0	+0·1

On the curves the black dots represent very good measures, and the small circles second class but still fairly good measures.

From the actual measuring of the differences in intensity between the components of H_β and those between the components of H_γ the former were far more easy to measure than the latter. Greater weight should therefore be given to the H_β curve, although the apparent differences are not large : in fact it was rather surprising, when plotting the curves, to find such a close similarity between them.

Through both series of points smooth curves are shown : these have been drawn freehand and made to pass, as far as possible, through the mean positions of the points.

In both cases the maxima and minima occur at dates which closely correspond to those calculated from the minimum of 1924 December 3, namely, Julian Day 2424440·0 and J.D. 2424503·4 respectively, as indicated by the vertical arrows in fig. 1. Further, these epochs occur midway between those of zero velocity, as was noted in the case of the 1924–25 observations.

It will be noticed that in places there are considerable divergences from the mean curve which cannot be attributed to errors of measurement. Thus between phases 50 and 56 a group of points lies below both the mean curves. Between phases 106 and 110 another group falls below the mean curves, while from phase 114 to 120 a group falls above the curves. Again, about phases 18 to 25 the mean curve falls below another group of points, especially in the case of the H_β curve.

In the previous paper * it was stated that " at three points of the curve, namely, at phases 25, 51, and 106 days, there seem to be suggestions of changes of curvature. . . ." These may possibly correspond to the 18 to 25, 50 to 56, and 106 to 110 phases noted above.

There are three other points of interest attached to these curves.

The first is that the amplitude of the H_β curve is greater than that of H_γ. This is possibly due to the fact that the components of H_β preserve their narrowness in spite of great variations in their relative intensities, while those of H_γ increase more in their width, while their differences of intensities do not become so marked. These remarks would apply still more to the line at H_δ if a curve for this line were given.

The second point is that both the H_β and H_γ curves indicate closely similar epochs for zero velocity both on the upward and downward grades, namely, at phases 32 and 93 and 94, suggesting that these epochs would be the best to derive the length of the star's period.

The third and last point, although not a very prominent feature of the smooth curves, yet suggests a fact which may give an important clue to the solution of the riddle of this star. By examining the curves for H_β and H_γ in fig. 1, it will be seen that both reach a little greater distance above the zero line at maximum negative velocity than they do below that line at maximum positive velocity. This was also the case of the same components in the smooth curves representing the 1924–25 observations (see fig. 3 for the H_β components).

This peculiarity of the curves suggests that the central absorption

* *M.N.R.A.S.*, **85**, 587.

line of Hydrogen, at the epoch of maximum negative velocity, is displaced towards the violet more from its normal position than it is displaced towards the red from its normal position at the epoch of maximum negative velocity.

In other words, this indicates that the velocity in the line of sight is greater at maximum negative velocity than it is at maximum positive velocity, provided the assumption is correct that zero velocity takes place when the central absorption is placed midway between the bright components or when the intensities of the bright components are exactly equal.

Now the actual facts are the exact opposite. Ludendorff,* Cannon,† Jordan,‡ and Frédette§ have all published normal curves of velocity for this star, and the following values are taken from these curves :—

	Maximum Velocities.	
	Positive.	Negative.
Ludendorff	51	32
Cannon	43	18
Jordan	43	22
Frédette	45	20

Thus the greater velocities occur at the maximum positive velocity phase, and not at that of the maximum negative velocity phase.

It is quite possible, however, that the bright components of the hydrogen lines may not be symmetrically placed with regard to the normal wave-lengths of these lines. If this be so, then it will be seen that if a small positive velocity shift be given to them this would account for the discrepancy mentioned above.

Now of the above mentioned observers Jordan‖ is the only one who has measured the line of sight velocities for the bright components of the hydrogen lines. The measures are not so accurate as they are for the absorption lines owing to their nature. As he states, "Settings on the diffuse edges of those lines are, of course, more uncertain than those of the absorption lines, even though the latter may be diffuse : hence the accordance of the normal places with a mean curve is not as good as in the case of the absorption lines."

Nevertheless the published measures are sufficiently good to show without any doubt that these emission lines of hydrogen exhibit on the whole distinctly negative velocities, the only positive velocities, and these are very small, occurring at the epochs of maximum positive velocity. The actual figures read from his curve are 4 for maximum positive velocity and 23 for maximum negative velocity.

Again, therefore, the facts are contrary to the results that were expected.

Attention may here be drawn to the very striking and interesting differences in the appearance of the hydrogen lines on photographs

* *Astr. Nachr.*, **186**, 27, 1910.
† *Journ. R.A.S. Canada*, **4**, 200, 1910.
‡ *Pub. Allegheny Obs., Pittsburgh*, **3**, 39, 1913.
§ *Journ. R.A.S. Canada*, **19**, 189, 1925.
‖ *Pub. Allegheny Obs.*, **3**, 36, 1913.

taken with the Ottawa slit spectroscope and the Sidmouth prismatic camera, and it is very probable that these divergences may be due to the different instruments employed.

Thus, for instance, Frédette * states that sometimes the emission is so strong at H_β "as to completely obliterate the central absorption." No single instance of this occurs in any of the Sidmouth photographs throughout a whole cycle of the star's variation. In every case the bright components are very distinctly separated and their respective intensities easily measured.

Again, he says that "sometimes the emission may even be absent at H_ϵ." This also has not been observed on the Sidmouth photographs. It is true that the violet emission component is often absent, due no doubt to it being masked by the absorption line of ionised calcium at λ 3968·5, but the red component has always been noted as being present.

Lastly, he states that "H_ζ is present occasionally, always as a dark line." This line is one of the most prominent lines in the whole spectrum in all the Sidmouth spectra, being more conspicuous by the absorption displayed than by the emission. It is, however, always accompanied by an emission component on each side of it, although these are generally broad and weak in intensity.

At some of the phases of this star the central absorption lines of the hydrogen series, as will be shown later, increase in intensity and become very conspicuous, and at these phases the Balmer series of lines can be easily traced in the Sidmouth photographs down even to H_ρ (λ 3686·8). Reference to this will be made more fully towards the latter end of the following section (p. 489).

Cyclical Change of the Narrow Absorption Lines of Hydrogen.

It was pointed out in the previous paper † that the narrow absorption lines of hydrogen, separating the two bright components, appeared at times more conspicuous in some negatives by becoming broader. The discussion of the observations led to the conclusion ‡ that "there undoubtedly appears to be a variation of short period with quite a considerable amplitude, superimposed on the primary variation."

The new observations entirely endorse this conclusion, as will be seen from the following reduction.

The method of analysis employed was the same as that previously used—that is, the intensity of the H_ζ absorption line was measured against those of the H_ϵ and H_δ lines, the differences between the intensities being determined by the wedge method of measurement.

As in the case of the bright hydrogen lines, three settings were made on each line to form the first mean, and each negative was again similarly measured on two other separate dates, as shown in Table II. Further, the first twenty-four negatives were each similarly remeasured for the same reason as that stated for the bright hydrogen components.

All the measures were made by the writer, and the total number of settings amounted to 3618.

* *Journ. R.A.S. Canada*, **19**, 185, 1925.
† *M.N.R.A.S.*, **85**, 598. ‡ *Ibid.*, 601.

Table I. embodies all the facts. Columns 8 and 9 show the differences of intensities between H_ζ and H_ϵ and between H_ζ and H_δ respectively: the following two columns (10 and 11) display the differences from the

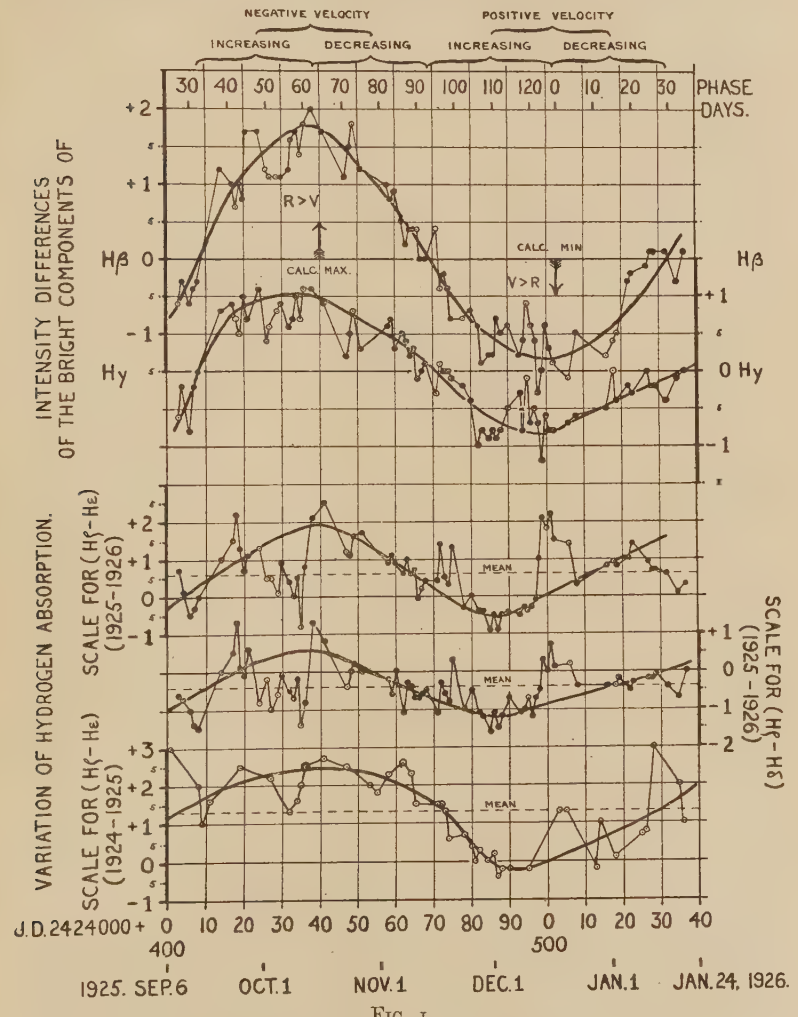

Fig. 1.

actual mean values of columns 8 and 9. The mean values employed are inserted in columns 8 and 9 just after the plate numbered 800 in column 1.

The data in columns 8 and 9 are all plotted in fig. 1 just below the two curves showing the intensity differences of the bright hydrogen lines. While the horizontal scale is the same as that for the bright

hydrogen lines, the vertical scale has been halved to economise space in the diagram.

As before, the black dots represent good measures and the small circles measures not quite so good, and these are all joined up by thin continuous lines. A smooth thick curve, drawn freehand, has been made to pass as far as possible through the mean positions of the measured points.

The first point to be noticed is the great resemblance of the curves to each other. They are based on absolutely independent measures. Dealing with the smooth curves first, it will be seen that the epochs of the maxima agree almost absolutely with those for the bright hydrogen components, and this was the case with the curves representing the observations made in 1924–25, one of which is again reproduced here at the bottom of fig. 1, representing the differences H_ζ–H_ε.

On the other hand, the recent observations clearly demonstrate that the minima are not coincident with those of the bright hydrogen components. The bright hydrogen components indicate distinct and pronounced minima at phase 126, while the absorption of hydrogen shows equally marked minima at phase 112, giving a difference of 14 days. In the case of the 1924-25 observations the phase dates were 127 and 114 respectively, giving a difference of 13 days.

The observations, then, clearly show that the epoch of maximum hydrogen absorption precedes that of maximum positive velocity by about 14 days, and that the epochs of minimum hydrogen absorption and maximum negative velocity are coincident.

The smooth curves for the hydrogen absorption display other points of interest. The first is that the amplitude of variation is much greater for H_ζ–H_ε than it is for H_ζ–H_δ. Why this should be so is not at first sight easy to explain. It may possibly have its origin in the fact that while H_δ has no other line closely adjacent to it, H_ε, on the other hand, is very close to the ionised calcium line at λ 3968·5. This calcium line, if it behaves like the other calcium line at λ 3933·8, varies, as will be seen further on, in intensity with the star's period, being very pronounced just before the time of maximum positive velocity and weak at all other times.

As the absorption at H_ε is at a maximum just before the epoch of maximum positive velocity, at which time the calcium line also exhibits its greatest absorption, the two working together might increase the total absorption at H_ε, and thus tend abnormally to lower the curve about this epoch and thus increase the amplitude.

A further point to which reference should be made is that H_ζ (fig. 1) exhibits on the average much stronger absorption than H_ε, as shown by the predominant number of points above the zero line or line representing the intensity of H_ζ as equal to that of H_ε. On the other hand, H_δ displays stronger absorption than H_ζ, as shown by the greater number of points below the zero line. On both curves a broken line representing the mean of each set of observations is given, differing greatly from the zero lines. The same peculiarity was shown by the 1924–25 observations, as illustrated by the H_ζ–H_ε curve given at the bottom of fig. 1.

Referring now to the secondary fluctuations in the curves illustrating the variation of hydrogen absorption, it will be noticed that they have a

very much larger amplitude than those exhibited in the curves of the bright components placed just above them in fig. 1. The dominant features are the excesses about phases 25, 42, 64, 98, and 125—all of which, with the exception of that at 98, were indicated in the 1924–25 observations, as shown in the curve at the bottom of fig. 1. The excess depicted at phase 86 in the earlier observations does not seem to have its counterpart in the recent observations. There appears to be only one prominent feature which seems to be common to all the four curves, and that is the group of points, which in all cases falls below the smooth curves between phases 50 to 58.

In the writer's previous paper * the tentative suggestion was made that "the only regular variation that seems to fit the measures is one having a period of 21 days, or equal in length to a sixth of the primary." The new observations, which are considerably more numerous and better distributed over the curve, fail, however, to corroborate any such regular periodicity. There seem to be indicated undoubted pulses of activity as exhibited by the hydrogen absorption, which appear to increase up to the epoch of maximum negative velocity and decrease down to that of maximum positive velocity, where another great impulse takes place.

A second graphical representation of this variation of the hydrogen absorption is given in fig. 2 and is shown as the second horizontal strip. It is given here in this form so that comparison can be made with the variations of the line intensities of calcium and helium which are described further on. The figures on which this is based are given in column 14 of Table I., and are so derived from those in column 10 that all the values are made positive to simplify plotting.

The cyclical nature of the absorption lines of hydrogen can be determined in quite another manner, although not in such great detail.

It was noticed, in examining several negatives, that when H_γ, H_δ, and H_ϵ exhibited greatest absorption, the other lines of hydrogen towards the ultraviolet became very sharp and clearly defined, and so could be traced far down into the ultraviolet. In fact, while in some negatives the hydrogen lines on the violet side of H_ζ could only be seen as far down as H_θ or H_ι (λ 3770·6), because they were so broad and ill defined, in others they were so sharp that they could be followed as far as H_ρ (λ 3686·8) or even a little further. These characteristics were conspicuous even in negatives that could not be called first class.

An attempt was therefore made to note the limiting hydrogen line visible in each negative. The actual method adopted was to give a number to each hydrogen line, thus 1 to H_β, 2 to H_γ, 3 to H_δ, and so on, and to record for each negative the corresponding number up to the last line that could be identified. When more than one negative was taken on the same evening the mean was adopted. The counts were made by Mr. D. L. Edwards and are tabulated in the last column (21) of Table I. The figures were then plotted, using the phase days as the abscissa.

The following was the result obtained:—

Between phases 30 to 100 no hydrogen line could be traced in any negative further down than H_λ. From phase 100 to phase 118 every

* *M.N.R.A.S.*, **85**, 601.

negative, without a single exception, displayed the hydrogen lines further into the ultraviolet than H_λ, and they extended in the mean to the line $H_\circ$. One negative at phase 104 showed the series down to

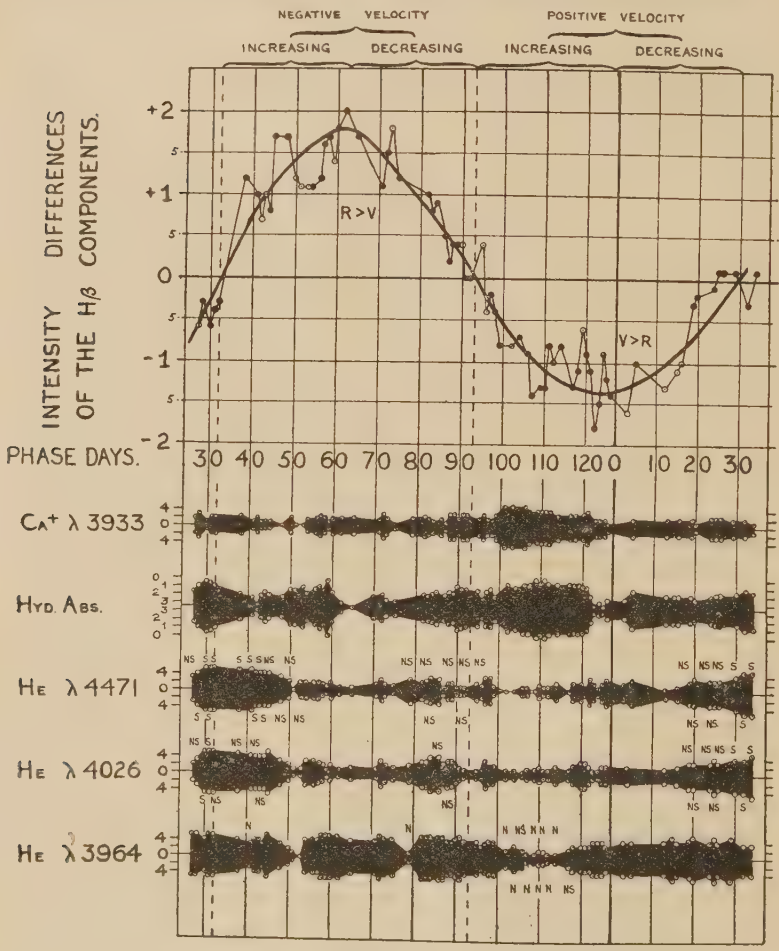

Fig. 2.

H_7. After phase 118 up to phase 30 again no line could be traced further into the ultraviolet than H_λ with one exception only.

By looking at the third and fourth curves in fig. 1, illustrating the variation of hydrogen absorption, it will be seen that the maximum absorption occurs at phase 112. Now this phase falls nearly midway between phases 100 and 118, thus showing that the extension of the visibility of the hydrogen lines in the ultraviolet is an indication or measure of greater hydrogen absorption in the star.

Cyclical Changes in the Intensities of the Calcium and Helium Absorption Lines.

From the 1924–25 observations of ϕ Persei it was shown that the absorption lines of ionised Calcium and the lines of Helium exhibited changes which were cyclical in nature but not similar to each other. Reference was made to the difficulty of determining their intensities, as all lines in the spectrum were variable in intensity at some phase or other. The method that was finally adopted was to make estimates of them on the basis of five categories of intensity, namely, (5) very strong, (4) strong, (3) moderate, (2) weak, and (1) very weak.

For the new series of measures another method has been employed. This consisted in selecting very carefully from all the negatives three typical samples which exhibited the intensity of the particular line to be examined as very weak (intensity 1), very strong (intensity 5), and intermediate or moderate (intensity 3). These three chosen negatives were then placed in a specially made frame backed by a plane glass reflector placed at an appropriate angle, in the order of the intensity of the line in question. The mode of operation was then to take the negatives at random and compare them with the samples, and see whether the special lines in them were similar in intensity to any of them or represented an intermediate stage between any two of them. In this way five categories of intensity were discriminated. The intensity represented by " 0 " indicated that the line was invisible.

The intensities of the individual lines of Ca^+ λ 3933·8 and He λ 4471·7, λ 4026·3, and λ 3964·9 were investigated, the comparisons being made by Mr. D. L. Edwards. All the reduced intensities, together with the character of the lines, are tabulated in Table I., columns 12, 13 and columns 15 to 20.

As some of the lines display varying characteristics, the following is the notation used to express them :—

(N) nebulous ; (S) sharp ; (NS) a narrow sharp absorption line superposed on a broad nebulous absorption band ; (V) very ; ($S^\times$) the absorption line is accompanied by bright borders, or, in other words, is " double bright."

In the accompanying subsections the behaviour of each line is dealt with individually.

The Ionised Calcium Line at λ 3933·8.

This line, as was formerly noted, is a sharp absorption line and in the best negatives is accompanied by bright borders. It has been treated here as an absorption line only and its intensity determined. For the intensity estimates the following three negatives were selected to serve as standards :—

No. 672 for intensity (1) ; No. 761 for intensity (3) ; and No. 747 for intensity (5).

All the data are contained in Table I., columns 12 and 13, and graphically displayed in fig. 2 in the first horizontal strip under the

intensity-difference curve, the greater breadth of the strip indicating increased intensity.

The main conclusion is fairly obvious, namely, that at the time of negative velocity the intensities are small, and at the time of positive velocity the intensities are great and very pronounced for the period embracing 24 days before maximum positive velocity. This result completely endorses the previously published conclusions from the 1924–25 observations.

The Helium Lines at λ4471·7 and λ4026·3.

The following negatives were selected to serve as standards for the intensity determinations of these lines, namely :—

No. 688 for intensity (1) ; No. 800 for intensity (3) ; and No. 647 for intensity (5).

These absorption lines are the strongest of the diffuse doublet system of helium, and they were each treated independently.

They appear sometimes as very sharp lines (S) (see Plate 6), sometimes as very nebulous lines (N), and, lastly, as very broad nebulous lines in the centre of which is a very sharp line (NS). These characters, as will be seen, are of a cyclical nature.

The data for the discussion are given in Table I., columns 15 to 18, and are graphically shown in two horizontal strips in fig. 2. The letters against some of the points of observation refer to the character of the lines as previously described, but where no letter is given the character is nebulous (N).

It will be seen that both strips are almost identical and so can be treated as one in the discussion.

Their general behaviour is as follows: At the maximum positive velocity phase the lines are weak to moderate and nebulous. They then increase in intensity, and at the same time the sharp line appears in the centre of the nebulous line. About the intermediate phase at zero velocity they become exceedingly strong and sharp, the nebulous character disappearing altogether. Approaching the phase of maximum negative velocity they become purely nebulous again and weaken. Just before the next zero velocity phase is reached the lines again strengthen, and here the nebulous lines are accompanied by a sharp central line. They then become again very weak and nebulous and so complete the cycle.

The behaviour of these helium lines is practically the same as that recorded by the 1924–25 observations, considering the comparative paucity of the observations then dealt with.

It will be noted that both the character and the intensity of these helium lines suggest a period of variation equal to half that of the main period.

Curiously enough Frédette * reproduces a half-period curve for the behaviour of the hydrogen lines, and these lines seem to vary both their intensities and characters not only in a similar manner but at the same epochs. Thus the maxima of his curves correspond, as he says, to lines

* *Journ. Roy. Astr. Soc. Canada*, **19**, 189, 1925.

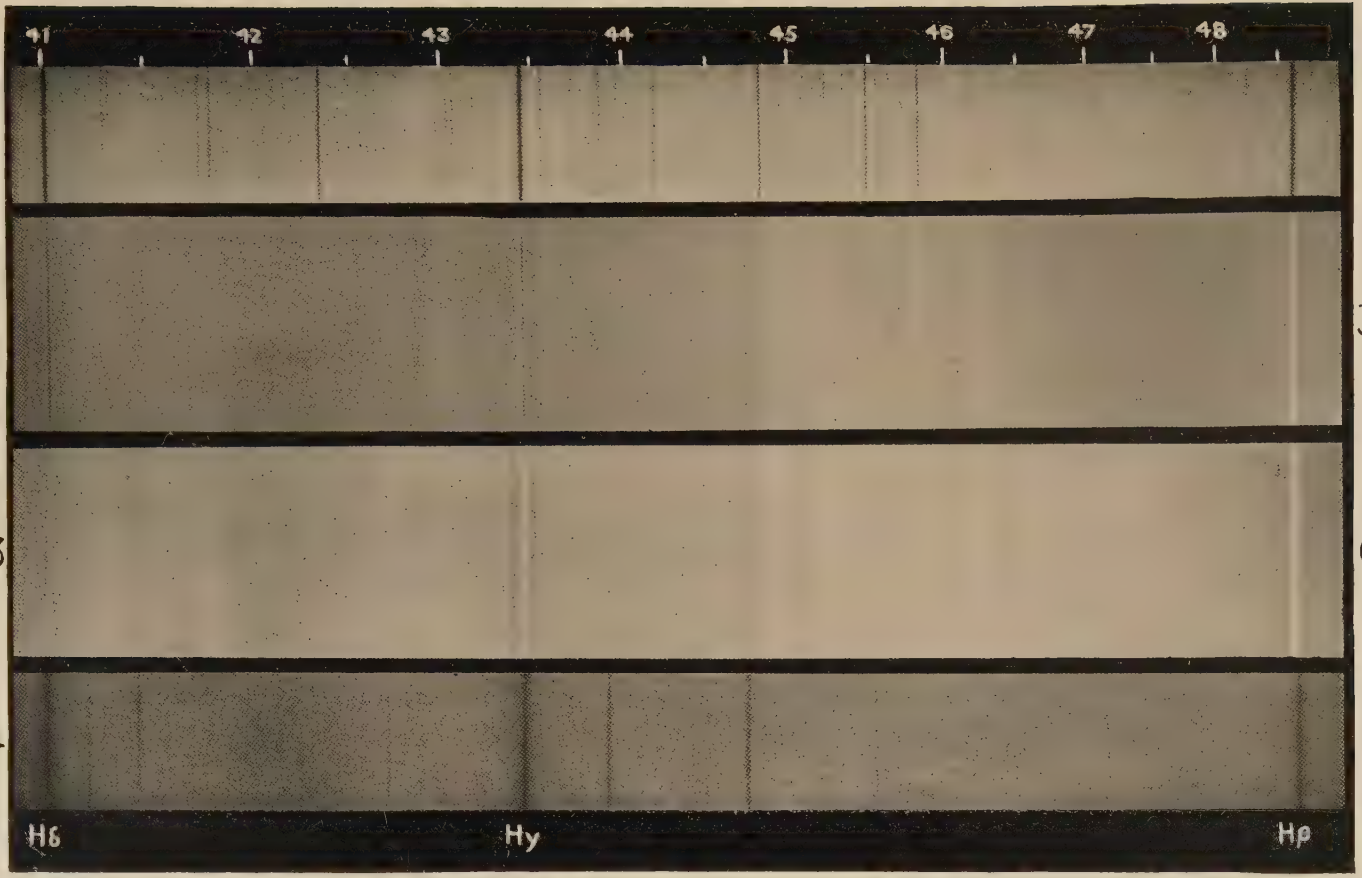
41
42
43
44
45
46
47
48
1
2
3
4
32
62
Hδ
Hγ
Hρ

which are " sharp, intense, and narrow," and the minima to lines which are " broad, weak lines with diffuse borders." No such half-period variation has been deduced from the hydrogen lines discussed from the present series of observations, as will be observed by comparing in fig. 2 the hydrogen absorption strip with those for the two helium lines dealt with above.

The fact that at some phases either the nebulous or the sharp lines appear separately, and at other phases they appear simultaneously, suggest that there probably may be two separate sources responsible for the helium absorption.

The behaviour of these helium lines throughout the complete cycle is thus very different from that indicated by the ionised line of calcium, and might be stated generally to be almost the inverse.

Attention may be drawn here to a peculiar character sometimes assumed by the helium line at $\lambda 4471{\cdot}7$. It appears as a double absorption line, the distance between the components being about the same as that of the components of the bright ionised lines adjacent to it. The red component is always stronger than the violet component, and in only one instance is the other line of the same series, namely, $\lambda 4026{\cdot}3$, observed to be of the same double character. In all cases the red components of the hydrogen lines at H_β and H_γ are simultaneously brighter than the violet components.

An examination of all the negatives, with special relation to this feature, has been made, and ten cases were recorded. They fall into two distinct groups. Four of the negatives are included between the phases 28 to 41, and six between the phases 83 to 91. A glance at fig. 2 will show that this special feature occurs just at those two phases at which the helium line at $\lambda 4471{\cdot}7$ (as there indicated in the middle strip) is marked as exhibiting sharp or sharp on nebulous lines.

A re-examination of the negatives taken during the 1924–25 observations showed that three negatives exhibited the same characteristic, one occurring at phase 33 and the other two at phases 82 and 86. Thus the phases are coincident in both series of observations.

The Helium Line at $\lambda 3964{\cdot}7$.

This helium line belongs to the principal singlet system, and is the only member which falls within the photographic region of the plates used that is suitable for intensity determination. The following negatives were used for the selected standards of the three intensities, namely :—

No. 751 for intensity (1) ; No. 765 for intensity (3) ; and No. 678 for intensity (5).

Exactly the same procedure of reduction was adopted as in the cases of the other helium lines, and the estimated intensities with the characters of the line are given in Table I., columns 19 and 20. The variations in intensity and characteristics are graphically shown in fig. 2 at the very bottom.

Unlike the other helium lines, this line is nearly always sharp, but is occasionally nebulous, and in two instances has a thin absorption line

down its centre. On this account only the nebulous intensity observations are lettered in the diagram, all the other points representing the line as of a sharp character.

It will be seen that this line is for the most part of the cycle strong, but it shows a distinct brief weakening at about phase 50, and a more prolonged weakening between phases 100 and 120. Both these occurrences are echoed in the case of the two other helium lines. On the other hand, where the other helium lines are distinctly weak the line at λ 3964·7 is comparatively strong. The strengthening of both the lines of the diffuse doublet system at about phase 85 corresponds to the maximum intensity of the line λ 3964·7 at the same phase.

The variation in the intensity of this line approximates fairly closely to that previously deduced from the comparatively few observations dealt with in the 1924–25 estimates, and the character of the line varies in almost the same manner as was described on that occasion.

Comparison with the 1924–25 *Results.*

In order to display graphically the results derived in the preceding paragraphs in comparison with those given by the 1924–25 observations, the diagram published in the earlier communication in a slightly altered form has been reproduced here (fig. 3) on a very much smaller scale and placed alongside a reduced copy of fig. 2. It is to be noted that no horizontal representation is given for the variation of intensity of the bright ionised lines in the 1925–26 diagram, but a strip is given showing the behaviour of the helium line at λ 4026·3 in relation to that of λ 4471·7. Again, in the 1925–26 diagram for the line at λ 3964·7 all the points indicate sharp lines except where otherwise indicated, while in the 1924–25 diagram all the points represent nebulous lines except where otherwise shown.

The result of this comparison seems to be that, in spite of the very much larger number of observations utilised in the 1925–26 reduction, the main features of the changes exhibited in the 1924–25 reduction are fairly closely upheld.

The Absorption Line of Ionised Magnesium at λ 4481·3.

It was pointed out in the previous paper * that the absorption line of ionised magnesium at λ 4481·3 was practically on the verge of invisibility or absent in most of the photographs. This statement is fully corroborated by the new series of observations.

Its presence seems to occur very occasionally at about the phase of maximum negative velocity, and becomes a little more conspicuous from phases 107 to 125 when hydrogen absorption is at its maximum.

The Bright Ionised Lines.

So far as can be gathered from a thorough examination of all the negatives, the most conspicuous bright ionised lines of iron and titanium

* *M.N.R.A.S.*, **85**, 602, 1925.

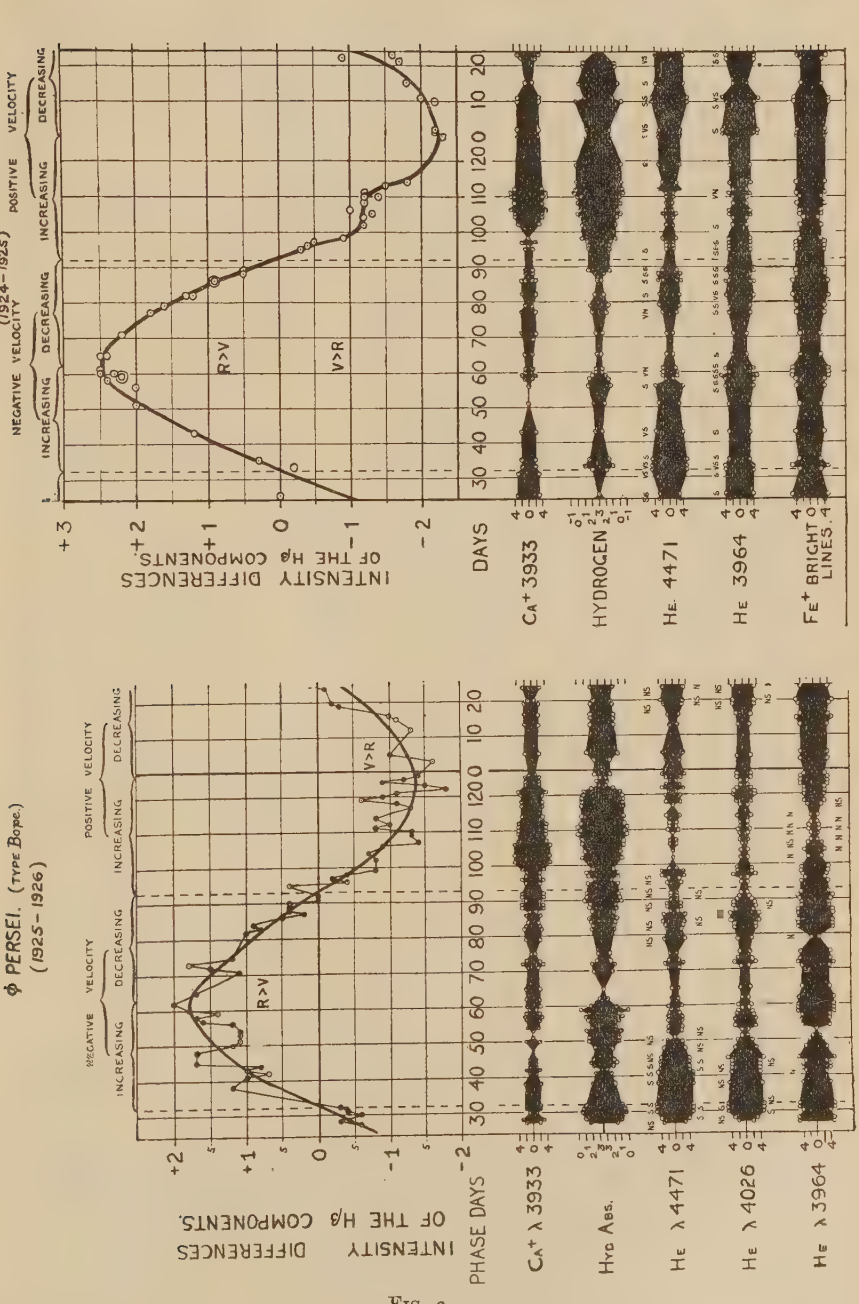
φ PERSEI. (Sp. Type Bope.)
(1924–1925)
NEGATIVE VELOCITY
INCREASING
DECREASING
POSITIVE VELOCITY
INCREASING
DECREASING
R>V
V>R
INTENSITY DIFFERENCES OF THE Hβ COMPONENTS.
DAYS
Ca+ 3933
HYDROGEN
He 4471
He 3964
Fe+ BRIGHT LINES.
φ PERSEI. (Type Bope.)
(1925–1926)
PHASE DAYS
Ca+ λ 3933
Hyd Abs.
He λ 4471
He λ 4026
He λ 3964

Fig. 3.

do not seem to vary in intensity to any appreciable extent : they are a very conspicuous feature of all the negatives and are always moderately strong, sharp, and double. The wave-lengths and origins of these lines were tabulated in the previous communication.*

From the observations of 1924–25 it was stated that these lines behaved in a similar way to those of hydrogen—that is, that when the red components of the bright hydrogen lines were stronger than the violet components, so the red components of the bright ionised lines were stronger than the violet components. This conclusion, however, must now be modified in the light of the greater number of the new observations and their more even distribution over the whole period.

To inquire more minutely into their behaviour four fairly conspicuous double-ionised iron lines were selected, namely, λλ 4179·0, 4233·8, 4351·9, and 4576·5, and in the case of every negative the brighter of the two components was determined.

It was finally concluded that in the case of the lines at λλ 4233·8 and 4576·5 the red component was on the average the brighter, and in the case of the lines at λλ 4179·0 and 4351·9 the violet component was more frequently the brighter. These changes, so far as could be determined, had no connection with phase.

A feature conspicuous in all negatives taken at any phase, and more especially noticed in every enlargement that has been made, is that between the ionised iron double at λλ 4173·5 and 4178·9, and the ionised iron line at λ 4238·8, this region shows almost continuous homogeneous absorption. It is clearly visible in the original enlargement from which Plate 6 has been taken, although it may be a little less obvious in the reproduction. It is also easily seen in the reproductions of the spectra published in the account of the 1924–25 observations.†

As there seems to be no reason for any absorption to be present here it must be due to an effect of contrast, indicating the absence of many bright lines in this region. If this be so, then the general spectrum must contain very many more bright lines than have been identified so far, lines, however, that will be relatively weak.

A more detailed investigation of these lines would no doubt prove of interest, and it is hoped that this may be undertaken in the near future.

φ Persei as a Variable Star.

It was on the basis of the discovery of the cyclical variability of the hydrogen absorption in this star that the writer previously suggested that φ Persei should present changes of magnitude and thus be found to be variable with a period of 126·8 days.

The present observations not only endorse this view, but go a step further by showing that this change of magnitude should exhibit a secondary variation corresponding to the changes indicated in the curves showing the variation of the hydrogen absorption (fig. 1).

Just as it was important to observe the star every available fine night

* *M.N.R.A.S.*, **85**, 590, 1925.
† *Ibid.*, Plates 16 and 17.

to record the changes in the intensities of the bright hydrogen components, so observations for magnitude should also be very frequent owing to the large amplitudes of the secondary variation of the hydrogen absorption.

The Period of Velocity Variation.

An important result of the reduction of this new series of photographs is the corroboration of the fact, mentioned in the former communication, that the prismatic camera is a very serviceable instrument for accurately determining the form of the curve representing line of sight velocities for this particular type of star.

Further, for the precise determination of the length of the period the epochs when the line of sight velocities are zero can be most easily and accurately ascertained, for these depend simply on the determination of the equality of brightness of the red and violet components of the hydrogen lines, an observation which can readily be made by the wedge method or even by direct observation. The curve cuts the zero velocity line at a very acute angle, both on the ascending and descending side, thus clearly defining the point of intersection with the time scale.

Lastly, the revised length of the period of this star, namely, 126·8 days, deduced by the writer from the observations made in 1924–25 is endorsed by the present series of observations, the observed and calculated main phases agreeing very closely.

Summary.

(1) This paper contains a discussion of 106 photographs comprising a complete cycle of ϕ Persei from 1925 September 9 to 1926 January 13.

(2) It was undertaken to discuss in greater detail the variations in the spectra suggested in the previous paper (*M.N.R.A.S.*, **85,** 580).

(3) The results corroborate in the main the deductions previously made.

(4) The earlier suggestion of a secondary period of 21 days is here modified. It is now indicated that there appear to be pulses of activity, as exhibited by the absorption of hydrogen, which seem to increase up to the epoch of maximum negative velocity and decrease down to that of maximum positive velocity.

(5) The epoch of greatest hydrogen absorption is shown to occur about 14 days before that of maximum positive velocity, while those of least hydrogen absorption and maximum negative velocity are coincident.

(6) The strongest hydrogen absorption is further indicated by the greater extension of the series of hydrogen lines into the ultraviolet.

(7) The character and intensity of the helium lines suggest a period of variation equal to half that of the primary variation.

(8) The components of the bright ionised lines occasionally alter their relative intensities. They do not all, however, behave alike, neither do they present any apparent cyclical change.

Description of the Plate.

Plate 6. Comparison of two spectra of φ Persei with No. 1 α Cygni (typical of ionised lines) and No. 4 γ Orionis (typical of helium lines) between H_β and $H\delta$, and enlarged 3·6 times from the original.

The φ Persei photographs Nos. 2 and 3 were taken at two important phases. The first at phase 32 (Negative No. 648) shows prominently the equality in brightness of the components of the bright hydrogen lines and the sharp and strong helium line at λ 4471·7. The second at phase 62 (Negative No. 695) illustrates the greatest difference in the relative intensities of the bright hydrogen components, and the weak and nebulous character of the same helium line. Both photographs exhibit clearly the duplicate character of the bright ionised lines.

Attention may be drawn to the fact that the spectrum of φ Persei is extremely difficult to reproduce satisfactorily owing to the admixture of bright and dark lines, none of which except hydrogen are very strong.

All the photographs were broadened by means of the clepsydra apparatus.

On the Spectrum of Nova Pictoris. By Joseph Lunt, D.Sc. (Plates 7–10.)

(*Communicated by H.M. Astronomer at the Cape.*)

Nova Pictoris was discovered on the morning of 1925 May 25, by Mr. R. Watson of Beaufort West, South Africa. It was of about the second magnitude at discovery, situated near α Pictoris. We are greatly indebted to Mr. Watson for his vigilance and for his prompt telegraphic notification to the Cape Observatory, which enabled spectrograms to be secured on the evening of the day of discovery.

This is the second Nova which Mr. Watson has discovered, the first being his independent discovery of Nova Aquilæ No. 3, of which he also sent prompt notification to this Observatory. These are the rewards which fall to amateur astronomers who keep a constant watch on the skies and learn the configurations of the constellations well enough to detect a stranger in the familiar groupings.

The Nova was in a very favourable position: $\alpha = 6^h\ 34^m\ 57^s$, $\delta = -62^\circ\ 34'\ 34''$, for, although the hour angle of the early observations was from 5^h to 7^h West, it was possible to photograph its spectrum without a break until the spectrograph was dismounted on 1926 March 15.

When the star became too far West to observe in the evening sky, which happened fortunately in the Cape winter with its long nights, it was possible to observe it—from July 6—more and more favourably placed in the sky before dawn. It was on the meridian at dawn, with an altitude of 61° 22′ on October 21.

Four plates were secured on May 25, and thereafter no opportunity was lost of securing additional observations when the sky permitted; 133 plates were secured before the termination of observations.*

* The plates were taken by Drs. Jones and Lunt and Messrs. Cheeseman, Jackson, Mullis, Turner, and Baines, and developed usually by Turner.

The four-prism slit spectrograph of the 24-inch Victoria telescope, with the short camera, was used throughout. The spectrograph was designed for radial velocity work in the region of spectrum near H_γ, and, although excellent for that work, it is not ideal for work on Novæ spectra where it is desirable to secure as long a range of spectrum as possible in good focus. The camera was not designed to take thin bent plates or films, and the curvature of the field of the camera necessitated a change of tilt when it was desired to photograph either the K region or the region near H_β. The differences of focus of the objective for different wave-lengths was an added difficulty, which is not met with when using a reflector. The spectral region covered by the observations extends from the nebular line λ 3869 in the ultra-violet, to the enhanced iron line λ 5019 beyond H_β towards the red. Imperial Eclipse plates were used throughout.

The measures were made by the writer on the Toepfer machine and reduced by Hartmann's formula. The scale of the plates is given in *M.N.*, **79**, 418. Iron comparison lines were measured frequently along each Nova spectrum, and corrections were applied to each measured wave-length in accordance with the deviations of the iron lines from their positions in Rowland's tables. For the sake of uniformity in computing, all wave-lengths have been reduced to hundredths of an A° and velocities to tenths of kilometres. Final velocities are rounded off to kilometres. Wave-lengths, of course, vary very much in accuracy from fine sharp lines to diffuse nebulous lines or bands, and the accuracy of the wave-lengths must be judged from the O–T columns.

The life-history of the Nova, as far as these observations are concerned, may be divided into eleven periods, throughout each of which the spectra were more or less constant in character. In each period certain plates were selected as typical and of good quality for measurement, and it would have been superfluous to have attempted to measure all the plates secured.

The periods are as follows :—

Period.	Dates.		Plate Nos.
I.	1925 May 25 to	June 5	7290–7307
II. (transition)	June 8 ,,	June 10	7308–7319
III.	,, 12 ,,	,, 17	7320–7327
IV.	,, 20 ,,	July 3	7332–7356
V. (transition)	July 6 ,,	July 18	7357–7371
VI.	,, 25 ,,	Sept. 3	7375–7410
VII. (transition)	Sept. 4 ,,	,, 15	7411–7417
VIII.	,, 17 ,,	Oct. 24	7419–7434
IX.	Nov. 3 ,,	Dec. 21	7439–7475
X.	1925 Dec. 28 ,,	1926 Jan. 18	7476–7485
XI.	1926 Jan. 23 ,,	Mar. 13	7486–7501

The spectrum of each period will now be considered in detail.

Notes on Plate 7.

Plate 7301, 1925 June 4.—A typical spectrum of Period I. H_γ is the strong dark line on the right of the dotted iron line λ 4337.

Plate 7322, 1925 June 12.—A typical spectrum of Period III. Note the triple H_γ (dotted), the right one in its original position on the right of Fe 4337, another on the left of the same Fe line, and a third, heavy and strongly displaced, on the left of Fe 4326. Note the bright H_γ band and other bright bands broken up by dark lines and the duplication of lines on the right of spectrum.

Plate 7326, 1925 June 17.—Note the diminished shift of the strongly displaced H_γ, showing a *retardation* of the radial velocity as compared with June 12. The lower strip of Plate 7326 shows bright H_β (dotted) with the very heavy, strongly displaced dark line on the left (dotted). The bright band extends to $H_\beta{}^2$ and is similarly extended to the red. Note the normal bright bands, bordered on the violet side by dark lines, on the left of H_β.

Plate 7346, 1925 June 27.—A typical spectrum of Period IV.; the continuous spectrum fading and the bright bands more definitely emerging. The dark lines are fading out. A fine bright line and the oblique white mark pointing to it are scratches on the glass side of the negative. On the lower strip of plate 7346, note the bright H_δ showing the dark line belonging to Period I. (dotted). Fe_E 4233 (dotted), now definitely emerged (compare plates 7322, 7326). Note the bright H_γ also showing the original dark H_γ (dotted), and the extension to the red due to Fe_E 4352 (dotted).

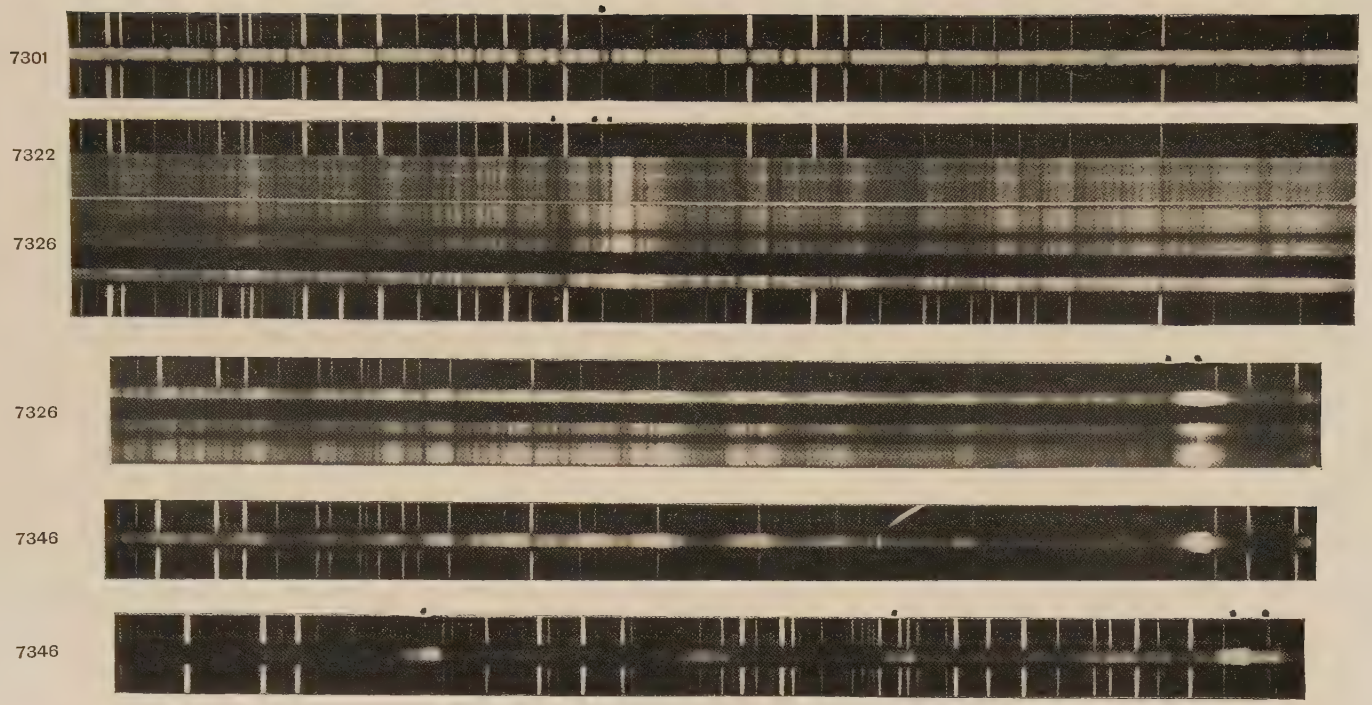

Spectra of Nova Pictoris 1925 June 4 to June 27.

Period I. 1925 May 25 to June 5. Plates 7290–7307.

This is a period of fluctuating brightness, leading up to the first maximum. The magnitude curve, divided into periods, is shown in fig. 1.* It is based on all the available observations by numerous observers.† Fuller details will, no doubt, be given elsewhere, but it is sufficient for our present purpose to show the general trend of the magnitude variations. The constancy of the magnitude about 4·8 since the beginning of 1926 is worthy of note as an indication that the Nova will be observable over a very lengthy period.

The spectrum is a continuous one crossed by heavy broad absorption lines, many of them bordered on the red side by an ill-defined bright line or shading (see Plate 7, 7301). Measures on three plates were made between H_ζ and Fe_E (enhanced iron) λ 4584. The lines may be summarised as under, including the components of blends which could not be resolved :—

	$Ti_{E\cdot}$ Ti.	$Fe_{E\cdot}$ Fe.	$Sc_{E\cdot}$	$V_{E\cdot}$ V.	$Cr_{E\cdot}$ Cr.	$Y_{E\cdot}$	$Zr_{E\cdot}$ Zr.	$Ca_{E\cdot}$ Ca.	$Sr_{E\cdot}$	Al.	$Mn_{E\cdot}$ Mn.	$Mg_{E\cdot}$	Totals.
	44	23	10	10	5	3	1	2	2	..	1	1	102
	9	32	..	1?	4	..	3	2	..	2	1?	..	54
Totals,	53	55	10	11	9	3	4	4	2	2	2	1	156

Details are more fully given in Table I. The measured wave-lengths corrected for shift can be obtained from the columns, Tabular and O–T.

Nearly two-thirds are enhanced lines, testifying to the relatively high temperature of the absorbing layer. Over two-thirds of the lines belong to iron and titanium. The scandium lines are very strong, but most of them occur as blends. V, Cr, Y, and Zr are next in importance. The above does not include the hydrogen lines and five lines which have not been traced to their origins, including the strong solar line at λ 3938·55. It is noteworthy that many lines correspond to unorigined lines in Rowland's solar spectrum. It is particularly fortunate that records of the spectrum were secured at this early stage when the spectrum was almost a normal star spectrum, and the displacement of the lines was quite ordinary. No speculations as to the meaning of the spectra will be attempted at this stage ; they are better left until the spectra have been described.

The lines show a weighted mean radial velocity of about −71 km./sec.

Radial velocities are given in Table VII.

* The two peak observations 1·2 and 1·0 are placed a day too early in the figure.

† In South Africa : Messrs. Watson ; Smith ; Long ; Ensor ; Reid ; Houghton ; Cousins, A. W. J. ; Cousins, C. A. ; and the observers on duty at the Cape Observatory (Victoria telescope). In Australia : Johnson. In South America : Dawson ; Hartmann ; Paraskevopoulos, Dr. and Mrs. See *Ast. Nach.*, 5413, and *Harvard Bulletins*, 822–826.

TABLE I.

Period I. 1925 May 25 to June 5. Plates 7291–7307.
„ III. „ June 12 „ June 17. „ 7320–7327.
„ V. „ July 6 „ July 18. „ 7357–7371.

Origin.	Tabular λ.	O–T. I.	O–T. III.	O–T. V.
$H\zeta$	3889·20	+·06		
V ?	96·28	+·01		
Ti_E	3900·68	−·28	..	+·07
V_E	03·40	−·08		
Fe_E	06·04	−·06		
Ti_E	13·61	+·20	..	+·06
Fe	16·88	−·12		
Fe	30·45	+·15		
Ca_E (K)	33·83	−·29	..	+·07
Co ?	*36·12*	..	..	*+·34*
Un	38·55	+·07	..	−·18
Al	44·16	+·06	..	+·23
V_E	52·10	+·32	..	−·01
Zr_E	58·36	+·30		
Fe	60·42	+·02		
Al	61·67	−·04	..	+·01
Ca_E (H)	68·63	−·16	..	−·05
	(69·41)	−·44		
H_E	70·18	..	+·08	+·37
V_E	73·80	+·37	..	−·09
Fe	74·54	−·18		
?	[78·38]			
Ti (du)	82·27			
	(82·50)	−·08	−·03	
Y_E	82·74			
Ti_E	87·76	+·04	−·07	
Zr	91·33	+·31	−·05	
V_E	97·30	..	−·02	−·09
	(97·43)	+·09		
Fe	97·55			
Zr	99·12			
	(99·21)	−·05		
V_E	99·30	..	−·06	
Fe_E	4002·65	−·11	−·45	
Fe	05·41			
	(05·64)	+·04	−·04	
V_E	05·86	..	..	+·01

Origin.	Tabular λ.	O–T. I.	O–T. III.	O–T. V.
Ti_E	4012·54			
	(12·59)	+·01	−·09	−·04
Cr_E	12·63			
Fe (Sc_E)	14·68	+·06	+·09	
V_E	23·53	+·12	+·01	−·01
Ti_E	25·29	−·03	−·05	+·05
Ti_E	28·50	+·05	−·09	+·02
V_E	35·88	−·06	−·07	−·02
Fe	45·98	−·04	−·06	−·01
Fe_E	48·82			
	(48·87)	+·03	+·07	
(Mn, Cr)	48·91			
Fe (du)	52·26	+·18	−·02	
V_E	53·80			
	(53·89)	+·14	+·17	+·01
Ti_E	53·98			
Fe	63·76	−·05	−·07	·00
Cr, Fe	67·14	−·02	−·09	−·03
Fe	71·91	+·08	−·04	+·01
Fe	*73·92*			
	(*74·43*)	..	..	*+·14*
Fe	*74·95*			
Sr_E	77·89	−·12	+·07	
$H\delta$	4101·89	−·14	+·30	+·12
Fe	*04·29*	..	..	*−·01*
Cr_E	11·25	+·21	−·02	
Fe	18·71	−·14		
	(18·88)	..	+·01	
Fe	19·05			
Fe	22·67	+·33	+·22	+·16
Y_E	25·10	−·06	−·04	
Mn_E	28·36	+·13	+·02	−·14
Fe	44·04	−·06	−·15	
Zr	49·36	+·06	−·01	
Ti_E	61·68	+·08	−·02	+·02
Ti_E	63·82	−·02	−·02	−·01
Ti_E	72·07	+·17	+·04	+·01

Note.—The wave-lengths in italics in Period V. only.

TABLE I.—*continued.*

Origin.	Tabular λ.	O–T. I.	O–T. III.	O–T. V.
Fe	4173·48			
	(73·60)	..	−·01	+·06
Ti_E	73·71	+·08	+·06	
Y_E	77·77	+·17	−·14	
Fe_E	79·03	+·13	+·37	−·02
Fe	*81·92*	..	..	*−·44*
Fe	4202·20	+·35	·00	
V_E	05·24	+·03	+·04	
Sr_E	15·70	−·15	−·04	
Fe	24·34	..	−·11	
	(24·88)	−·20		
V_E	25·41	..	·00	
Ca	26·90	+·15	+·16	−·06
Fe_E	33·33	−·09	−·03	−·05
Fe	*36·11*	..	..	*−·23*
Cr_E (Mn_E)	42·54	−·01	·00	+·05
Sc_E	47·00	−·03	+·08	+·01
Fe (du)	50·62	+·04	+·24	
Cr	54·51	+·16	+·02	+·02
Fe	58·48	+·03		
Fe	60·64	+·15	−·04	
Cr_E	62·15	+·16	−·04	−·01
Fe (Ti_E)	71·93	−·13	−·23	+·05
Fe	73·48	+·37	−·01	−·12
?	[75·91]			
Fe, Ti	78·39	−·06	+·11	
Ti	87·57	+·09		
Ti_E	88·04	−·06	−·06	−·01
Ti_E	90·38	−·08	−·36	−·02
?	[*93·17*]			
Ti_E	94·20	+·11	−·26	+·13
Fe_E	96·74	+·14	+·03	−·09
Ti_E	4300·21	·00	−·27	+·02
Ti_E	*02·09*	..	..	*−·04*
Fe_E	02·35			
	(02·52)	+·05	−·02	
Ca	02·69			
Fe_E	03·34	−·03	+·21	+·03
Ti, Sc_E	06·08	+·14		
(Ti_E) Fe	08·08	−·02	+·03	·00
Ti_E	13·03	+·10	−·18	−·08
	(13·64)	+·17		
Sc_E	14·25	..	−·25	−·03
	(14·70)	+·03	+·18	
Ti_E	15·14	..	+·14	+·06
Sc_E	4320·91	..	..	+·03
	(21·02)	−·02	+·07	+·16
Ti_E	21·12			
Sc_E	25·15	..	−·02	−·02
	(25·55)	−·12	+·08	
Fe	25·94	..	..	−·08
Ti_E	30·50			
	(30·69)	−·02	+·13	−·01
Ti_E	30·87			
Ti_E	38·08	−·10	+·05	+·01
H_γ	40·63	+·02	+·01	+·08
Ti_E (Mn_E?)	44·45	−·03	−·18	
Fe_E	51·93	−·15	−·06	−·01
Sc_E	54·80	+·03		
?	[59·30]			
Ti_E	67·84	+·01	−·07	+·13
Sc_E	74·63	+·19	+·15	+·11
Fe	83·72	..	+·11	+·02
	(84·64)	+·05		
Fe_E	85·55	..	−·03	+·07
Ti_E	*87·01*		..	*−·05*
Ti_E	91·19	+·02	−·10	
Ti_E	95·20	−·23	+·09	+·04
Ti_E	99·94	..	..	+·01
	(4400·25)	−·05	−·10	−·19
Sc_E	00·56			
Fe	04·93	−·05	−·06	+·05
Ti_E	11·24	+·16	−·05	+·04
Fe	15·29			
	(15·51)	+·08	+·13	+·08
Sc_E	15·72			
Ti_E	17·88	−·05	+·21	−·11
?	[*19·89*]			
?	[22·48]			
Ti_E	43·98	+·13	+·09	+·06
Ti_E	50·65	+·09	+·02	−·23
Ti_E	64·62	+·02	+·02	+·07
Ti_E	68·66	−·16	+·09	−·03
Ti_E	71·02	+·38	+·13	−·28
Fe	72·88			
	(72·93)	+·02		
Mn ?	72·97			
Mg_E	81·40	+·08	+·16	
?	[*84·75*]			

TABLE I.—*continued.*

Origin.	Tabular λ.	O–T. I.	O–T. III.	O–T. V.
Ti$_E$	4488·49	..	..	−·07
(88·92)		−·07	−·04	
Fe$_E$	89·35			
Fe$_E$	91·57	+·20	−·03	
Ti$_E$	4501·45	−·05	+·01	+·12
Fe$_E$	08·46	+·06	−·21	−·04
Fe$_E$	15·51	−·03	−·14	
Ti (du ?)	18·20	+·56	+·23	+·59
Fe$_E$	20·40	+·14	−·17	−·14
Fe$_E$	22·80	+·13	−·04	+·13
Fe	28·80			
(29·23)		−·01		
Ti$_E$	29·66			
Ti$_E$	34·14	+·06	−·13	−·11
Fe$_E$	4541·51	+·13	−·54	
Ti	44·86	+·03	−·11	
Fe$_E$	49·64			
(49·73)		+·07	+·21	+·21
Ti$_E$	49·81			
Ti	55·66			
(55·86)		−·15	+·10	
Fe$_E$	56·06	..	·00	
Cr$_E$	58·83	+·25	−·08	
Ti$_E$	63·94	+·08	+·16	
Ti$_E$	72·16	−·05	·00	−·06
Fe$_E$	76·51	+·09	−·25	
Cr	80·23	−·02		
Fe$_E$	84·02	−·15	−·52	−·11

Period II. 1925 June 8 to 10. Plates 7308–7319.

This is a very important transition period of three days, coinciding with the first and highest maximum of light, bridging Period I. and Period III. Violent changes are now in progress, the lines begin to broaden towards the violet, become very diffuse and unfit for measurement in many cases, gradually settling down to a spectrum much more displaced to the violet than in Period I. In many cases the remnants of the original spectrum remain in their old positions and form doubles with the shifted lines (see Plate 7, 7322–7326).

The doubling of the lines is well seen in the following measures of Plate 7317 on June 10:—

Measured λ in Nova Spectrum.	Rowland's λ in ⊙.	Origin.	Shift in Km./sec. (1).	Shift in Km./sec. (2).	Corrected λ's.	Mean Corrected λ.	O–T.
4484·31	4488·49	Ti$_E$	−279·3		4488·64	4488·44	−·05
87·05				−96·2	·23		
96·83	4501·45	Ti$_E$	307·7		4501·17	4501·30	−·15
4500·23				81·3	·42		
10·97	15·51	Fe$_E$	301·5		15·32	15·32	−·19
14·12				92·3	·31		
18·10	22·80	Fe$_E$	311·6		22·46	22·46	−·34
21·26				102·1	·45		
45·26	49·73	Fe$_E$ Ti$_E$	294·6		49·64	49·81	+·08
48·78				62·6	·98		
51·97	55·86	Ti$_E$ Fe$_E$	256·0		56·36	56·18	+·32
54·80				69·8	·00		
68·00	72·16	Ti$_E$	272·8		72·41	72·41	+·25
71·21				62·3	·41		
79·65	84·02	Fe$_E$	285·8		84·07	84·16	+·14
83·04				64·1	·25		
Mean displacement,			−288·7	−78·8			
Correction to ⊙,			− 2·4	− 2·4			
			−291	−81 km./sec.			

Numerous new lines appear, and a bright band spectrum develops by the extension of the original bright area towards the red on one side and to the shifted dark lines on the violet side. The narrowing of the lines is a noticeable feature. More complete measures are better deferred until the next more stable period (III.) has set in.

Period III. 1925 June 12 to 17. Plates 7320–7327.

This period coincides with the beginning of the rapid drop in magnitude shown in the magnitude curve of fig. 1.

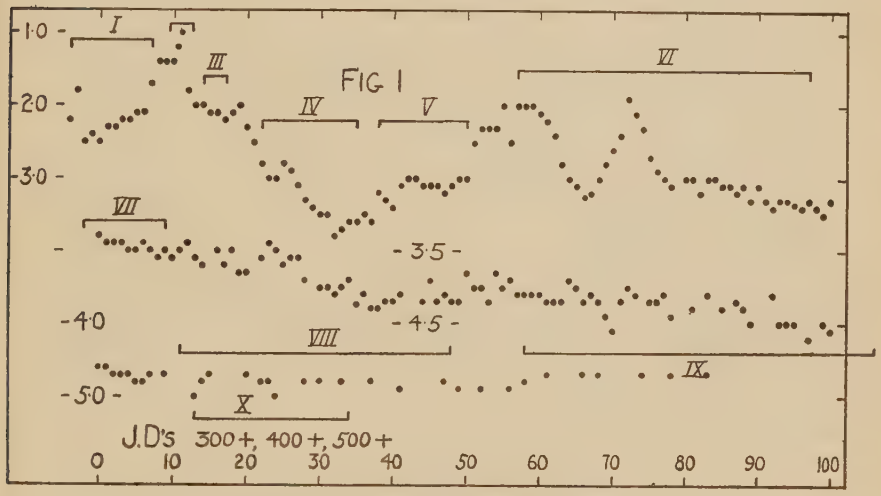

Fig. 1.—Magnitude Observations of Nova Pictoris 1925–1926.

The lines measured on four plates may be summarised as under (compare with Period I.) :—

Ti_E. Ti.	Fe_E. Fe.	Sc_E.	V_E. V.	Cr_E. Cr.	Y_E.	Zr_E. Zr.	Ca.	Sr_E. Sr.	Al_E.	Mn_E. Mn.	Mg_E.	Co.	He.	Totals.
45	20	8	10	7	5	2	..	1	1	5	1	..	..	105
10	67	..	4	5	..	6	4	1	..	5	..	1	1	104
Totals, 55	87	8	14	12	5	8	4	2	1	10	1	1	1	209

The wave-lengths, corrected for shift, are given in column four of Table I. as far as they are common to Period I.; the additional lines are given in Table II.

The measures do not extend further than H_ϵ towards the ultraviolet, as the spectrum fades off there. To make the two lists comparable

nineteen lines should be omitted from Period I. (beyond H_ϵ); then we have

Period I., 137 lines. Period III., 209 lines.

The increase is mainly due to the appearance of numerous lines of iron of lower temperature classes. The four strong manganese lines λλ4031, 4033, 4035, and 4042 became prominent and the helium line λ4472 appears between the Ti and Fe lines λλ4471 and 4473. The above table takes no account of the duplication of lines, but refers only to the new spectrum shifted further to the violet. The lines have become narrower and sharper than in Period I., and the spectrum, apart from the duplicated lines, the strong hydrogen lines of large displacement, the helium line and the bright bands, is very comparable with that of Canopus.

The weighted mean radial velocity of the principal spectrum is −306 km./sec. compared with −71 km./sec. in Period I. The metallic lines remaining of the Period I. spectrum show a radial velocity of −92 km./sec., whilst the hydrogen lines (omitting H_β in 7326) show a radial velocity of −55 km./sec.

In addition to these two spectra a strong hydrogen spectrum appears, displaced −1203 km./sec. on the 13th, diminishing to −1055 on June 17 (see Plate 7, 7322–7326).

The centres of the bright bands are only slightly displaced to the red, showing a radial velocity of +18 km./sec. On June 17 the red edges are displaced +349 and the dark lines bounding the violet edges −308 km./sec. The mean displacement is +20·5; sun correction −2·4; radial velocity +18 km./sec. The width of the bands (657 km./sec.) is equivalent to 9·5 A° at H_γ, with narrower bands to the red and wider bands to the violet side of H_γ.

TABLE II.

Period III. 1925 June 12 to 17. Plates 7320–7327.

Lines Additional to those in Table I.

Origin.	Class.	Tabular λ.	O–T.	Origin.	Class.	Tabular λ.	O–T.
Fe	III.	3977·89	+·08	Fe	III.	4062·60	+·02
Fe	..	79·78	+·02	Fe	..	73·92	−·26
Cr, Fe	III.	84·09	+·03	Fe	..	87·25	+·05
Fe	..	4000·40	+·06	Fe	III.	4107·65	+·03
Un	..	03·08	+·21	Fe	IV.	09·95	+·02
Ti, Fe, V	III.	22·02	−·03	Zr	..	21·65	+·03
Fe	V.	29·80	−·11	Fe	II.	32·24	+·10
Mn	..	30·92	+·01	Fe	IV.	34·84	−·05
Mn	..	33·22	+·07	Cr_E	..	45·91	+·10
Mn	..	34·64	−·07	Fe	III.	47·84	−·13
Mn	..	41·53	+·09	Fe (du)	III. IV.	4154·82	−·11
Fe	IV.	44·77	+·02				
Fe	V.	57·50	+·06	Zr, Fe	..	56·73	−·08

TABLE II.—*continued.*

Origin.	Class.	Tabular λ.	O–T.	Origin.	Class.	Tabular λ.	O–T.
Fe	III.	4175·81	−·12	Ti_E	..	4316·96	+·21
Fe	III.	81·92	+·16	Ca	..	18·82	−·06
V_E ?	..	83·60	+·24	Fe	III.	69·94	−·22
Zr, Fe	III.	99·27	+·11	V, Zr_E	..	79·76	+·04
Fe	III.	4204·10	−·01	Ti_E	..	87·01	+·06
Fe	IV.	07·29	+·08	Ti ?	..	94·23	+·28
Fe	V.	08·77	+·18	Y_E ?	..	98·18	+·04
Zr	..	12·05	−·04	Fe	III.	4407·87	+·17
Fe	IV.	4217·72	−·25	Ti_E	..	09·68	+·01
Fe	IV.	19·52	+·04	V	..	16·64	+·15
Fe	III.	22·38	+·11	Ti_E	..	18·50	−·16
Fe	IV.	38·97	−·14	Ca (du)	..	35·49	−·10
Fe	III.	40·01	+·07	Fe	..	37·11	+·44
Mn_E (du)	..	52·50	+·29	Ti_E, V	..	41·89	+·16
Zr_E	..	58·20	+·05	Fe	III.	47·89	−·27
Fe (du)	IV.	67·55	−·08	Fe	III.	54·55	+·16
Cr	..	74·96	+·27	Fe	II.	66·73	+·05
Fe	III.	82·57	+·30	Fe *	II.	4528·80	−·21
Cr_E	..	84·38	−·05	Al_E ?	..	29·80	+·08
Sr	..	4305·61	+·24	Ti_E	..	37·35	−·28
Y_E	..	09·81	−·01	Ti	..	52·63	+·05

* Ascribed to Fe, Ti_E in Table I.

No origins have been found for the following :—

(Wave-lengths corrected for the displacement of the principal spectrum.)

4015·43	4137·67	4389·47
37·23	51·73	4461·47
42·95	67·01	94·29
56·04	4229·32	4530·62
61·12	45·02	36·69
76·02	49·29	66·34
88·11	56·50	79·52
96·56	69·29	

It is only in the region on the red side of λ 4584 that the bright bands are sufficiently separated to allow of satisfactory measurement (see Plate 7, 7326, lower spectrum). On the violet side of this point the dark lines—already in many cases duplicated—are so numerous that it is not profitable to attempt to identify all the overlapping bands which, from the appearance of the region to the red, may be supposed to accompany them. The overlapping of bands produces fictitious bands,

and the strong dark lines split them up in a manner which renders it exceedingly difficult to determine where the bright bands begin and end. Narrow bright bands in some cases fill up the space between the −71 and the −306 km./sec. spectra, the portion of the normal band to the red being partly obscured. The significance of this will be further referred to later.

The following bright bands are regarded as definitely present :—

Fe_E	4233·3	Ti_E	4708·9
H_γ	4340·6	?	4731
Fe_E	4351·9	Ti_E	4764·1
Ti_E	4417·9	Ti_E	4780·2
Ti_E	4444·0	Ti_E	4805·3
He_E	4471·7	Cr_E	4824·3
Cr_E	4588·4	H_β	4861·5
Cr_E	4619·0	?	4872
Fe_E	4629·5	Fe_E	4924·1
Cr_E, Fe_E	4634·3	Fe_E	5018·6
?	4670		

The band at λ 4731 is a strong isolated one, which is not satisfactorily accounted for by Cr or Fe. The band at λ 4872 appears to be the red edge of a wide H_β corresponding to the dark H_β^2. On this supposition its red edge is displaced +1058 km./sec., the mean of the three dark lines (Plate 7326) being −1053 km./sec. The band at λ 4670 is doubtfully ascribed to scandium. The measures beyond λ 4584 to the red fall off in accuracy, the scale being so much smaller.

Period IV. 1925 June 20 to July 3. Plates 7332–7356.

This period, in which the magnitude falls to its first minimum and begins to rise again, is characterised by a great diminution in the strength of the continuous spectrum and the more definite emergence of the bright bands. The dark lines, from want of a continuous background, are few, and diminish in strength and in sharpness. The following dark lines were measured on Plate 7340, June 25 :—

Origin.	Tabular λ.	O–T.	Origin.	Tabular λ.	O–T.
Ti_E	4028·50	+·13	Fe (du)	4250·62	[−·83]
Fe	45·98	−·15	Cr	54·51	+·07
V_E, Ti_E	53·89	+·02	Ti_E	4300·21	[+·07]
Fe	63·76	−·17	Ti_E (du)	30·69	+·10
?	[4244·19]	..	Ti_E	4534·14	−·08

The details become very unsatisfactory for measurement, and definite identification a matter of great difficulty except in the regions where the bands stand out clearly without too many overlaps and interference from dark lines (see Plate 7, 7346).

The identifications of bands made in Period III. hold good for Period IV. The bright bands of hydrogen and enhanced iron are the most prominent, Fe_E λ4233·3 and λ4351·9 particularly so. The following bands were measured :—

Origin.	Tabular λ.	O–T.	Origin.	Tabular λ.	O–T.
Ti_E	4025·29	−·16	Fe_E	4351·93	−·09
Fe_E	4179·03	−·10	Ti_E	4417·88	−·07
Fe_E	4202·20	+·18	Ti_E	43·98	−·10
Fe_E	33·33	−·04	Fe_E	62·17	+·03
Fe ?	58·48	·00	Fe_E	89·35	−·05
Ti_E	90·38	+·20	Fe_E	4584·02	+·24

Ca (H and K) and hydrogen bands, bright.

The radial velocity shown by the bright bands is +14 km./sec.

There are very few measurable dark lines. The mean radial velocity from 8 dark lines has increased to −327 km./sec.

Period V. 1925 July 6 to 18. Plates 7357–7371.

In this period the magnitude is rising again towards the second rather flat principal maximum. The latter part of this rise was not observed spectroscopically owing to cloudy weather. The continuous spectrum brightens up again, and as a consequence the bright bands are merged in the bright background. The dark lines reappear, excellent for measurement, but greatly reduced in numbers as compared with Period III. Enhanced lines are again the most prominent feature of the spectra, which are very comparable with the earlier spectra in Period I., except that the lines are sharper.

They may be summarised as follows :—

	Ti_E.	Fe_E. Fe.	Sc_E.	V_E.	Cr_E. Cr.	Ca_E. Ca.	Al.	Mn_E.	Co. ?	Totals.
	41	10	7	7	3	2	..	1	..	71
	..	18	..	..	1	1	2	..	1	23
Totals,	41	28	7	7	4	3	2	1	1	94

The wave-lengths are given in the fifth column of Table I.

About three-fourths of the lines are enhanced lines. As compared with Period I., the enhanced titanium lines are more prominent and the iron lines are diminished by half. Y, Zr, and Sr lines no longer appear in the measures.

The weighted mean radial velocity of the principal spectrum is −320 km./sec. On July 7 and 8 additional hydrogen lines appear with a radial velocity of −620 km./sec. (8th), not present on the 18th. The few measurable bright bands show approximately the same displacement and width as in Periods III. and IV.

Notes on Plate 8.

Plate 8 shows the extraordinary changes in Hδ in Periods VI. and VII. The four iron comparison lines are : 4064, 4072, 4119, 4132. They give the scale of the spectra. The central dark Hδ has a constant displacement of -320 km./sec. up to the end of August, increasing rather abruptly about September 8–10 to -400 km./sec. (see Tables). Note the progressive narrowing of many of the additional lines, the drift to the red of the least refrangible additional line from August 25 to September 17, and the disappearance of the most refrangible additional line on August 12.

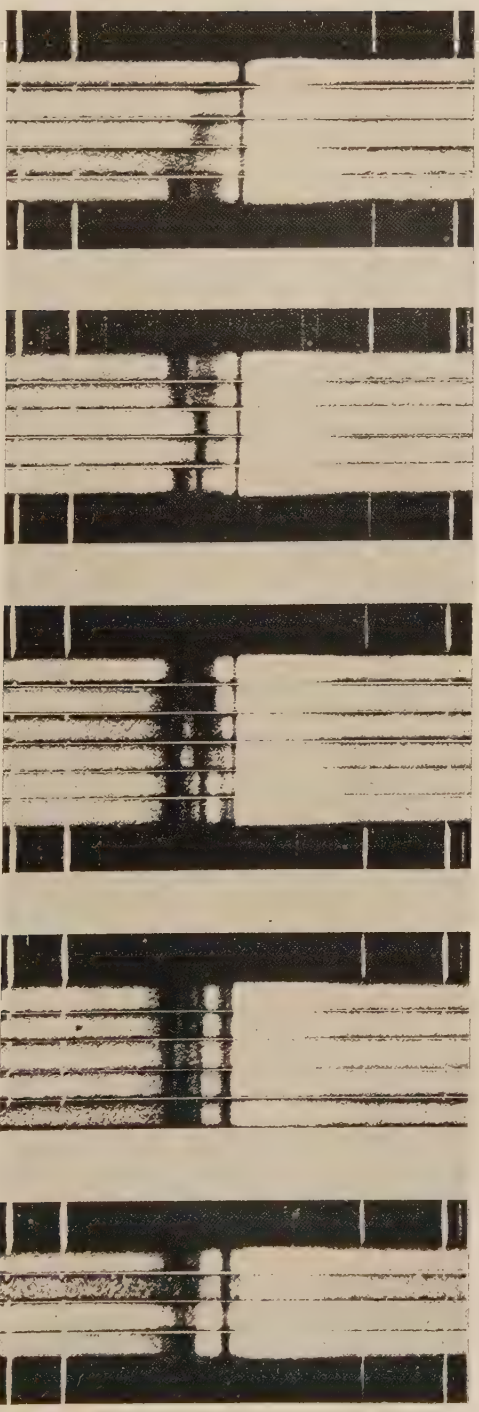

Spectra of Nova Pictoris.

Period VI. 1925 July 25 to September 3. Plates 7375–7410.

The weighted mean radial velocity of the principal spectrum remains, within the errors of measurement, constant at the same figure as in Period V., viz. −320 km./sec. The composition remains as before in its main features, but the lines show a gradual fading out and become fewer. They may be summarised as under :—

	Ti_E. Ti.	Fe_E. Fe.	Sc_E.	V_E. V.	Cr_E. Cr.	Y_E.	Zr_E.	Ca_E. Ca.	Co. ?	Totals.
	37	8	7	4	3	(1 ?)	1	2	..	62
	2	11	..	2	2	..	..	1	1	19
Totals,	39	19	7	6	5	..	1	3	1	81

The wave-lengths are given in the third column of Table III.

The hydrogen lines and three unknown lines are not included. Enhanced lines are still predominant. The magnitude curve shows a marked drop from the second rather flat maximum, followed by a rather steep peak which occurs before the very gradual fall in magnitude sets in. Unfortunately, cloudy weather prevented spectroscopic observations at the peak.

The chief interest in this period is the extraordinary behaviour of the hydrogen lines. The changes in number of extra lines, in breadth and intensity and in displacement, are worthy of careful scrutiny (see Plate 8). The progressive narrowing which is well seen in some of the lines should be noted, as should the temporary disappearance of the violet component of the triplet on August 12, and the drift to the red of the component (on August 23), which approaches and then passes the −320 km./sec. line. Throughout these disturbances the −320 km./sec. line remains unmoved, and there seems little doubt that the absorbing layer producing it is, by this time, well away from the centre of disturbance. The strong extra lines are regarded as due to successive minor explosive outbursts of hydrogen giving rise to broad heavy lines, whilst the material is near the nucleus, but becoming gradually finer as the material expands and becomes more tenuous and under lower pressure. The fine most displaced component on September 19 appears to have had a continuous existence since August 19. A temporary disappearance on August 12 may have been caused by an increase in temperature, carrying the gas from the absorbing state to the emissive state. Bridging this gap, the line may be traced back to July 31. The pair of very heavy additional hydrogen lines on August 4 coincides with the beginning of the sharp peak maximum on August 10.

The λ4233 line of enhanced iron follows more or less closely the behaviour of the hydrogen lines, as do, less clearly, other lines of enhanced iron and titanium.

On July 25 λ4233 Fe_E^2 coincides with and strengthens the calcium line λ4227 (−320), afterwards showing a steady shift to the violet. Throughout these changes no evidence of orbital motion has been found. With the diminution in the strength of the continuous spectrum the bright bands gradually emerge into prominence again.

TABLE III.

Period VI. 1925 July 25 to September 3. Plates 7375–7410.
„ VII. „ September 4 „ September 15. „ 7411–7417.
„ VIII. „ September 17 „ October 24. „ 7419–7434.

Origin.	Tabular λ.	O–T. VI.	VII.	VIII.
$H\zeta$	3889·20	+·20		
?	[95·25]			
Ti_E	3900·68	+·03		
V_E	03·40	−·11		
Fe	08·08	−·02		
Ti_E	13·61	+·06		
Ca_E (K)	33·83	−·07	+·10	−·01
Co ?	36·12	+·16		
Zr_E	58·36	−·25		
?	[67·28]			
Ca_E (H)	68·63	−·07	+·17	−·05
$H\epsilon$	70·18	+·15	+·27	+·10
Fe	79·78	−·15		
Fe	4005·41			
	(05·64)			
V_E	05·86	·00		
Ti_E	12·54			
	(12·59)	·00		
Cr_E	12·63			
V_E	23·53	−·04		
Ti_E	25·29	−·05		
Ti_E	28·50	+·05		
Fe	45·98	+·04		
V_E, Ti_E	53·89	+·07		
Fe	63·76	−·02		
Cr, Fe	67·14	+·08		
Fe	71·91	−·02		
$H\delta$	4101·89	+·02	+·15	+·16
Ti_E	61·68	+·13		
Ti_E	63·82	−·01	−·05	
Ti_E	72·07	−·02	−·10	
Fe_E, Ti_E	73·60	+·02		
Fe_E	79·03	−·02		
Ca	4226·90	+·15		
Fe_E	33·33	−·08	−·06	−·11
Sc_E	47·00	−·08		
Cr_E	62·15	−·17		
Fe (Ti_E)	71·93	+·13		
V	84·24			
Cr_E	84·38	−·17		
Ti	86·17	+·21		
Ti_E	88·04	−·17		
Ti_E	90·38	−·03	+·05	−·15
Ti_E	94·20	+·02		
E	4300·21	−·07	−·10	−·20

Origin.	Tabular λ.	O–T. VI.	VII.	VIII.
Ti_E	4302·09	−·08		
Fe_E	03·34	+·03		
(Ti_E) Fe	08·08	−·07	..	−·01
Ti_E	13·03	−·12	−·12	
Sc_E	14·25	−·08		
	(14·70)	+·27		
Ti_E	15·14	+·05	+·02	
Sc_E	20·91	−·04		
	(21·02)			
Ti_E	21·12			
Sc_E	25·15	+·04		
Ti_E (du)	30·69	−·22		
Ti_E	38·08	+·03		
$H\gamma$	40·63	+·05	+·18	+·12
Fe_E	51·93	−·02		
Ti_E	67·84	+·11		
Sc_E	74·63	+·09		
(Y_E ?)	75·10			
Fe	83·72	+·10		
Fe_E	85·55	−·04		
?	[88·99]			
Ti_E	95·20	−·01	·00	−·17
Ti_E	99·94	−·06		
	(4400·25)	−·06		
Sc_E	00·56			
Ti_E	11·24	−·04		
Fe, Sc_E	15·51	+·05		
Ti_E	17·88	+·09		
Ti (+ ?)	38·36	+·05		
Ti_E	43·98	·00	+·01	+·05
Ti_E	50·65	+·08		
V	62·53	+·02		
Ti_E	68·66	+·03	−·01	−·46
Ti_E	88·49	+·11		
Ti_E	4501·45	+·05	−·45	
Fe_E	22·80	..	..	−·09
Ti_E	34·14	−·04	+·23	
Fe_E	49·64			
	(49·73)	−·05	−·01	+·10
Ti_E	49·81			
Ti_E	63·94	+·08		
Ti_E	72·16	−·02	−·16	+·08
Cr	80·23	+·05		
Fe_E	84·02	+·06	−·18	+·11

Period VII. (transition). 1925 September 4 to 15.
Plates 7411–7417.

This is a transition period in which the radial velocity of the principal spectrum undergoes a rather abrupt change. During July and August the velocity was constant within the errors of measurement at −320 km./sec. On September 4 it had increased to −337, and on the 17th to −395 km./sec. The plates of September 8 and 10 show blurred lines, and it was mainly on those dates that the change was accomplished. After the change the velocity settled down again to a value of about −400 km./sec. This change in radial velocity may possibly be the result of a drift of faster moving material carrying it between us and the nucleus, the material causing the lines of smaller displacement at the same time drifting laterally out of the central line of sight. The multiple hydrogen lines are still in evidence, the most displaced component narrowing to a fine line.

The magnitude is slowly and steadily declining, the continuous spectrum weakening and the dark lines becoming fewer. The bright bands are growing in distinctness.

The red component of the additional hydrogen line, which has been moving to the red, has now crossed the principal line and appeared on the red side of it.

The dark lines measured in the principal spectrum consist, apart from the hydrogen lines, entirely of enhanced lines of Ti, Fe, and Ca.

The measures are given in the fourth column of Table III.

Period VIII. 1925 September 17 to October 24.
Plates 7419–7434.

This is a rather uninteresting period as far as the dark lines are concerned. They consist, as in the previous period, only of the enhanced lines of Fe, Ti, and Ca and the hydrogen lines. The lines are fading out with the further diminution in the strength of the continuous spectrum, and the bright bands are becoming more apparent. The bands of unknown origin present so conspicuously in η Argûs are now becoming evident,* but, as they are stronger at a later stage, they are not considered here. Heavy additional hydrogen lines are still present, but these disappear temporarily on October 24. Their multiple structure is no longer seen. The radial velocity shown by the principal spectrum shows no further marked change, but remains at about −400 km./sec. The magnitude curve shows a further decline, marked with minor irregularities which appear to be real.

The wave-lengths of lines measured are given in the fifth column of Table III.

Period IX. 1925 November 3 to December 21.
Plates 7439–7474.

The centre of interest in this period is the appearance of a variable dark line helium spectrum, having the same large displacement as the

* Sir David Gill calls attention in *Proc. Roy. Soc.*, **68**, 456, to "the very exact agreement between the spectrum of η Argûs and that of the Nova Aurigæ."

Notes on Plate 9.

Dots are placed *above* the lines or bands noted below.

Plate 7465, 1925 December 3.—Dark lines, left to right: (1) K^1; (2) He^2 3965; (3) $H\epsilon^2$; (4) (Ca)H^1; (5) $H\epsilon^1$; (6) He^2 4026; (7) $H\delta^2$; (8) $H\delta^1$.

Plate 7495, 1926 February 11, 12, 13.—(1) Neb. 3869; (2) $H\zeta$; (3) double band He 3965 and $H\epsilon$ 3970; (4) He 4026.

Plate 7469, 1925 December 8.—I. Lightly printed. (1) Fe_E 4924; (2) Fe_E 5019.
" " " II. Deeply printed. (1) Overlapping bands, Fe_E 4550, 4556; (2) Fe_E 4584; (3) Fe_E 4630; (4) He^2, dark, 4713; (5) η Argûs band 4815; (6) He^2, dark, 4922.

Plate 7481, 1926 January 8.—(1) η 4815; (2) $H\beta$; (3) He 4922, Fe_E 4924.

Plate 7496, 1926 February 15, 16, 17.—I. Lightly printed. (1) He 4472; (2) Fe_E 4584; (3) η 4815.
" " " " II. Deeply printed. (1) He 4472; (2) Fe_E 4584; (3) Fe_E 4630; (4) unknown band 4658.

Plate 7498, 1926 February 27, March 1, 2.—(1) N_2, 4959 (2) N_1 and He, Fe_E overlapping $\lambda\lambda$ 5007, 5016, 5019.

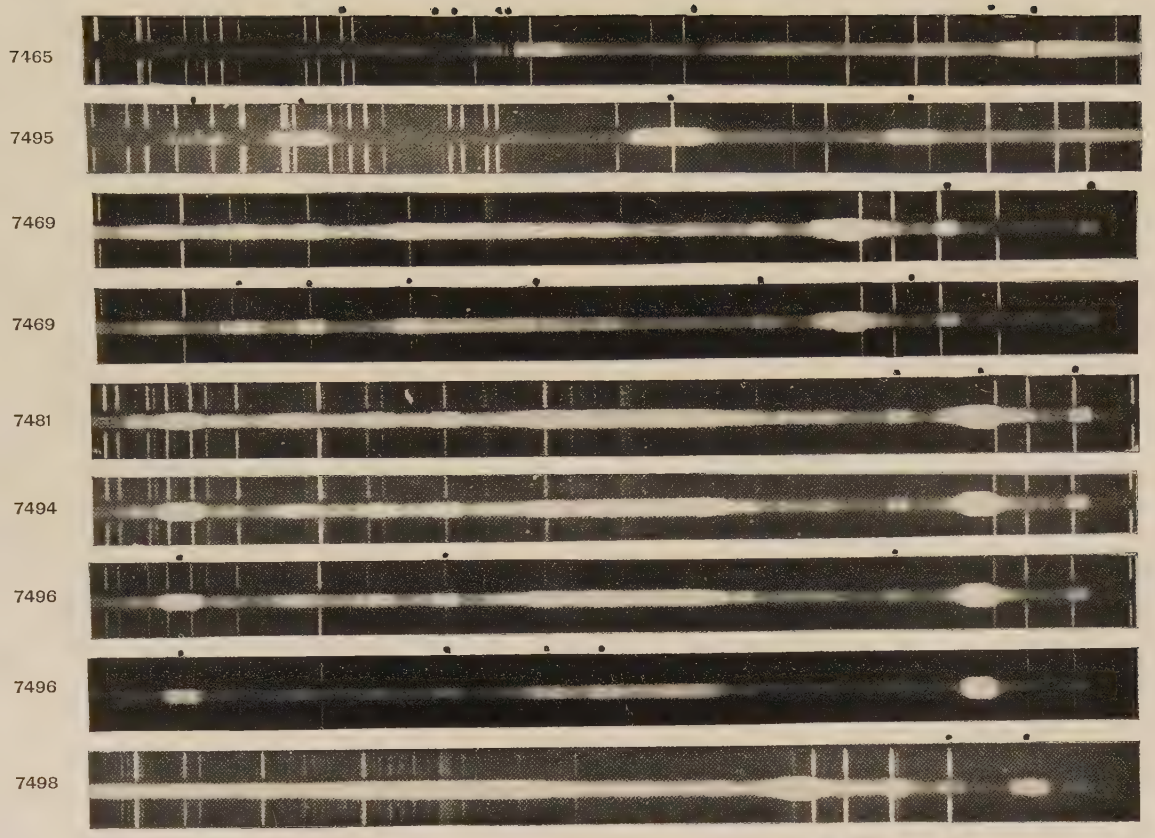

Spectra of Nova Pictoris 1925 Dec. 3 to 1926 Mar. 2.

additional hydrogen lines (see Plates 9 and 10, 7465). The helium lines measured are: λλ 3965, 4026, 4144, 4388, 4471, 4713, 4922, and 5016. The variations in strength and sharpness are well seen in the line λ 4026, prominent on December 3 and absent on December 1. The helium line λ 3965 forms a double with H_ϵ^2 between the H and K lines of calcium (see Plate 9, 7465). The helium lines λ 4922 and λ 5016, owing to the large difference in their displacement, are now separated from Fe_E λ 4924 and Fe_E λ 5019, with which they would be blended if they had the same displacement.

The η Argûs bands of unknown origin, designated η in Table V., are now sufficiently developed to allow of the measurement of the strongest of them. They have the same breadth as the other measurable bands, and their wave-lengths can be determined from either the violet or red edges where both edges are not measurable through overlapping (see Plate 10).

η 4244 overlaps Fe_E λ 4233, η 4277 overlaps η 4287. H_γ is extended on the red side, terminating at the red edge of η 4359.

The red side of the H_γ band is of interest throughout. It is first extended by Fe_E λ 4352, then by η 4359, and then by the nebular and Nova band λ 4363. The double band η 4414 and 4416 is sometimes difficult to measure, as the wings on each side of the broad overlap are not always distinct. The violet edge of η 4416 is sometimes marked by a faint dark line; η 4815 is an isolated band on the violet side of H_β; η 4277, only just recognisable in plate 7465, is better seen in plates 7481 and 7496 (see Plate 10).

The measures are given in Table IV.

TABLE IV.

Period IX. 1925 November 3 to December 21. Plates 7439–7475.

Dark Lines.

Origin.	Tabular λ.	O–T.	Origin.	Tabular λ.	O–T.	Origin.	Tabular λ.	O–T.
H_ζ	3889·20	+·02	Ti_E	4290·38	+·09	Fe_E	4541·51	+·04
Ti_E	3900·68	+·04	Ti_E	94·20	−·23	Fe_E	49·64	
Ti_E	13·61	+·13	Ti_E	4300·21	−·13		(49·73)	+·03
Ca_E (K)	33·83	·00	Fe_E	03·34	+·04	Ti_E	49·81	
He	**64·88**	**+·03**	H_γ	40·63	−·08	Fe_E	56·06	+·23
Ca_E (H)	68·63	+·03	**He**	**88·10**	**+·20**	Fe_E	84·02	+·07
H_ϵ	70·18	+·03	Ti_E	95·20	−·04	**He**	**4713·25**	**+·15**
He	**4026·34**	**+·14**	**He**	**4471·65**	**−·11**	H_β	4861·53	+·05
H_δ	4101·89	+·01	Fe_E	4508·46	+·06	**He**	**4922·10**	**+·15***
He	**43·92**	**−·01**	Fe_E	20·40	+·16	Fe_E	24·11	−·46
Fe_E	79·03	+·14	Fe_E	22·80	−·11	**He**	**5015·73**	**−·34***
Fe_E	4233·33	−·07	Ti_E	34·14	−·26	Fe_E	18·63	−·40

Note.—The dark helium lines in heavy type are in the strongly displaced spectrum. The bright η Argûs bands are present, but better for measurement in Period X. (Table V.).

* These two helium lines are separated from the enhanced iron lines 4924, 5019 by the great difference in their displacements.

Notes on Plate 10.

Plate 7465, 1925 December 3.—(1) $H_{\gamma}{}^{1}$; (2) dark He 4388; (3) He^{2} 4472, dark and strongly displaced.

Plate 7495, 1926 February 11, 12, 13.—(1) He 4144, He 4472; bright bands (compare 7465).

Plate 7469, 1925 December 8.—I. Lightly printed. (1) He^{2} 4472, dark.

„ „ „ II. Deeply printed. (1 and 2) overlapping bands Fe_{E} 4713, 4719; (3 and 4) overlapping bands Fe_{E} 4233 and η Argûs 4244; (5) η 4287; (6) $H_{\gamma}{}^{2}$; (7) $H_{\gamma}{}^{1}$; (8) red edge of η 4359; (9) dark He^{2} 4388; (10 and 11) double η band 4414, 4416, latter showing dark line on violet edge; (12) dark He^{2} 4472.

Plate 7481, 1926 January 8.—(1 and 2) double η bands 4277, 4288.

Plate 7494, 1926 February 8, 9, 10.—(1) He 4144.

Plate 7496, 1926 February 15, 16, 17.—I. Lightly printed. (1) He 4144; (2 and 3) double η band 4277, 4288; (4) neb. 4363. Compare with plate 7469, η 4359.

„ „ „ „ II. Deeply printed. (1) Neb. 4363.

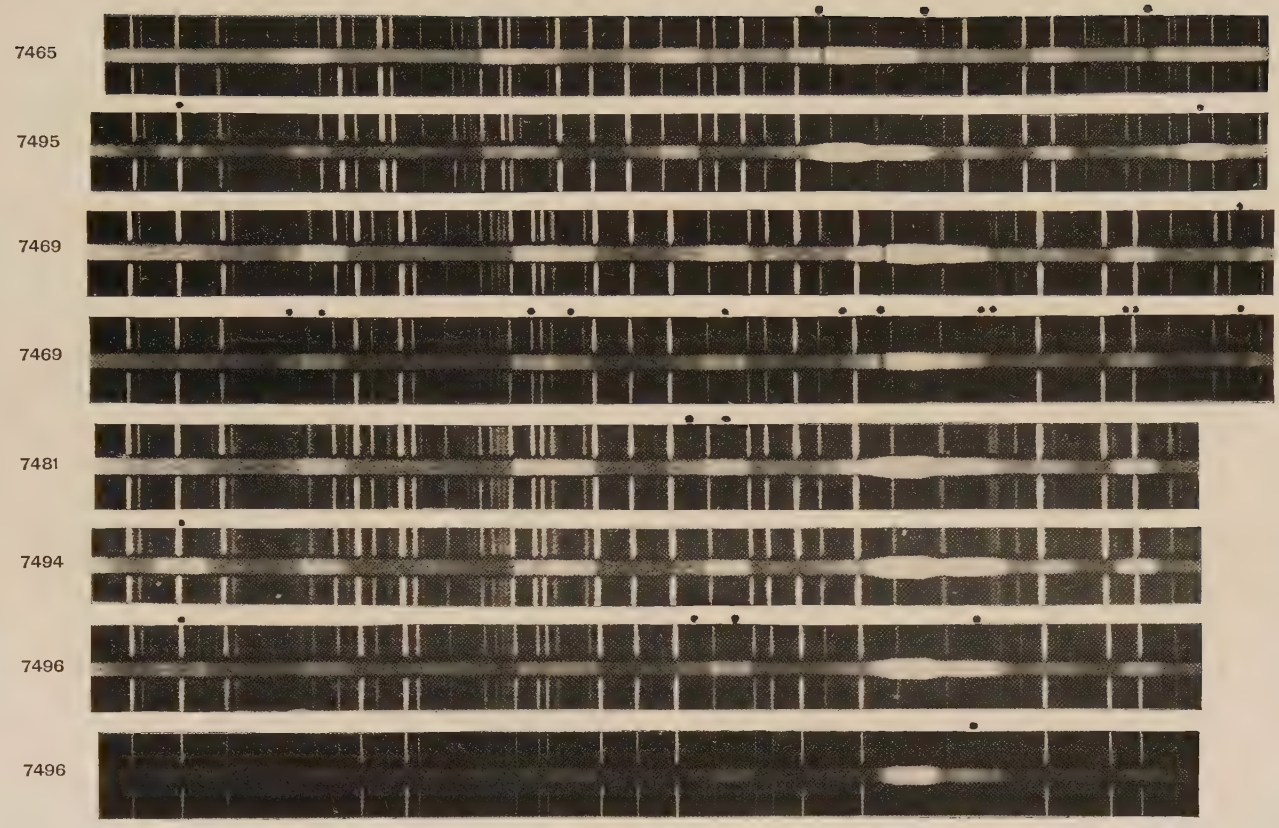

Spectra of Nova Pictoris 1925 Dec. 3 to 1926 Feb. 17.

Period X. 1925 December 28 to 1926 January 18.
Plates 7476–7485.

This period is characterised by strong bright hydrogen lines, and the further development of the η Argûs bands $\lambda\lambda$ 4069, 4244, 4277, 4287, 4359, 4414, 4416, and 4815. Helium λ 4472 becomes a very prominent bright band (see Plate 9). A number of enhanced iron bands complete the spectrum. The dark lines gradually vanish. The radial velocity given by the dark lines shows a further slight increase to −411 km./sec., as compared with −405 km./sec. in Period IX.

On January 5 He $\lambda\lambda$ 4026 and 4472, with H_γ, show very diffuse broad absorption lines displaced −1457 km./sec. The H and K lines of calcium show as dark lines in the principal spectrum.

The dark lines and bright bands measured are shown in Table V.

TABLE V.

Period X. 1925 December 28 to 1926 January 18. Plates 7476–7485.

Dark Lines and Bright Bands.

Origin.	Tabular λ.	O–T.		Origin.	Tabular λ.	O–T.	
Ca_E (K)	3933·83	+·02	d	η	4413·88	−·28	v
Ca_E (H)	68·63	−·01	d	η	16·64	+·01	v r
H_ϵ	70·18	+·16	d r	Fe_E	51·75	+·39	d v[r]
He	4026·34	−·20	d	He	71·65	+·31	d v r
η	68·71	+·13	d r	Fe_E	91·57	+·20	r
?	[89·74]	..	d	Fe_E	4508·46	+·27	d v
?	[98·64]*	..	v	Fe_E	15·51	+·04	d v
$H\delta$	4101·89	−·08	d	Fe_E	49·64	+·11	d v
Fe_E	73·48	−·03	v r	Fe_E	56·06	−·17	d v r
Fe_E	79·03	−·14	d v r	Fe_E	84·02	−·07	d v r
Fe_E	4233·33	+·12	d v	Fe_E	4629·52	+·27	v r
?	[38·76]	..	d	?	[58·29]	..	v r
η	43·93	+·04	r	?	[4742·05]	..	d
η	76·89	−·26	v	?	[73·92]	..	r
η	87·46	−·22	v r	η	4814·58	+·37	v r
?	[93·75]	..	d	?	[24·66]	..	d
Ti_E	4308·08	+·09	d	$H\beta$	61·53	−·27	d
?	[26·29]	..	d	He, Fe_E	4923·11	+·27	d
H_γ	40·63	−·21	d	Fe_E	4924·11	+·10	v r
η	59·42	−·10	v r				

d=dark line. v=violet edge of bright band. r=red edge.

Note.—The bright helium spectrum is more fully developed in Period XI.

* Wing to $H\delta$. Not N. 4097·43.

Period XI. 1926 January 23 to March 13.
Plates 7486–7501.

This period is characterised by the further development of the helium bright bands λλ 3965, 4026, 4144, 4388, 4472, 4713, and 4922. The η Argûs bands are prominent, but the enhanced iron bands less so. H_β, H_γ, H_δ, H_ϵ, H_ζ are bright (see Plates 9 and 10).

The spectrum now shows signs of a transition to a more normal late stage Nova spectrum, as the nebular band λ 3869 appears beyond H_ζ in the ultra-violet (see Plate 9, 7495). It is no doubt the same line which is recorded as λ 3868 Int. 10 in the spectrum of the later stages of Nova Persei. H_γ is extended on its red side by the nebular band λ 4363 (see Plate 10, 7496). The principal nebular bands N_1 and N_2 begin to appear, but they are weak and not fully developed even with nine hours' exposure—three hours on each of three nights—until early in March, when N_2 becomes strong enough to show plainly on an enlargement (Plate 9, 7498). N_1, overlapping helium and iron enhanced λλ 5016, 5019, now becomes strong. Next to the hydrogen bands, helium λλ 4026 and 4472 (Plate 9, 7495, 7496) are the strongest bands. The nebular band λ 4363 is strong.

The region between Fe_E λ 4630 and the He band λ 4713 is occupied by strong continuous spectrum, the only detail being a strong band of unknown origin at λ 4658, stronger than the background (Plate 9, 7496). The position of the λ 4640 band, regarded as typical of Novæ, is overlapped by Fe_E λ 4629–52 and the unknown band λ 4658. The edges of these two bands (plate 7496, February 15, 16, 17) are :

v. 4623·9, *r.* 4636·9 and *v.* 4652·6, *r.* 4664·5.

The λ 4640 band cannot be identified. In Nova Aquilæ I showed that five bands were present in this complicated region. The band λ 4658 is an additional one.

The enhanced helium band λ 4686 likewise cannot be identified against the continuous spectrum. The unknown band at λ 4658 was also present in Period X.

The radial velocity derived from the few dark lines H_γ, H_δ, H_ϵ, and He λ 3965 is −436 km./sec. (February 11, 12, and 13). Some of the bands show maxima near their two edges, best seen in Plate 10, 7469 λ 4287. The centre of the two maxima is at zero radial velocity, the mean velocities being −331 and +332, the edges being at −375 and +439. The bands differ from those in Nova Aquilæ No. 3 in this respect, the latter having a wide maximum almost central (see *M.N.*, **80**, 527). The dark lines and bright bands measured are shown in Table VI.

Theory of the Nova and Conclusion.

For a long time there was a disposition not to accept any explanation of the phenomena of Novæ in terms of Doppler displacements of lines. There is now, however, a growing body of considered opinion which regards the pronounced displacements of the lines as representing the real radial velocities of the absorbing gases. No other explanation is forthcoming.

Table VI.

Period XI. 1926 January 23 to March 13. Plates 7486–7501.

Origin.	Tabular λ.	O–T.						
Neb	**3868·88***	+·10		v	r			
$H\zeta$	89·20	−·07		v	r			
He	3964·88	+·09	d					
H_ϵ	70·18	−·02	d		r			
He	4026·34	+·02		v	r	M	m	
η	68·71	·00		v	r			
$H\delta$	4101·89	+·11	d		r			
He	43·92	−·03		v	r		m	
Fe_E	79·03	−·02		v	r			
Fe_E	4233·33	−·04		v				
η	43·93	−·02			r			
η	76·89	−·73		v				
η	87·46	−·17		v	r	M	m	
$H\gamma$	4340·63	+·10	d		r			
η	59·42	−·40		v				
Neb	**63·37**	−·01			r	M	m	
He	88·10	+·35		v	r			

Origin.	Tabular λ.	O–T.		
η	4413·88	+·10	v	
η	16·64	−·74	r (see Table V.).	
He	71·65	−·14	v	r
Fe_E	4549·64	−·27	v	
Fe_E	56·06	−·53	r	
Fe_E	84·02	−·22	v	r
Fe_E	4629·52	+·50	v	r
?	[58·14]	..	v	r
He	4713·25	−·07	r	
η	4814·58	+·47	r	
$H\beta$	61·53			
He	4922·10	+·78	v	r
Neb (N_2)	**59·05**	+·53	v[r]	
Neb (N_1)	**5006·89**	−·56	v	
He	15·73	−·11	r	

d=dark line. Bright bands: v=violet edge, r=red edge.
M=violet maximum. m=red maximum.

Evershed † was, I believe, the first to formulate the ideas which are now known as the "explosion theory." The latest to adopt them is Hartmann, who cabled to the *Astronomische Nachrichten* from Buenos Aires, "Nova problem solved, the star swells up and bursts."

This is very pithily put, and, whilst making the reservation that Novæ still offer us many unsolved problems, I fully subscribe to the latter part of his cablegram. Nova Pictoris exhibits phenomena which I consider strengthen very much the grounds for believing that the star "swells up and bursts." It shows us a slow-motion picture of the entire process in a unique manner. It is exceedingly fortunate that Mr. Watson discovered the star when he did, so that it was possible to secure a series of photographs of the spectrum whilst it was still in the *simmering* stage and before the *explosive ebullition* took place.

In Period I. the absorption lines are broad and heavy and, it is important to note, show the quite ordinary mean radial velocity of only −71 km./sec. These conditions prevailed for twelve days after discovery. No sign of any "explosion" here, only a "simmering" of gases which their spectra—in which enhanced lines predominated—showed to be at a relatively high temperature and probably in turbulent motion, hence the broad lines. But whilst the spectra remained without much change, the magnitude was steadily rising to a maximum. This

* Strong in Nova Persei, later stages. λ 3868 Int. 10.

† *M.N.*, **79**, 481.

TABLE VII.

Radial Velocities.

	Date.	Plate.	Km./s.	Lines.	Km./s.	Lines.	Additional Lines. Km./s.	Lines
Period I.	1925 May 25	7291	−77	51				
	June 4	7301	−68	91				
	5	7307	−71	31				
	Weighted mean		−71					
Period II.	1925 June 8	7308	..	..	−125	9		
	10	7317	−81	8	−291	8		
	Weighted mean		−81		−203			
Period III.	1925 June 12	7320	H −61	2	−309	49	−1195	2
			Fe_E −90	3				
	12	7322	H −56	3	−306	99	−1210 *	2
			Fe_E −92	17	−309	39		
	13	7324	H −51	3	−298	58	−1204 *	2
	17	7326	−94	6	−310	46	−1055 *	3
	Weighted mean		..	..	−306			
Period IV.	1925 June 25	7340	..	..	−327	8	Dark lines fading, brig bands emerging.	
Period V.	1925 July 6	7357	..	..	−323	48	−629	H_γ
	8	7362	..	..	−317	23	−621	H_δ
	18	7371	..	..	−320	66		
	Weighted mean		..	..	−320			

							Additional Lines.	
Period VI.	1925 July 28	7377	−319	42	..	..	-826_{13}	
	Aug. 4	7387	−319	45	..	-683_5	-946_1	−1008
	6	7390	−320	39	..	H -698_2	..	H −1029
						Fe_E-722_2	..	Fe_E−964
	12	7393	−319	27	..	H -737_2		
	15	7399	−320	41	-497_9	-743_5	..	−1054
	19	7400	−320	35	-513_7	-748_4	-932_5	
	23	7403	−323	31	Fe_E-549_1	?	Blended	?
	25	7404	−320	20	-539_4	-763_2	-947_1	−100
	29	7408	−325	29	-494_2	-694_2	..	−102
	Weighted mean		−320					

Suffixes indicate number of lin

* Note this real change. See Plate 7.

TABLE VII.—*continued.*

	Date.	Plate.	Km./s.	Lines.	Km./s.	Lines.	Additional Lines. Km./s.	Additional Lines. Lines.
riod III.	1925 Sept. 4	7411	−337	12	-419_2	-673_3	-828_2	-1039_2
	8	7414	Lines blurred, acceleration occurs here.					
	10	7415						
	15	7417	−395	16	[H_δ only −223	−719	−861, −952	−1071]
riod III.	1925 Sept. 25	7424	−388	15		H_γ	−899	
	Oct. 17	7433	−410	9		No extra lines.		
	Weighted mean, 3 Plates		−396					
eriod IX.	1925 Nov. 3	7439	−398	14	−1162	3		
	10	7446	−410	11	−1157	9		
	23	7454	−405	7	f and v diff.			
	Dec. 3	7465	−403	12	−1305	7		
	4	7468	−411	11	−1275	6		
	Weighted mean		−405					

	Date.	Plate.	Km./s.	Lines.	Km./s.	Lines.	Neb. Km./s.
eriod X.	1926 Jan. 5	7478	−408	11	−1455	3 (H_γ and He)	+24
	7	7480	−412	8	..	..	+16
	8	7481	−423	3	−1537	2 (H_β and 4923)	[+5]
	Weighted mean		−411				

	Date.		Km./s.	Plate
eriod XI.	1926 Feb. 11, 12, 13.	Dark H_γ, H_δ, H_ϵ and He 3965 give a mean of	−436	7495
		The mean of the violet and red edges gives	+32	7495
		,, ,, ,, maxima gives	+0·4	7495
	,, ,, 15, 16, 17.	,, ,, ,, edges gives	+26	7496

indicates, to my mind, not an increase in intrinsic surface brightness, but an increase in surface area, a "swelling-up," in fact, as Hartmann puts it.

How long this preliminary heating up had lasted it is difficult to say; certainly for twelve days at least, and as Harvard reports the star as of third magnitude on April 13, six weeks before Mr. Watson's discovery, the process had been a comparatively gradual one. In view of the Harvard * observation of April 13, and the freedom from violent changes in the spectrum for twelve days after visual discovery, too much weight should not, in my opinion, be placed on Mr. Reid's † negative evidence for the low magnitude a few days before discovery. The star was fainter than 12th magnitude ‡ on February 18.

Period II., June 8, 9, and 10, brings us to a real crisis in the history

* *Harvard Bulletins*, 823.
† *The Observatory*, **48**, 261.
‡ *Harvard Bulletins*, 826.

of the Nova. The magnitude has risen to a maximum of about 1·0 and the spectrum shows the disturbed state of the absorbing gases. There is no absolutely abrupt explosive change, the process is a comparatively gradual one; the lines gradually move to the violet, showing an increasing radial velocity over a period of at least three days, ending with a radial velocity of about −300 km./sec.

As the speed of a rifle bullet is only about 1 km./sec. we may, without impropriety, regard this as an "explosive outburst."

The steady expansion which preceded it, and the consequent release of pressure from the deeper layers, may have been the trigger which set in motion the "explosive ebullition." That this occurred in the deeper layers, the spectra seem to show conclusively, for the following reasons: The duplication of many of the lines shows (in addition to the spectrum displaced −300 km./sec.), another spectrum—remnants of the original spectrum—presumed to be due to the outer layers which have travelled furthest from the star in the preliminary expansion and still retaining approximately the original displacement, as though too far from the seat of disturbance to be immediately affected by it. Between the components of the duplicated lines we have in many cases narrow, bright bands, which are only the violet edges of the normal bands, showing that they originate at a lower level, and that the remainder (red end) of the band is dimmed by absorption from the undisturbed outermost layers.

Following this explosive change the spectrum becomes much more complicated by the appearance of many more iron lines of lower temperature classes—the enormous expansion would be expected to be accompanied by a cooling of the gaseous envelope—and the lines become sharper partly owing to reduced density and also due to greater distance from the central body. This coincides with the drop in the magnitude curve after the first and highest maximum. It would appear that, at this stage, the increase in brightness due to increasing surface area is more than counterbalanced by the cooling which the spectra show has taken place, hence the drop in magnitude.

Evershed is quite definite in regarding the wide bright bands as Doppler effects, and it may be pointed out that I so regarded them in the case of Nova Aquilæ No. 3,* giving the displacements of the edges in km./sec. and computing the radial velocity of the nebula corrected for the earth's motion. The same procedure has been followed in the present case. On this view the widths of Nova bright bands are simply a measure of the rate of expansion of the gaseous envelope expelled from the Nova. Nova Pictoris shows a much less violent explosion than did Nova Aquilæ No. 3. The nebula may be regarded as a transparent gaseous shell, for, as Evershed points out, "the gas on the side towards Earth would not obstruct the radiation from the opposite side, because owing to the change of wave-length it would be transparent to the radiation from the receding gas. The result would be wide emission bands with edges defined by the velocity of the expansion."† There

* *M.N.*, **80**, 524.

† Evershed's proviso, "If the star, etc.," is not important, as we may assume the nucleus to be very small in comparison with the nebula.

is a close relationship between the displacement of the dark lines and the widths of the bright bands. The broad bright bands have a dark absorption line on their violet edges, but only when the nucleus gives a sufficiently strong continuous spectrum to show it up by contrast. In the later stages, when the continuous spectrum fades, the bright bands show no dark line.

The explanation of the violet edge dark line appears to be that we are dealing with a gaseous shell with a cooler outer layer, thin in comparison with the emitting layer. Every radial line from the nucleus passes through an emitting and an absorbing portion of the gaseous shell. The further portion of the shell and the peripheral portions of the disc of the nebula produce no absorption, as the cool layer is on the outside and the emission through it does not reach us. It is only the centre of the shell nearest us, where the radial velocity is a maximum, that is responsible for the violet edge of the band. There the cool layer interposes itself completely and gives the maximum absorption at this shortest wave-length. Intermediate radial lines between centre and periphery (as seen from the earth) pass through portions of shell where the hotter and cooler layers have the same wave-length, but the cooler layer does not completely mask the hotter layer, and we have emission superposed on absorption and obliterating it, the precise effect depending on the relative thicknesses of the hotter and cooler layers, and on their difference of temperature. The additional strongly displaced hydrogen lines accompanied to some extent by enhanced iron and titanium are regarded as successive eruptions of these materials from the nucleus, eruptions of greater or less intensity, each component of the multiple lines being regarded as due to a separate mass ejected with the velocity indicated by its displacement. In November and December (Period IX.) the strongly displaced hydrogen spectrum is accompanied by a similarly displaced spectrum of helium. Bright helium bands occur at a later stage and form a very prominent feature of the later spectra, but it is not likely that these bright bands are due to the same helium which produced the much more strongly displaced dark lines at an earlier stage, as the bright helium bands have the same widths as the other bright bands—associated with them—which belong to the outer nebular envelope. The later appearance of the nebula bands as well as the earlier appearance of the η Argûs bands of unknown origin are phenomena on which we can only speculate. Are they due to atoms in the process of building, or did they exist before and only become luminous under some change of physical condition ?

As to the root cause of the heating up of the Nova there are many theories. The one which seems likely to survive is that the disturbance originates within the star itself,* due to some release of atomic energy and atomic or even molecular rearrangements. The evidence of the presence of stationary H and K lines is very weak in this Nova. A few plates, *e.g.* 7423, 7424, show the stationary K line feebly.

The above remarks on the theory of Novæ may form a basis of discussion. Barnard's observation that Nova Aquilæ No. 3 had a

* See Lundmark, *Publ. Astl. Soc. Pac.*, **35**, 115 (1923); and Hartmann, *Ast. Nach.*, **5413**, p. 206, 1925.

sensible expanding disc lends support to the theory. He also found a planetary disc in the case of Nova Ophiuchi. On 1920 June 10 the diameter of the nebulosity was 2″·3, in the centre of which the star itself appeared as a very small point of light. Observations of this nature have not yet been reported in the case of Nova Pictoris, but they may come later. From the width of the bright bands we should expect a smaller disc in this case than in the case of Nova Aquilæ, if they are at the same distance from us.

A nebulous envelope expanding at the rate of $\frac{1000}{3}$ km./sec. would take five months to become as large as the orbit of Neptune, and a disc of this size might easily be invisible to us at the distance of the Nova. There is less likelihood of seeing a measurable disc in the case of Nova Pictoris than in that of Nova Aquilæ No. 3, as the rate of expansion (on our theory) is so much smaller. The size of the nebulous disc, when measurable, and the widths of the bands—representing rate of expansion—seem to offer a means of determining the parallax. Nova Ophiuchi * passed into the nebular stage about $7\frac{1}{2}$ months after the light maximum of September, or 6 months after that of 1919 November. Nova Pictoris has been equally tardy, in great contrast to Nova Aquilæ No. 3.

The large number of spectrograms of Nova Pictoris secured at this Observatory would repay a deeper and more extended study than has been found possible in the limited time at my disposal prior to my retirement, but the present account probably contains most of the essential details.

I have great pleasure in acknowledging the invaluable assistance rendered throughout the work by Messrs. J. W. Jackson and J. B. Turner, and also the interest and encouragement shown by H.M. Astronomer, Dr. H. Spencer Jones, which are much appreciated. Fuller details and many enlargements of spectra are being prepared for publication in the *Annals* of this Observatory.

Royal Observatory,
Cape of Good Hope :
March 1926.

On the Line Absorption in Spectra of G, K, and M Types.

By F. E. Baxandall, A.R.C.Sc.

(*Communicated by the Director, Solar Physics Observatory, Cambridge.*)

Although the banded portions of spectra of the G, K, and M groups vary considerably both in nature and extent, it is well known that the superposed line absorption of the same spectra, in its general aspect, does not vary from star to star in such a great degree, especially as regards the actual lines in the spectra. That is to say, there are very few lines special to any one of these spectral types. When studied in

* "The Spectra of the Temporary Stars," Wright, *Publ. Lick Observatory*, **14**, 26.

detail, however, the lines show many changes in relative intensity, and it is the purpose of the present paper to give the results of a detailed comparison of the lines in spectra of the G_0 type, the available subdivisions of the K type, and the Ma type.

There has been far less work published relating to the details of the line spectra in this part of the stellar sequence than in the various parts of the sequence O—B—A—F. The papers bearing on this subject may be shortly referred to here.

In 1897 Miss Maury gave,* under the heading "Tables of Solar Lines," a comparison of solar lines with those occurring in α Bootis (K_0), α Orionis (Ma), and earlier spectra of F and A types. The group letters given here refer to the more recent nomenclature of the Harvard classification, and not to that adopted by Miss Maury. This comparison simply showed the relative intensities of the lines in the various groups, and had no reference to the chemical origins of the lines. The region of spectrum dealt with in the Harvard tables was from λ 3970 to λ 5896, and the spectra from which the results were obtained were taken with an objective-prism spectrograph.

In 1903, in a publication on "The Spectra of Stars of Secchi's Fourth Type," † Hale, Ellerman, and Parkhurst included in their comparison tables lines which had been measured by Professor Keeler in the spectrum of α Orionis (Ma), and sent by him in manuscript to the authors of the above paper. These lines referred only to the region less refrangible than Hβ, and thus afford no comparison with the list of lines given in the present paper.

In 1906 Hale and Adams published a paper on "Sun-spot Lines in the Spectra of Red Stars," ‡ in which they showed that many lines in the region λ 5393 to λ 5606 which are affected in sun-spots are similarly affected in α Orionis as compared with the sun. The strengthening in α Orionis was much more marked than that from sun to sun-spot.

In the same year, Walter S. Adams published a paper on "Sun-spot Lines in the Spectrum of Arcturus." § The region of spectrum discussed was λ 4352 to λ 4900, and a tabular comparison was given of lines in star, sun, and sun-spot. This paper did not record all the lines of these spectra in the region indicated, but in general referred to the lines showing changes of relative intensity in the various spectra discussed. The chief result was that lines strengthened and weakened in sun-spot spectra were also strengthened and weakened respectively in passing from the solar spectrum (G_0) to that of Arcturus (K_0). Lines of titanium and vanadium were particularly prominent amongst the strengthened lines, and many of the weakened lines were found to be "enhanced" lines of various chemical elements.

In 1914, in a paper "On the Line Spectrum of α Orionis and its Relation to that of Arcturus and the Fraunhoferic Spectrum," ‖ the

* *Annals Harv. Coll. Obs.*, **28**, pt. 1, 58.
† *Decennial Publications Univ. of Chicago*, **8**, 370.
‡ *Ast. Phys. Journ.*, **23**, 400.
§ *Ibid.*, **24**, 69.
‖ *Publications of the Solar Physics Committee.*

present writer discussed the origins and intensities of the lines which were strengthened or weakened in passing from the solar spectrum to that of α Orionis (Ma), and similarly from Arcturus (K_0) to α Orionis. The spectra investigated for this purpose were taken at South Kensington with two 6-inch objective prisms. For the solar spectrum a collimator was introduced into the spectroscope, and the resulting spectrum showed considerably better definition and separation of the lines than in the case of the objective-prism spectra of the stars named. The region of spectrum over which the comparison was made is from λ4318 to λ4930. One of the chief results was that the majority of lines which were affected in intensity from sun to stars were strengthened, and that lines of titanium, vanadium, and chromium were prominently involved in such strengthened lines.

The photographs which have been investigated as the basis of the present paper are from the Cambridge collection, and were taken in 1902 with a four-prism slit spectrograph attached to the Newall telescope. The stars whose spectra have been discussed are α Bootis (K_0), α Arietis (K_2), α Tauri (K_5), and α Orionis (Ma). A solar spectrum taken with the same spectrograph has also been compared with these stellar spectra in the elucidation of the probable origins of the stellar lines. The region over which the changes in the spectra have been investigated is from λ4236 to λ4716 for the sun, α Bootis, and α Orionis, but for α Tauri and α Arietis the extension towards the red was rather curtailed, owing to the definition deteriorating. Thus for α Tauri no lines are included in the tables beyond λ4584, and for α Arietis beyond λ4655.

All the lines in α Bootis and α Orionis were measured under the micrometer and their wave-lengths and intensities estimated. The wave-lengths were corrected for the radial velocities of the stars so as to give their normal values. As there appeared to be no lines in either α Arietis or α Tauri which do not occur in either α Bootis or α Orionis, and as the former two showed definition rather inferior to that of the K_0 and Ma spectra, it was decided not to make separate measurements of the lines in the K_2 and K_5 spectra. Instead of this an intercomparison was made of each of these spectra with those of α Bootis and α Orionis, and the relative intensities of the common lines were estimated under the micrometer. The wave-lengths adopted are the means of the estimated wave-lengths of the lines in α Bootis and α Orionis, in cases where the lines are common to the two, but where a line occurs in only one of these spectra the single estimated wave-length is used. The results are given in Table I.

It may be said here that, owing to finer definition and consequent better separation of the stellar lines, the Cambridge slit-spectra used in this inquiry furnish considerably more detail than did the Kensington objective-prism spectra which formed the basis of the earlier paper by the writer referred to previously in the present paper. The slit-spectra lend themselves to more accurate estimation of the wave-lengths of the stellar lines, and, where the two investigations cover common ground, the present results may be held to supersede the former.

Explanation of the Table.

The intensities given in Table I. are on a scale of 1 to 10; a line of intensity 1 being the weakest of the lines which could be satisfactorily measured.

Column 1 gives the wave-lengths as estimated from the Cambridge plates. Column 2 gives the intensities of only those solar (G_0) lines which were estimated to have a difference of intensity of 2 or greater from those of the corresponding lines in α Bootis. Thus these lines can be discussed as showing a decided and considerable change of intensity from the solar or G_0 type to the K_0 type. The solar intensities given here do not refer to Rowland's intensities, but to those estimated from the Cambridge low-dispersion solar spectrum with which the stellar spectra have been compared. Many of these lines are blends of several lines separately recorded in Rowland's tables.

Columns 3, 4, 5, 6 give respectively the intensities of the corresponding lines in K_0 (α Bootis), K_2 (α Arietis), K_5 (α Tauri), and Ma (α Orionis) spectra. To keep the table within reasonable limits, only those stellar lines which show an intensity-range of 2 or greater in the spectral range G_0 to Ma are included. These represent about 45 per cent. of the total number of lines measured.

Column 7 gives the chemical origins of the solar lines which are thought to be involved in the stellar lines, and column 8 Rowland's wave-lengths for these solar lines. The origins used are mainly those given in Rowland's tables, but in some cases revised or additional origins have been taken from a manuscript copy of a revision of Rowland's origins which was started here some years ago, and which has been recently resumed and completed for the region λ 3900 to λ 5900.

" Un " in column 7 signifies that the line is of unknown origin, and, if followed by a wave-length number, the latter represents Rowland's wave-length for the particular solar line of unknown origin which is supposed to be involved in the stellar line.

Where the symbol for an element is followed by " + " it means that the line is of the " enhanced " type.

The symbol (H_mC_n) is provisionally used here to indicate that the line is probably identical with one of the " structure " lines forming the well-known hydrocarbon band whose chief head is near λ 4314.

TABLE I.

Wave-lengths, Intensities, and Probable Origins of Lines in the Spectra of G_0, K_0, K_2, K_5, *and* Ma *Types.*

Wave-length.	Intensities. G_0	K_0	K_2	K_5	Ma.	Probable Origin.	λ of Solar Lines probably involved.	Remarks.
42 38·96	..	4	3	3	2	Fe	42 38·97	
42·65	..	5	5	2	3	Cr+, Mn, (H_mC_n)	42·54	
						(H_mC_n)	·62	
						Fe	·77	
						Fe, Ce	·90	
43·65	..	5	4	4	3	Fe, (H_mC_n)	43·52	
						Un	·61	
						Un	·71	
46·07	..	3	3	2	1	Fe	46·25	
46·90	..	4	4	3	6	Sc	47·00	
48·41	..	4	5	3	5	Fe, Co	48·38	
49·65	..	2	2	1	..	(H_mC_n)	49·65	
						(H_mC_n), Ca ?	·76	
50·15	..	3	3	2	4	Fe	50·29	
50·89	..	5	6	7	6	Fe	50·95	
52·38	1	3	3	3	5	Cr	52·39	
53·62	..	..	..	..	2	Ce	53·52	
						Zr	·70	
54·44	..	6	8	9	10	Cr	54·51	
55·73	..	3	2	4	4	Fe, Cr	55·66	
						(H_mC_n)	·79	
56·26	2	5	5			Ti	56·18	
						Ce	·29	
						Un	·37	
58·44	3	5	5	4	7	Fe, Mn	58·48	
59·33	1	3	3	2	3	(H_mC_n) ?	59·25	
						Cr	·30	
						Mn+, V	·46	
64·35	..	4	3	3	2	Un	64·13	
						Fe	·37	
65·26	..	2	1	3	2	Fe, Ti	65·42	
66·97	1	3	3	3	3	Fe	67·12	
68·00	..	5	5	3	4	Fe	67·99	
70·02	..	3	3	1	1	(H_mC_n), V	69·90	
						Un	70·02	
						Ti, Ce	·33	

TABLE I.—*continued.*

Wave-length.	Intensities. G_0.	K_0.	K_2.	K_5.	Ma.	Probable Origin.	λ of Solar Lines probably involved.	Remarks.
42 72·52	..	4	4	..	2	Ti, (H_mC_n)	42 72·59	Probably masked in K_5 by adjacent Fe line.
73·43	..	2	4	1	2	Fe, Ti	73·48	
						Zr+, (H_mC_n)	·64	
73·75	..	3			1	(H_mC_n)	73·95	
						(H_mC_n), Fe	4·05	
74·90	..	6	6	8	9	Cr	74·75	
							·96	
75·67	..	4	4	4	2	(H_mC_n), Cr	75·71	
76·69	1	4	2	3	3	Ti	76·59	
						Fe	·84	
77·57	2	4	4	4	3	Un	77·54	
						Un	·69	
80·58	..	3	4	2	2	Cr	80·56	
84·11	2	4	4	3	2	Mn, V, (H_mC_n)	84·22	
						Cr+	·38	
85·61	..	2	1	4		Fe	85·61	
86·01	2	5	5		5	Co	85·97	
						Ti	6·17	
87·12	..	2	2	..	..	(H_mC_n) ?	87·03	
						Fe, La	·16	
89·15	2	4	4	8	5	Fe	89·12	
						Ti	·24	
89·73	..	5	7		7	Ca	89·53	
						Cr	·89	
90·32	..	4				Ti, Ce	90·08	
						Ti+, Co	·38	
						Fe	·54	
91·49	..	5	5	5	8	Ti	91·28	
						(H_mC_n)	·38	
						Fe	·63	
92·30	..	5	5	4	2	(H_mC_n)	92·21	
						Un	·29	
						Fe, Mn+	·45	
93·17	..	3	1	..	1	Un	93·19	
						(H_mC_n)	·27	
94·27	..	7	6	8	7	Un	94·20	
						Ti+, Fe	·30	

TABLE I.—*continued.*

Wave-length.	Intensities. G_0.	K_0.	K_2.	K_6.	Ma.	Probable Origin.	λ of Solar Lines probably involved.	Remarks.
42 94·85	..	..	..	..	4	Zr, Sc	42 94·94	Not the same line. Ma line is the more refrangible one.
95·10	..	5	2	2	..	(H_mC_n), Dy (H_mC_n)	95·19 ·38	
95·98	1	4	4	4	4	Cr, Ti Ni, Co	95·91 6·04	
96·97	..	4	3	3	2	Fe+ (H_mC_n) (H_mC_n)	96·74 ·84 97·11	
97·96	2	4	3	4	2	Cr, V (H_mC_n), Co Fe, V	97·91 8·14 ·20	
43 05·57	4	2	1	1	6	(H_mC_n) Fe, Sr+, Ti, Cr, (H_mC_n)	43 05·48 ·61	
06·43	..	5	4	5		Ti, Co (H_mC_n)	06·08 ·31	
06·83	..	2	2	..	..	(H_mC_n) (H_mC_n), Ce Un	06·76 ·86 07·02	
07·33	..	..	..	..	2	Un	..	
08·01	..	8	7	7	4	Ca Fe, Ti+, (H_mC_n)	07·91 08·08	
09·76	2	4	4	4	5	Fe, (H_mC_n) Co (H_mC_n), Y Cr, Ce	09·54 ·62 ·79 ·88	
20·95	3	5	5	5	6	Sc, Ce Ti+	20·91 21·12	
23·43	..	5	6	3	3	Chiefly (H_mC_n)	..	Group of Solar-hydrocarbon lines from λ4323·16 to λ4324·57.
24·20	..	2						
25·15	3	5	6	6	4	Sc, Fe Ti, Cr	25·15 ·31	
27·10	2	4	3	4	3	Fe, Mn+ Fe, Pt ?, Gd	26·92 27·27	
30·21	1	3	3	4	3	V Ti+	30·19 ·41	
30·86	1	3	3		3	Ti+	30·87	
31·71	1	3	2	3	3	Un Ni	31·61 ·81	

TABLE I.—*continued.*

Wave-length.	Intensities. G_0.	K_0.	K_2.	K_5.	Ma.	Probable Origin.	λ of Solar Lines probably involved.	Remarks.
						Cr	43 32·75	
43 32·94	2	4	4	4	4	V	·99	
						Un	33·08	
34·10	2	4	4	4	4	La	33·93	
						Un	34·83	
34·94	1	3	3	3	3	Un	·97	
						La	35·10	
37·24	..	5	6	6	6	Fe	37·22	
38·03	1	3	3	5		Cr, Co	37·73	
38·72	..	2	1		..	Ti +	38·08	
						Un	..	
39·67	3	5	4	5	5	Cr	39·62	
							·88	
40·81	..	6	5	4	9	Hγ	40·63	
						V	41·17	
41·38	..	3	3	4		Ti+	·53	
42·28	1	3	2	2	2	V, Gd	42·35	
43·41	..	4	4	4	2	Cr	43·37	
						Fe	·43	
43·88	..	3			2	Fe, Cr	43·86	
						Ti+	44·45	
44·63	2	4	4	4	5	Cr	·67	
						Fe, Ti	46·73	
46·73	..	2	3	4	..	Cr	·99	
47·37	..	2	4	4	7	Fe	47·40	
						Fe, Zr	48·00	
48·12	1	3			1	(H_mC_n)	·13	
						Ti +, V	51·00	
51·16	..	4	4	6	6	Cr	·22	
						Fe, Ce	52·91	
53·02	3	5	5	5	5	V	53·04	
56·04	1	3	3	2	3	Ni	56·06	
56·90	..	2	2	1	..	Un	..	
58·30	..	1	1	..	3	Un	..	
59·79	2	4	4	4	4	Cr, Ni	59·78	
61·02	..	3	3	5	4	Fe, Zr, Co	60·96	
						(H_mC_n)	63·46	
63·50	1	3	3	4	3	Un	·63	
66·10	..	1	2	2	3	Fe	66·06	

TABLE I.—*continued.*

Wave-length.	Intensities. G_0.	K_0.	K_2.	K_5.	Ma.	Probable Origin.	λ of Solar Lines probably involved.	Remarks.
43 66·56	1	3	3	3	1	Zr, (H_mC_n)	43 66·66	
						(H_mC_n)	·84	
68·82	..	1	..	..	2	V	68·80	
73·57	..	2	1	} 3	5	Cr, V	73·42	
						Fe, Ni	·73	
74·63	..	2	1		4	Sc, Fe, Co	74·63	
75·13	..	3	..	..	..	Y+, Mn, Co, Nd	75·13	
76·11	3	5	5	6	7	Fe	76·11	
79·40	2	4	4	4	5	V	79·40	
80·90	..	4	4	3	1	(H_mC_n)	80·88	
82·99	..	4	5	2	..	Fe, (H_mC_n)	82·93	
						(H_mC_n)	83·16	
84·94	..	6	} 8	6	5	V, Er	84·88	
						Sc	·99	
						Cr	85·14	
85·57	..	2		2	4	Fe ?	85·41	
						Fe+	·55	
86·79	..	..	..	..	..	..	..	Apparent head of faint band in K_0 fading to red.
89·38	..	1	} 3	3	5	Fe	89·41	
90·16	1	3			3	V, Co	90·15	
91·17	1	3	2	2	2	Fe	91·12	
						Ti+	·19	
92·08	2	4	4	3	4	Cr	91·92	
						Co	92·03	
						V	·24	
93·39	..	2	2	} 4		Un	..	
94·11	2	4	4		2	V ?	93·97	
						Ti	94·09	
						Ti, Co	·23	
97·28	..	2	2	1	..	Un	97·13	
98·31	1	3	2	3	5	Y+	98·18	
						Ti	·46	
44 00·70	1	4	4	5	5	Sc	44 00·56	
						V	·74	
01·65	..	5	4	4	3	Fe	01·46	
						Fe	·61	
						Ni	·71	

TABLE I.—*continued.*

Wave-length.	Intensities. G_0.	K_0.	K_2.	K_5.	Ma.	Probable Origin.	λ of Solar Lines probably involved.	Remarks.
44 08·61	2	4	4	4	4	V	44 08·36	
						Fe	·58	
						V	·68	
09·51	1	3	3	3	3	Fe, Ni	09·29	
						Ti	·68	
12·36	2	5	5	5	5	V	12·30	
						Cr. Ca ?	·42	
16·82	1	3	3	3	3	V	16·64	
						Fe +	·99	
17·64	1	3	3	3	3	Ti	17·45	
						Ti+	·88	
21·75	2	4	4	4	4	V	21·73	
23·01	3	5	5	5	5	Fe, Y	22·74	
						Ti	·99	
						Fe, V	·30	
24·41	2	4	4	4	3	Cr	24·46	
30·24	3	5	5	7	6	V	29·96	
						Fe	30·36	
30·71	..	4	5			Fe	30·79	
33·44	..	2	2	3	3	Fe, Ni	33·39	
34·02	1	3	3			Fe	33·95	
						Ti, Cr	34·17	
35·32	..	4	4	4	6	Ca	35·13	
						Fe	·32	
36·61	1	3	3	3	3	V	36·31	
						Mn	·52	
						Ti	·75	
38·12	1	4	4	5	5	V	38·01	
39·74	..	..	..	..	..	..	..	Apparent head of faint band in K_0 fading to red.
45·67	1	3	2	2	4	Fe	45·64	
49·40	..	3	3	4	5	Ti	49·31	
50·75	2	4	4	3	4	Fe, Cr	50·48	
						Ti+	·65	
						Ti, V	51·09	
52·06	1	3	2	2	3	Mn, Fe, Nd	51·75	
						V	52·17	

TABLE I.—*continued.*

Wave-length.	Intensities. G_0.	K_0.	K_2.	K_5.	Ma.	Probable Origin.	λ of Solar Lines probably involved.	Remarks.
44 53·24	1	3	3	5	5	Mn	44 53·17	
						Ti	·49	
53·74	..	2				Ti	53·88	
57·58	1	3	2	2	3	Ti, V	57·60	
						Mn	·71	
58·40	..	2	1	2	..	Fe	58·24	
						Mn	·41	
61·88	5	7	7	6	8	Fe	61·87	
						Fe	62·16	
63·46	1	3	3	3	3	Ti, Ni, Ce	63·57	
70·90	..	1	1			Ni, Zr, Cr	70·65	
						Ti	71·02	
71·70	1	3	3	3	6	Ti, Ce	71·41	
						Co	·72	
						Co	·97	
75·02	1	3	2	2	3	V	74·91	
						Ti	75·02	
79·99	2	4	4	3	3	Fe	79·78	
						Fe	80·31	
82·35	3	5	5	4	8	Fe	82·34	
						Fe	·44	
83·05	..	2				Ti, Fe	82·90	
88·17	1	3	3	2	1	Cr	88·22	
						Fe	·31	
						Ti+	·49	
89·26	1	3	3	4	4	Fe, V, Ba	89·08	
						Ti	·26	
						Fe+	·35	
90·02	1	3		2	7	Fe	89·91	
						Mn, Fe	90·25	
96·43	1	3	4	5	5	Fe	96·12	
						Ti, Fe ?, Ca ?	·32	
96·97	..	3	3		5	Cr	97·02	
						Zr+	·14	
45 01·46	..	4	5	5	6	Ti+, V	45 01·45	
06·88	..	2	3	3	4	V	06·78	
12·91	..	3	2	2	4	Ti, V	12·91	

TABLE I.—*continued.*

Wave-length.	Intensities. G_0.	K_0.	K_2.	K_5.	Ma.	Probable Origin.	λ of Solar Lines probably involved.	Remarks.
45 26·48	2	4	4	3	3	Un, Cr, Fe	45 26·58, ·63, ·73	
30·04	2	4	4	2	2	Fe, Cr	29·85, 30·02	
37·79	..	1	..	..	2	Fe, V	37·84	
40·24	..	1	1			Un		
41·05	2	4	3	4	5	Cr	40·67, ·88, 41·24	
43·93	1	3	3	2	2	Co, Ti	43·99, 44·19	
46·01	..	2	1	3	2	Cr, Co	46·13	
49·04	..	2	1	..	4	Ti	48·94	
54·29	..	4	4	4	6	Ba	54·21	
60·42	1	3	3	3	4	Ni, Ti; Fe	60·10, ·27	
61·39	..	1	1	..	3	Un	61·59	
62·71	1	3	2	3	5	Ti	62·81	
71·31	3	5	4		6	Mg	71·28	
72·10	..	5	5	6	4	Cr, V, Ti+	71·85, ·98, 72·16	
75·77	..	..	..	..	3	Zr, Ti	75·72	
77·51	..	2	1	..	4	V	77·36	
78·99	..	3	2	2	4	Ca, V	78·73, ·91	
80·42	2	5	4	4	6	Cr, La; V; Fe, Ni	80·23, ·59, ·76	
81·65	..	5	3	3	3	Ca, Fe	81·58, ·69	Beyond here the K_5 spectrum is too weak to estimate line intensities.
86·35	..	6	4	..	6	Ca, V, Un, V	86·05, ·16, ·41, ·55	
91·50	1	3	2	..	5	V, Cr, Co, Un	91·42, ·57, ·69	

TABLE I.—*continued.*

Wave-length.	Intensities. G_0.	K_0.	K_2.	K_5.	Ma.	Probable Origin.	λ of Solar Lines probably involved.	Remarks.
45 94·27	2	4	3	..	5	V, Eu, Mn	45 94·30	
95·39	1	3	3	..	2	Fe, Mn	95·54	
96·39	..	3				Ni	96·13	
						Fe	·25	
						Cr, Mn	·59	
						Ni	46 05·17	
46 05·47	..	2	2	..	..	Mn	·54	
						Un	·57	
06·43	..	2	2	..	5	Ni, Co	06·40	
07·77	..	3	3	..	5	Sr, Co	07·51	
						Fe	·83	
16·21	..	3	3	..	6	Cr	16·31	
						Fe	19·47	
19·78	..	4	5	..	6	Cr	·71	
						V	·96	
23·30	..	3	3	..	5	Ti	23·28	
26·40	..	3	3	..	5	Cr	26·26	
37·93	..	5	5	..	3	Fe	37·69	
							38·19	
						Ti	39·54	
39·89	..	5	5	..	5	Ti, Cr	·85	
						Ti	40·12	
46·58	..	3	4	..	5	Cr	46·35	
						Un	·82	
47·68	..	3	2	..	1	Fe	47·62	
51·61	..	2	2	..	4	Cr	51·46	
52·48	..	2	2	..	4	Cr	52·34	Beyond this point the K_2 plate is too poor for estimation of intensities.
						Ti	56·23	
56·39	..	3	..	..	6	Cr, Mn	·37	
						Ti, Cr	·64	
69·66	1	3	..	..	3	Fe	69·35	
						Cr	·50	
70·71	1	3	..	..	3	Sc	70·59	
75·15	2	4	..	..	6	Ti, Cr	75·29	
						Ti	82·09	
82·32	..	4	..	..	6	Fe	·30	
						Co	·53	
						Fe	·75	

TABLE I.—*continued.*

Wave-length.	Intensities. G_0.	K_0.	K_2.	K_5.	Ma.	Probable Origin.	λ of Solar Lines probably involved.	Remarks.
46 83·82	..	2	..	..	..	Fe	46 83·75	
87·57	..	3	..	..	5	Fe	87·57	
90·98	..	1	..	..	3	Ti	90·98	
91·50	..	2	..	..	4	Ti	91·52	
						Fe	·60	
93·70	..	2	..	..	5	Co	93·37	
						Ti	·85	
95·30	..	..	..	..	2	Fe	95·04	
						Cr	·33	
98·97	3	5	..	..	6	Co, Ni	98·58	
						Cr	·64	
						Cr	·80	
						Ti	·95	
47 10·23	..	3	..	..	5	Mn, V, Nd	47 09·90	
						Ti	10·37	
						Fe	10·47	
15·57	1	3	..	..	5	Ti	15·47	
						V	·63	

Some of the differences in intensity from star to star as revealed by the table may now be discussed. A comparison of columns 2 and 3 shows that in almost all cases where there is a difference of intensity of 2 or greater between a solar line and the corresponding K_0 line the lines are " strengthened " in the K_0 spectrum. There are few cases of the reverse order.

Lines Considerably Strengthened from Solar Spectrum (G_0) to α Bootis (K_0).

There are 84 lines in all which come under this category. Table II. shows the chemical elements whose lines are probably involved in the strengthened lines. The number after a particular element represents the number of stellar lines in whose origin that element is presumed to take part.

TABLE II.

Fe 33	Ni 8	Y 2	Mg 1
V 28	Ti+ 8	La 2	Eu 1
Cr 26	Ce 6	Gd 2	Cr+ 1
Ti 25	(H_mC_n) 6	Fe+ 2	Y+ 1
Co 11	Sc 4	Mn+ 2	
Mn 9	Ca 2	Ba 1	

It is fairly evident from this that lines of the elements Fe, V, Cr, Ti play a prominent part in the strengthened lines. Certainly the evidence

for these is greater than for most of the elements in the list with small numbers following their symbols. Some of the latter may be haphazard appearances, as in a fair number of cases they come in stellar lines which are blends of several solar lines, among which may be lines of Fe, V, etc. —elements prominently represented in the strengthened lines.

It is rather surprising to find so many "Ti+" lines involved in the strengthened lines. The Ti lines of this class first appear at about B_8 and strengthen through the A group to the F group, where at about F_5 they attain their maximum intensity. They then decline in intensity through the remainder of the F group and through the G group. One would therefore expect them to decline still further in passing from G to K-type stars. The probable explanation of the apparent anomaly is that in almost every case of a line in α Bootis in which a Ti+ line apparently takes part, it is blended with an ordinary line of either Fe, Ti, Cr, or Sc, all of which elements are known to be often associated with strengthened lines from sun to sun-spots, or from sun to α Bootis (K_0). It is very likely that the Ti+ line is really weakened, but its partner or partners in the blend are strengthened to such a degree that the resultant effect is one of strengthening.

The (H_mC_n) lines in the preceding table also probably come in the same category as the Ti+ lines, as it will be shown later in this paper that they take a conspicuous part in the lines that are "weakened" from the K_0 stage to that of Ma.

For the Ba, Mg, and Sc lines in the table there is clear evidence that the strengthening is real, as the former two and at least one of the Sc lines are free from blending.

For the four outstanding elements—so far as number of lines is concerned—in the preceding table, an analysis has been made of how their lines are distributed among King's temperature classes. The results are given in Table III.

TABLE III.

Distribution of the Lines of Fe, V, Cr, *and* Ti *in King's Temperature Classes.*

Element.	Total Number of Lines.	King's Temperature Class.					Not given by King.
		I.	II.	III.	IV.	V.	
Fe	38	7	0	1	4	1	25
V	31	15	4	9	2	0	1
Cr	29	9	2	10	5	0	3
Ti	29	0	8	17	0	1	'3

This shows fairly decisively that the large majority of the lines belong to King's Classes I. to III. inclusive. The lines of Classes I. and II. are regarded by King as being of a low-temperature type, Class III. as medium temperature, and Classes IV. and V. as high-temperature. There are about three times as many lines here of Classes I. and II. as those of Classes IV. and V.; which indicates evidence of lines of comparatively low temperature being mainly involved in the lines strengthened from sun to star.

The absence of any lines of Class I. in the case of titanium seems rather a striking result, but on examination of King's list of Ti lines

it is found that, for the region covered by this inquiry, only three lines are placed in Class I. In effect, therefore, the lowest temperature lines of Ti may almost be said to start at Class II., and the differentiation of Ti from the other three elements is more apparent than real.

The fact that 25 of the 38 Fe lines associated with the strengthened stellar lines are not given in King's list suggests that the majority of Fe lines involved are of comparativly low intensity.

Changes in the Stellar Spectra from K_0 to Ma.

An examination of Table I. will show that there are far less decided changes in relative intensity of the lines from K_0 to K_5 than from K_5 to Ma. In this sense the step from K_0 to K_5 seems to be less than from K_5 to Ma. An analysis is now given of the chemical elements which probably take part in the lines which are considerably affected in intensity in passing from the K_0 type to the Ma type. For the sake of simplicity and emphasis it has been decided to include only those lines which show an intensity-difference of 2 or greater in the two spectra. The strengthened lines can be considered first.

Lines Strengthened from K_0 to Ma.

Table IV. summarises the chemical elements involved in the strengthened stellar lines with an intensity-difference of 2 or greater. The total number of lines in this class is 53. The numbers opposite the symbols represent the number of strengthened stellar lines in which the particular element is presumed to take part.

TABLE IV.

Fe	20	Ni	2	Ce	1
Ti	17	Ca	2	(H_mC_n)	1
Cr	16	Zr	2	Fe+	1
V	9	Ti+	2	Zr+	1
Co	7	Ba	1	Y+	1
Mn	4	Sr	1		
Sc	3	La	1		

The best evidence for real strengthening of lines of a particular element is, of course, obtained from stellar lines which are pure, and not blends of several lines belonging to different elements. For each of the first four elements in the above summary there are several lines quite free from blending, and there can be little doubt that the majority of lines of these elements which form parts of the blended stellar lines are real agents in the strengthening of the latter in Ma spectra.

Too much weight must not be given to most of the elements represented by the smaller numbers in the summary, as for all those below Sc—except Ba—their involved lines are blended with lines of other elements which are known to be associated with the strengthened lines.

As enhanced lines in general are known to be weakened in passing through the later spectral types, those of that category which are

apparently contained in the strengthened lines occupy an anomalous position. In each case, however, they are blended with ordinary lines of some other element, and their apparent strengthening is probably illusory. Thus the Ti+ lines are each blended with a line of vanadium, the Fe+ line with an unenhanced Fe line, the Zr+ line with a Cr line, and the Y+ line with a Ti line. As nearly all the lines with which the enhanced lines are blended belong to elements at the head of the summary it seems almost certain that the strengthening in these blends is due to the " unenhanced " and not the " enhanced " lines.

Some of the elements represented in Table IV. may be referred to in more detail.

Barium.—Only one line of this element occurs in the origins of the stellar lines. The particular line (λ4554·2), however, is quite an isolated one, and the strengthening cannot be questioned.

Scandium.—The isolated Sc line λ4247·0 seems to have an anomalous behaviour here. It is a fairly prominent line in A and F types, and decreases in intensity in passing from these to the G (solar) type. One would, therefore, expect it to decline still further through the K types to Ma. It is, however, considerably stronger in Ma than in K_0, although there appears to be no suspicion of its being blended with a line of another element, and certainly not with an adjacent solar line.

Chromium.—Some of the lines of this element show a great increase in intensity from K_0 to Ma, so that the line 4254 is about the strongest line in the whole spectrum, and 4274·9 one of the strongest. Whether the Cr lines attain their maximum intensity at Ma, or increase still further in lower types in the sequence, it is impossible to say here, as the Cambridge series of stellar spectra contains nothing of a later type than Ma.

Temperature Classes of the Lines Involved in the Strengthened Stellar Lines.

As the lines of Fe, Ti, Cr, and V evidently play a conspicuous part in the stellar lines strengthened from K_0—Ma, an analysis is now given of how these lines are distributed amongst King's temperature classes. This is shown in Table V. The figures in the second column give the total number of lines of each element which apparently take part in the strengthening of the stellar lines.

TABLE V.

Element.	Total Number of Lines.	King's Temperature Classes.					Not given by King.
		I.	II.	III.	IV.	V.	
Fe	21	7	0	0	1	1	12
Cr	18	8	2	3	1	0	4
Ti	17	2	5	7	1	0	2
V	9	2	0	1	4	0	2

Here, again, there are about three times as many lines in King's Classes I. and II. (low temperature) as in Classes IV. and V. (high temperature), so that, in general, low temperature lines may be said to

prevail in the strengthened stellar lines, whether blended or unblended. In the case of Fe, all the unblended lines which are strengthened in Ma are of Class I. Cr shows ten lines of Classes I. and II., and only one of Classes IV. and V. For Ti, King gives only three lines in Class I. in the region covered by this inquiry, and two of them occur in the strengthened lines, whereas only one Ti line of Classes IV. and V. is involved. Vanadium shows rather a curious differentiation from the other three elements in that about half its lines which apparently take part in the strengthening of the Ma lines belong to Class IV., which is associated with high-temperature lines.

Lines Weakened from K_0 to Ma.

In the same way as in the preceding summary, an analysis is given in Table VI. of the chemical elements represented in the stellar lines which decline in intensity from K_0 to Ma to such an extent as to show an intensity difference of 2 or greater. The total number of stellar lines in this category is 44.

TABLE VI.

Fe	24	Ce	3	Ti+	2
(H_mC_n)	21	Ni	2	Cr+	2
Cr	7	Co	2	Fe+	1
Ti	5	Ca	2	Mn+	1
Mn	5	Zr	2	Dy	1
V	4				

This shows at once that lines of iron and hydrocarbon play a conspicuous part in the lines weakened from K_0 to Ma. In addition to this there is a fair representation of the "enhanced" type of line which, for most elements, are far fewer in number than the ordinary or unenhanced lines. The hydrocarbon lines may be specially referred to here.

Hydrocarbon.—The lines under this heading (given in the tables as (H_mC_n) refer to detached lines or small groups of lines in the structure of the main band. This band, the main head of which is at λ4314, first appears in stellar spectra at about F_5, gradually strengthening through the lower F types to G_0 or solar type. There is little difference in its intensity in the G_0, K_0, and K_2 types, but from here to K_5 and Ma it falls off in intensity considerably, being quite weak at Ma. It may be mentioned that the changes in intensity in the hydrocarbon band may be best traced through the various stellar types, not by the general appearance of the main band, but by the changes in a small detached portion of the band near λ4324. There is a small compact group of solar lines here (λ4323·17 to λ4324·57), consisting almost wholly of hydrocarbon lines. In stellar spectra of small dispersion these lines coalesce into what appears to be a single line, and the changes in intensity of this in the stellar types may safely be taken as an indication of what is also happening to the main band, although the real changes in the latter may not be so obvious owing to so many lines of other substances being superposed on the band. In fact, this detached group of hydro-

carbon lines forms an important criterion in placing the subdivisions of lower-type spectra in their proper sequence. It may not be out of place to mention here that although the hydrocarbon band drops in intensity along the branch K–M of the stellar sequence, on the other recognised branch K–R it is far more prominent in the R stars than in the K stars. This is one of the features that makes it almost impossible to place the G, K, M, and R stars in one sequence.

Iron Lines.—An analysis of the iron lines which take part in the weakened stellar lines shows that of the twenty-six lines involved one belongs to King's Class V., five to Class IV., one to Class II., while nineteen are not given in King's list. What evidence there is tends to show that the weakened stellar lines relate to high-temperature lines, as distinguished from the low-temperature lines which occur amongst the strengthened stellar lines.

General Conclusions.

The majority of the stellar lines vary little in intensity in the range G_0 to Ma.

The lines showing considerable increase in intensity from G_0 (sun) to K_0 belong chiefly to iron, vanadium, chromium, and titanium. The majority of the strengthened lines of these elements fall in King's temperature classes I., II., and III.; the first two of which are associated with low temperatures. Very few of the lines occur in Classes IV. and V., indicative of high temperature.

Of the lines markedly strengthened from K_0 to Ma the great majority belong to the same four elements mentioned in the preceding paragraph; and here, again, the lines involved belong chiefly to the lower-temperature classes. There is, however, evidence from unblended stellar lines that lines of barium and scandium also strengthen from K_0 to Ma.

The lines which weaken considerably from K_0 to Ma consist chiefly of lines of iron and hydrocarbon. Those of the latter substance are detailed lines or groups of lines in the structure of the well-known band whose main head is at $\lambda 4314$. The weakened iron lines which are classified by King nearly all belong to Classes IV. and V., and are thus high-temperature lines.

There are less numerous and smaller changes in intensity of the stellar lines from K_0 to K_5 than from K_5 to Ma. The step from K_0 to K_5 thus seems less than that from K_5 to Ma.

Of the enhanced lines involved in the stellar lines few are free from blending with ordinary lines of other elements. Among those that are unblended there seems to be no very marked change of intensity from K_0 to Ma. One or two seem to be slightly stronger in Ma, which is contrary from what one would expect from their behaviour in earlier parts of the stellar sequence. These do not show an intensity-difference great enough to include them in Table I.

The behaviour of the hydrocarbon band in the range K to M where it weakens is different from that on the other branch K–R of the spectral sequence, where it strengthens considerably.

There are a few lines of unknown origin, but none with high intensity.

On the Inclination of the Orbits of Spectroscopic Binaries.

By G. Shajn.

(*Communicated by the Secretaries.*)

The observations of spectroscopic binaries allow us to evaluate the following mass-functions :

$$f_1(m)=(m_1+m_2)\sin^3 i \qquad \text{(two stellar spectra observed)}$$

$$f_2(m)=\frac{m_2{}^3\sin^3 i}{(m_1+m_2)^2}=\frac{\alpha^3}{(1+\alpha)^2}m_1\sin^3 i \qquad \text{(one stellar spectrum observed)}$$

where $$\alpha=\frac{m_2}{m_1}.$$

In most cases we know only the second function. It is easily seen that $f_2(m)$ depends to a great extent on the value of mass-ratio. For this reason it is to be expected that the dispersion of $f_2(m)$ for the same spectral class will be very large and, in fact, the observations confirm this expectation. However, for the group of stars the average value of mass-function is close to the truth (Ludendorff, Halm, O. Struve,* and others). The influence of the factor $\sin^3 i$ is also great. Usually $\sin^3 i$ is assumed to be equal to 0·59.

It is not impossible that the planes of the orbits of spectroscopic binaries have some peculiarity in their distribution in space. For instance, the orbital planes may be parallel to the Galaxy. It is of interest to study the connection between the mass-function $(m_1+m_2)\sin^3 i$ and galactic latitude to find if such a relation exists. The new *Third Catalogue of Spectroscopic Binary Stars*, by J. H. Moore, affords the best data for this purpose.† The valuable investigations by O. Struve show that we cannot consider all short periodic binaries as true binaries. For this reason we have excluded from Moore's *Catalogue* the Cepheids and spectroscopic binaries, the period of which is shorter than 2·3 days, with the exception of the binaries with two observed spectra (binary character certain). Some stars, the orbits of which are very uncertain, were also excluded, viz. Boss 384, 913, 1018, 1139, 1250, 1690, 4193, and 5469.‡ In addition to these binaries I have excluded some orbits of type B, which are computed from the velocity-curve from lines H and K.

For the spectroscopic binaries with two observed spectra $(m_1+m_2)\sin^3 i$ are taken immediately from Moore's *Catalogue*. For the binaries with one observed spectrum $(m_1+m_2)\sin^3 i$ was computed, assuming α to be equal 0·7. As we are concerned only with the ratios of $(m_1+m_2)\sin^3 i$ for different galactic latitudes, the assumed value of α is of no serious consequence. It is important to have groups of stars, which would be homogeneous in respect of the absolute magnitude,

* *M.N.*, **86**, 63.

† In addition to the orbits contained in Moore's *Catalogue*, I have used several orbits which have been published in *Public. of the Dominion Astrophys. Observatory, Victoria*, vol. iii, 5, 6, 7, 8.

‡ K=1·98.

because the galactic concentration depends in general on the luminosity. The influence of the selection of stars is then of no serious consequence.

In Table I. the average values of $(m_1+m_2)\sin^3 i$ for different spectral types and for different galactic latitudes are given (fig. 1).

TABLE I.

Spectrum.	$(m_1+m_2)\sin^3 i$.					
	$\beta=0°$–$15°$.	n.	$\beta=15°$–$30°$.	n.	$\beta=30°$–$90°$.	n.
B_0–B_5	25·46	24	9·92	17	3·94	17
,,	15·46*	22	,,	,,	,,	,,
B_8–A_5	6·95	25	2·66	19	2·84	28
F	2·08	6	2·30	16	1·06	15
G	3·45	9	3·70	9	0·79	10
K–M	5·75	5	1·56	5	0·69	11

No doubt there is a large dispersion in mass-function for the same value of galactic latitude. The factor $\frac{\alpha^3}{(1+\alpha)^2}$ decreases very rapidly with decreasing mass-ratio. For $\alpha=0·9$, 0·7, 0·5, and 0·3, for instance, this factor is equal 0·20, 0·12, 0·056, and 0·016 respectively. For this reason it is not so surprising that in fig. 1 we have a considerable number of spectroscopic binaries with very small improbable values of mass-functions. They relate in general to the binaries with only one spectrum observed.

It is easily seen that the average values of $(m_1+m_2)\sin^3 i$ for all spectral types decrease with increasing galactic latitude. This decrease is shown not only in Table I. (average values), but also by fig. 1, though, as is to be expected, the dispersion is very large. It must be noticed that this effect is smaller for binaries of type A than for other spectral classes. In fig. 1 the stars with mass-functions larger than 28·0 for B_0–B_5 and 7·0 for A, F, G, K-M are represented by the dots above the lines 28·0 and 7·0.

These results may be affected by several uncertainties and by want of homogeneity in the luminosities of stars. If in each group there are giants and dwarfs, and if the galactic concentration for giants is larger than for dwarfs, it is to be expected that in such a case the mass-function will be larger for low galactic latitudes. In Table II. are given the values of mass-functions for various groups of stars as a function of galactic latitude, with division of the later types into giants and dwarfs.

Among the binaries of type K there is only one dwarf (Lal. 46867, gal. lat.$-32°$). Among the binaries of types F and G there are giants and dwarfs. The division into giants and dwarfs is possible only for binaries of type F_5–F_8 and G. For F_0–F_2 this division is uncertain. The criterion for the division into giants and dwarfs was either absolute magnitude (for giants $M<2·5$) or proper motion.

It is easily seen that the data of Table I. are affected by the different

* Two stars with very large masses, $+6°·1309$ and Boss 1635, are excluded.

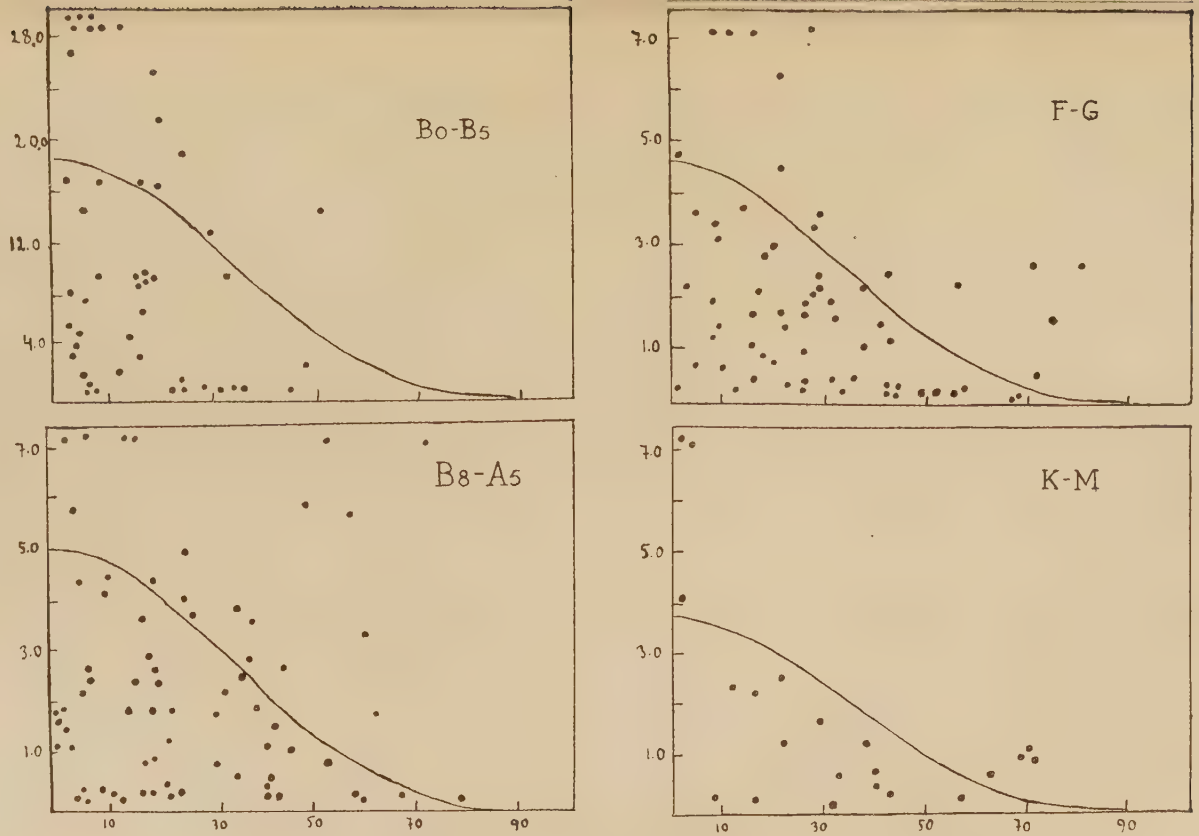

FIG. 1.—Relation between mass-function and galactic latitude for various spectral types.

Full line is function $y=\sin^3 x$.
Ordinate is function $(m_1+m_2)\sin^3 i$.

Table II.

Spectrum.	$(m_1+m_2)\sin^3 i$.			
	$\beta=0°-30°$.	n.	$\beta=30°-90°$.	n.
B_0-B_5	19·01	41	3·94	7
B_2-B_5	11·90	29	3·94	7
B_8-A_5	5·01	44	2·84	28
B_8-A_0	7·48	25	3·08	20
A_0-A_5	2·72	31	1·81	23
F	2·24	22	1·06	15
G	3·58	18	0·79	10
F–G	2·84	40	0·98	25
F_5-F_8 (giants)	2·86	10	1·50	5
F_5-F_8 (dwarfs)	1·67	8	0·94	9
G (giants)	4·40	14	1·53	2
G (dwarfs)	0·68	4	0·60	8
K–M (giants)	3·65	10	0·74	10

galactic concentration of giants and dwarfs. However, Table II., in which the stars are selected by luminosity, shows that there is a decrease of mass-function with increasing latitude. For the spectroscopic binaries of types F_5-F_8, G, and K–M this effect is very sensible, but for type G the number of stars is insufficient.

For the binaries of types B and A there is some uncertainty. We may consider that the results are affected by the fact that the absolute magnitude increases in general from B_0 to B_5 and from B_8 to A_5. But the difference in average absolute magnitudes within the limits B_0-B_5 and B_8-A_5 is smaller than the dispersion for one spectral subdivision. In Table II. are given $(m_1+m_2)\sin^3 i$ for B_2-B_5 and B_8-A_0, and within these close limits the difference in galactic concentration and absolute magnitude is very small. Thus for the groups of spectroscopic binaries of homogeneous luminosity the mass-function $(m_1+m_2)\sin^3 i$ in low galactic latitudes is larger than that in high ones.

It seems probable that the distribution of the orbital planes of spectroscopic binaries in space is not random, and that there is a tendency for them to be parallel to the Galaxy. To be sure, we cannot assert that the influence of non-homogeneity in the luminosities is excluded; however it is reasonable to conclude that the relation between $(m_1+m_2)\sin^3 i$ and galactic latitude is not accidental. It may also be supposed that the masses of stars of the same spectral class (giants and dwarfs separately) in the Galaxy are larger than that for high latitudes. But the difference seems to be too great for such an explanation.

For comparison, Eddington's and Seares' theoretical values of the masses are given in Table III. The comparison may be only an approximate one, because we do not know the absolute magnitudes of the stars under consideration, and in addition to this the assumed value for the mass-ratio is uncertain. Assuming the probable value of the absolute

magnitudes to be +1·0 for group A_0-A_5 and +0·5 for other spectral groups, we find :

Table III.

Spectrum.	$(m_1+m_2)\sin^3 i$.			
	$\beta=0°-30°$.	$\beta=30°-90°$.	Eddington.	Seares.
A_0-A_5	2·72	1·81	2·5	5·2
F_5-F_8 (giants)	2·86	1·50	3·0	3·3
G ,,	4·40	1·53	4·0	2·8
K–M ,,	3·65	0·74	4·8	2·4

The agreement of the mass-functions of galactic spectroscopic binaries with theoretical ones, especially with Eddington's masses, seems as good as could have been expected. On the other hand, the masses of non-galactic binaries are considerably smaller than the theoretical ones, and we may think that that is independent evidence in favour of a peculiar distribution of the orbital planes of spectroscopic binaries in space.

It must be remembered that Guthnick * had suggested that the orbits of eclipsing variables of type B are parallel to the galactic plane (on the basis of high galactic concentration of these stars). The writer † had suggested the same for the spectroscopic binaries. Aitken ‡ has found that spectroscopic binaries are concentrated to the Milky Way. In a recent paper Ludendorff § finds some evidence in favour of decreasing masses of B-type spectroscopic binaries with increasing galactic latitude.

The comparison of spectroscopic binaries of the same spectral type (Tables II. and III.) shows that the masses of giants are much larger than that of dwarfs. The spectroscopic binaries confirm our conceptions on the relation between mass and luminosity. As is to be expected, the difference between the masses of giants and dwarfs of types G and K is greater than that of type F_5-F_8. From the investigations of visual double stars it is known that the mass-ratio in giant systems is smaller than that for dwarfs. If the same is applicable to the spectroscopic binaries, the difference between the mass of giants and dwarfs must be still greater.

At various times investigations have been made with the object of finding whether the poles of double-star orbits showed any peculiarity of distribution (Doberck, See, Miss Everett, Lewis, Turner, and Bohlin). From the elements of double-star orbits we may find two sets of poles, and the inability to distinguish between the real and the spurious set is the great difficulty attending this research. The results are contradictory, and nothing of a decided character could be gathered from these investigations. The material is very scanty (50–60 orbits).

I think that the solution of this problem for double stars may be

* *A.N.*, **191**, 169.
† *Pop. Astr.*, 1924, May.
‡ R. G. Aitken, *The Binary Stars.*
§ *A.N.*, **211**, 115.

done conveniently in the following way.* For the sake of simplicity, we shall assume that the real orbits are circular ones. Let us suppose that the double-star orbits are parallel to the Galaxy. In such a case the apparent orbit will depend on the galactic latitude. In the Milky Way we shall have very elongated ellipses, and in very high latitudes almost circular orbits. Then the position angles (referred to the galactic pole) of the companion in close double stars in the Milky Way will show a marked preferential direction, but in very high latitudes the distribution of the position angles will be random.

Summary.

The mass-function of spectroscopic binaries $(m_1+m_2)\sin^3 i$ decreases with increasing galactic latitude.

Giants and dwarfs separately show this phenomenon.

In low galactic latitudes the values of $(m_1+m_2)\sin^3 i$ are in good agreement with those derived from Eddington's and Seares' masses, and in high latitudes the observed mass-functions are smaller than the theoretical ones. There is some evidence in favour of a tendency for the orbital planes of spectroscopic binaries to be parallel to the Galaxy.

The mass-function for dwarf systems is smaller than that for giants.

Attention is called to the possibility of the study of distribution of the double-star orbits in space by the investigation of the distribution of position angles in close pairs as a function of galactic latitude.*

Simeis, Branch Observatory of Pulkovo :
1926 *April* 15.

Fourth Note on W. Herschel's Diffused Nebulosities.

By J. G. Hagen, S.J., Assoc.R.A.S.

Madame D. Isaac Roberts has now sent us the complete set of the 52 positive prints on glass of her late husband's original plates referring to Herschel's fields. Without them the question of the long-forgotten observations of Herschel would not have been cleared up. Astronomers will therefore be grateful to Madame Roberts.

1. Among the following 13 fields there are 5 of especial importance, as they fall within some photographs taken by others and for other purposes.

To understand Table I. it is only necessary to remember that Roberts' plates cover an area of $2^\circ \times 2^\circ$, and that $\Delta\alpha$, $\Delta\delta$ denote the distances of the guiding star from the place given by Herschel, in the sense: star−H.

* This method has already been used by Prof. J. M. Poor. *Astr. Journ.*, **28**, 145 (1914).—*The Secretaries.*

TABLE I.

H.'s No.	Centre (1925).		Guiding Star (1925).			Mag.	$\Delta\alpha$.	$\Delta\delta$.
	h m	° ′		h m	° ′		′	′
19	4 53·8	+26 47	Camb. E. 2264	4 57·1	+26 34	7·2	+44	−13
20	5 17·4	+25 3	Berlin B. 1722	5 19·4	+24 54	7·8	+27	− 9
21	5 20·9	+25 2	Berlin B. 1722	5 19·4	+24 54	7·8	−20	− 8
22	5 30·1	− 6 55	Wien Ott. 1557	5 31·8	− 5 57	3·1	+25	+58
23	5 31·5	− 2 42	Strass. 1610	5 27·6	− 2 10	8·5	−59	+32
24	5 33·2	− 4 17	Strass. 1728	5 36·7	− 4 28	8·2	+54	−11
25	5 36·8	− 2 30	Strass. 1730	5 37·0	− 1 59	2·0	+ 2	+32
26	5 38·1	− 6 56	Wien Ott. 1586	5 35·2	− 7 15	5·8	−43	−19
27	5 44·5	+ 1 9	Nicolaj. 1467	5 42·7	+ 1 9	6·7	−27	0
28	6 2·3	+ 3 44	Albany 2011	6 1·0	+ 4 10	6·0	−19	+26
29	6 2·0	−20 27	Algiers 2040	5 58·3	−20 39	8·0	−50	−12
30	6 41·9	+41 15	N.G.C. 2281	6 44·1	+41 9	Cl.	+23	− 6
31	9 28·6	−18 33	Algiers 4251	9 28·9	−19 4	6·5	+ 4	−31

The second table contains Herschel's description of his fields, literally copied from the *Sc. Papers*, **2**, 463, and their extension in both co-ordinates counted from the centre, *i.e.* half of his totals, with the addition of the galactic latitudes.

TABLE II.

H.'s No.	Parallel.	Merid.	H.'s Description.	Gal. Lat.
	′	′		°
19	53	75	Strong suspicion of very faint milky neb.	−10
20	42	74	Very much affected	− 6
21	15	74	Affected	− 6
22	75	75	Affected with milky nebulosity	−19
23	15	80	Affected	−17
24	54	76	Visible and unequally bright neb. I am pretty sure this joins to the great nebula in Orion	−18
25	83	77	Diffused milky nebulosity	−15
26	58	75	A pretty strong suspicion of nebulosity	−17
27	33	79	Affected with milky nebulosity	−13
28	15	77	Much affected	− 9
29	54	84	Affected	−18
30	13	92	Affected	+16
31	15	75	Affected	+24

The second and third columns of Table II. make it probable that Herschel estimated the extension of the nebulosities by full degrees and by the unit of 15′ which was the diameter of his field of view.

2. Our own observations are recorded in what follows, denoting by the scale-number I the thinnest veils, and by V the densest nebulosities.

Herschel No. 19.—The nebulosities of this region vary between densities IV and V, both in the middle and in the four corners of the field.

Nos. 20 and 21.—The two regions form one continuous field, their centres differing only $3^m \cdot 5 = 47'$ in R.A. The single plate of Roberts was pointed to the middle between Herschel's positions. The density varies between IV and V, the latter prevailing in the southern half of the chart.

No. 22.—The general density of this field is similar to Nos. 19–21, varying between IV and V. The *np* quadrant, in particular, fades towards III, while in the *sf* quadrant density V prevails. The neighbourhood of the two brightest stars deserves special mention. Just *sp* the guiding star, to the extent of 8′, there is a cluster of stars, where the sky looks entirely void of nebulosity (zero on our scale of density). In the *sp* opposite quadrant, closely *np* the 5th mag. star (*BD*−7° 1106), there is a cloud of density V measuring about $15' \times 30'$.

The plate of Roberts shows in the *nf* quadrant a nebulous star which is not in the N.G.C. and which was estimated here on our light scale ($1' \cdot 2 \times 1' \cdot 2$) 10^N.* It is the star *BD*−6° 1253 (not 1252), mag. 9·3, and has the letter *b* on the key map of Dr. Max Wolf (see below, § 3). The surrounding nebulosity has density IV to V.

No. 23.—From Table I. it appears that the plate of Roberts was pointed one degree *p* Herschel's place. Still the chart serves its purpose. The guiding star is double (4″, but not in Burnham's Catalogue), and cannot be mistaken.

The general density of Herschel's field is IV to V, the latter prevailing in the *sp* quadrant, while in the *sf* quadrant the density is generally IV, sometimes III and II.

The centre has V, but immediately *p* there is a thinner band extending over one degree in length towards *n* and 25′ to 40′ in width in a *nf* direction. The density of the band is III, II, and even I. The whole field is remarkable for strong contrasts between lighter and denser portions.

No. 24.—The centre of Roberts' plate is 6^m late on Herschel's position, but the chart is serviceable since the guiding star falls on it and can easily be identified.

* In the notation of our *Preparatory Catalogue* (Specola Vaticana, X).

The general density of Herschel's field is III, IV, and V, number V prevailing in the *f* half and IV in the *p* half. Just *p* and *sp* the centre there are two open clusters of stars, where only faint nebular veils of grades I and II are visible.

This field, like 23, is remarkable for strong contrasts in density.

Herschel No. 25.—A print of this field was published by Roberts in *M.N.*, **63** (1903), 32, and in *Ap. J.*, **17** (1903), 76. It had been photographed by W. H. Pickering and others long before, though without reference to Herschel's field. In spite of the short exposure of 90^m, the star images on Roberts' plate are too diffuse for our purpose. Besides, our guiding star ζ Orionis should not be in the centre but 32′ to the north. Herschel's place coincides with the so-called "horse head" nebula exactly in Decl. and precedes it only 5′ of arc. We therefore made a new plate, with the astrographic reticle on it. This facilitated the exact locating of a chart published in our *Miscellanea Astr.*, p. 240. Although our plate was exposed an hour and a half it does not show the nebulous ribbon extending south from the star ζ, but the other two nebulæ that appear on the plate of Roberts are clearly impressed, viz. N.G.C. 2023 and the diffuse streaks closely *nf* ζ. Visually, however, our telescope shows only N.G.C. 2023.

The estimates of density around the "horse head" nebula were made this year quite independently from those made in 1922, and turned out about half a grade stronger, owing, perhaps, to a less transparent sky. On the whole the entire field of $2^\circ \times 2^\circ$ area varies between densities III and V, the greater density prevailing in the *s* and *f* portions, while the *np* quadrant has shades between II and III. Neither our plate nor that of Roberts show traces of these visual nebulosities.

No. 26.—The density of this region is IV to V at the centre, it is nowhere less than IV, and reaches V in the portions *s* and *sp*.

No. 27.—This field is the brightest portion of a spiral nebula encircling both belt and sword of Orion, the history of which is minutely recounted by Barnard in *Ap. J.*, **17** (1903), 79. His small print B on Plate VI. coincides almost exactly

with the plate of Roberts. Our guiding star of mag. 6·7 is a little *sp* Barnard's centre, close to the *p* margin of the nebulous band that crosses his print diagonally. As the three fields of Herschel, Roberts, and Barnard are practically central to one another and equal in extension, Barnard justly concludes that "there is therefore no question but that this nebulosity exists where Herschel saw it."

Roberts photographed this region four times, first in 1901 with an exposure of 90^m, and the last time in 1903 (February 23), a month or so after Barnard's protest had appeared. His last plate had an exposure of $2^h\ 57^m$, and the record appended reads: "Large areas void of stars, no nebulosity." Only in the *sp* quadrant there is a bright nebula 5′ in diameter which, in our 16-inch refractor, looks like a 12th mag. star. On Barnard's print it is easily found by its close *np* companion.

Visually the entire field has a density varying between grades IV and V except the *nf* quadrant, where the nebulosity is densest with grade V, and a few portions of the same density in the *sp* quadrant.

Herschel No. 28.—The portions *n* and *sf* Herschel's place have density V, the centre of the field has IV to V, and a few regions *sf* it have III to IV.

No. 29.—The pointing of Roberts' plate was about $15' = 1^m$ late on Herschel's place. The centre of the Herschel field has density IV. The portions *f* vary between IV and V, while *p* there are thinner nebulosities of grades III to IV.

No. 30.—From Table I. it appears that the guiding point is cluster N.G.C. 2281. Within this cluster, to the extent of 12′ *pf* and 25′ *ns*, only thin nebulosities of grade I are seen and somewhat denser ones immediately *p* and *f*, estimated as II to III. The rest of the field varies from III to V.

No. 31.—The centre of the field is of density IV to V., while the nebulosities of the entire region vary little around grade IV.

3. The three regions Nos. 22, 23, and 24 are remarkable for the fact that they fall within the great spiral nebula mentioned above under No. 27, and that they are contained in a photograph published by Dr. Max Wolf in *M.N.*, **63** (1903), 303.

As to No. 22 the comparison of our estimates with the photograph encounters the difficulty that the 3rd mag. guiding star and the clear

field *sp* it fall within the white patch marked on the photograph as the " great nebula."

Regarding No. 23 there is an advantage in the displacement of Roberts' plate in a *p* direction because Wolf's chart shows mainly that portion of Herschel's field. Possibly Roberts pointed purposely away from the right place to avoid the disturbing light of ζ Orionis, whose glare overlaps Herschel's centre on Wolf's chart.

Field No. 24 falls a little *sp* the place assigned to it by Wolf. Our 8·2 mag. guiding star is the one *sf* the cross, and Table I. shows that it lies nearly one degree east of Herschel's place. Field No. 24 is almost in line between ζ Orionis and the 3rd mag. guiding star of No. 22, and a little over a degree *nf* the nebula θ Orionis. Could Roberts have purposely avoided these objects ?

The nebula *h* 1180=N.G.C. 1977 marked on Wolf's key map falls within Herschel's field though it could not be on the plate of Roberts owing to the displacement. It was observed here in 1916 as involved in the θ nebula, agreeing with Herschel's conviction (see Table II.).

4. The existence of nebulous matter in the fields 22, 23, 24, 25, and 27 is thus photographically proved, though the chemical effect on the plates does not seem to match with our visual scale of densities. It can indeed hardly be expected that the visual part of the light spectrum should, in a few minutes, produce on the human retina the same picture that is impressed on a chemical plate by the photographic rays (even when filtered) in the long course of over six hours. The difference between visual and photographic pictures is strikingly apparent on the chart published in our *Miscellanea Astr.*, p. 240, when compared with photographs of Herschel's field No. 25. More systematic experiments, like those described by Barnard in *Pop. Astr.*, 2 (1894–5), 151–154, will be needed before photography can show what Herschel saw.

Vatican Observatory :
1926 April.